NEW VISUAL ASSESSMENT USING STEADY-STATE VISUAL EVOKED POTENTIAL (SSVEP) AND EYE TRACKING

Lin Sheng Tong

(BSc(Hons) in Vision Science, University of Melbourne)

A THESIS SUBMITTED

FOR THE DEGREE OF MASTER OF ENGINEERING

DEPARTMENT OF ELECTRICAL AND COMPUTER ENGINEERING

NATIONAL UNIVERSITY OF SINGAPORE

2016

Declaration

I hereby declare that this thesis is my original work and it has been written by me in its entirety. I have duly acknowledged all the sources of information which have been used in the thesis.

This thesis has also not been submitted for any degree in any university previously.

Parts of Chapter 1 and 2 have been published in the following journal article, "A Preliminary Study on Normalized Pattern-Reversal Peripheral Field SSVEPs as a Potential Objective Indicator of Useful Field of View Performance - A Potential Neural Indicator of UFOV" in Investigative Ophthalmology & Visual Science, 57(7), 3248-3256. The work in this published article is part of my M.Eng research during my candidature.

_____

Lin Sheng Tong

3rd November 2016

Acknowledgements

I would like to thank A/Prof Yang Zhi and Zhao Qi for their mentorship throughout my M.Eng candidature in NUS. I would like to thank DSO National Laboratories for the loan of equipment and facilities for the pursue of this dissertation. I would also like to thank Mdm Natesaperumal Hemamalini for her guidance in student administrative procedure during my stay as a part-time student.

Table of Contents

Summary

The useful-field-of-view (UFOV) is the visual area from which one captures visual information with a single glance without any eye movement. Currently, the test for UFOV typically relies on an individual's subjective attentional responses. Two physiological signals, namely, steady-state visual evoked potential (SSVEP) and pupillary oscillation (PO) have been frequently used as an objective alternative to replace subjective attentional responses. Our aim was to investigate the possibility of predicting UFOV performance objectively using these signals. Two sets of experiments, A & B, were carried out for this purpose.

Experiment A is a preliminary study that indicates the potential relationship between the two signals and UFOV using three tasks of different target difficulties; a simple peripheral task, a UFOV task without distractor and a UFOV task with distractor. It was found that only UFOV task with distractor can differentiate UFOV percentage accuracy performance between individuals and Deming regression analysis indicates that this performance is predictable by the normalised SSVEP ($F(1,6) = 16.250$, $r = 0.854$, $P < 0.01$, $n = 8$) and normalised PO ($F(1,6)=20.13$, $r = 0.878$, $p < 0.01$, $n = 8$).

Experiment B adopts the UFOV task with peripheral distractor to measure UFOV eccentricity size performance, to evaluates the ability of SSVEP and PO to an individual's UFOV eccentricity size. Deming regression analysis once again shown that UFOV can be estimated using normalised SSVEP ($F(1,51)=44.86$, $r = 0.684$, $p < 0.01$, $n = 53$), and pupillary oscillation ($F(1,51)=91.73$, $r = 0.802$, $p < 0.01$, $n =53$).

Finally, various structural configurations of feedforward neural network model were trained using the data in Experiment B by the Levenberg-Marquardt backpropagation function. These network models were evaluated using the 11-fold cross-validation method and step-wise elimination of least predictive input vector for the best network

structure with the least input vectors that yields the most accurate prediction of UFOV eccentricity size performance. The results shown that the network with 7-1-2-1 structure that takes in normalised SSVEP and OP signal from stimulus with 7.5° to 10° eccentricity size can best predict UFOV size performance with an accuracy of approximately ± 0.278° (MSE = 0.0775). The results indicated that neural network models trained to predict UFOV size performance using physiological signals, SSVEP and OP, can be used as an objective assessment tool for UFOV, to confirm subjective-based UFOV assessment results. By reducing the network to a 4-1-1-1 structure which takes in only 4 input vectors from OP signals, the network model is still able to predict UFOV size performance with an accuracy of approximately ± 0.545° (MSE = 0.344). The reduction in input vectors shortens signal collection time with a small compromise on prediction accuracy, allowing the network to become a quick objective UFOV screening tool.

List of Tables

List of Figures

List of Illustrations

List of Symbols

NIL

Chapter 1: Introductions

1.1 Background

Typically, current means of assessing attention is to put individuals through psychophysical tests. These tests rely on subjective feedbacks and critical reaction time response; hence time must be set aside for multiple trials to gather accurate averages and to minimize effects of noise on data. When a test has to be repeated to confirm results, the lengthy testing time multiplies with each repetition. Also, a subjective test tends to rely on the motivational level of an individual. In the case in which a subjective test is used to select suitable candidates for sportsmen or military vocation, those mandated by rules to participate may response suboptimally to avoid good scores while those who are keen but are not confident about passing the test may try guessing tricks to achieve high scores. Recruiters would prefer shorter testing times while avoiding subjectivity by having objective markers.

When attentional performance is a large determinant factor for a particular critical job (e.g. combat pilots) or high-paying sports (e.g. professional basketball players), a more reliable and faster way of testing attention for the purpose of selecting potential trainee or to monitor the actual progress of the attention improvement from training becomes important. Time and cost can be minimized with a fast and reliable objective attention test when a mass screening for potential candidates are necessary. In Singapore, the national call of duty that attracted thousands of young adults to undergo military pilot trainee selection is a good example.

In this study, the aim is to investigate steady-state visual evoked potential (SSVEP) and pupil oscillation (PO) as the physiological markers that can quickly and

objectively assess individuals for their attentional span around his/her primary gaze, or in another more recognized term, the useful-field-of-view (UFOV).

1.2 Literature Review

This section covers the three key aspects which are of critical importance to the research interest here. They are namely, the useful-field-of-view (UFOV), steady-state visual evoked potential (SSVEP) and pupillary oscillation (PO). This section ends with a summary of two sets of experiments to demonstrate how SSVEP and PO can be potential objective assessment of UFOV. Note that SSVEP and PO are forms of physiological signal from human.

The Useful-Field-Of-View (UFOV)

UFOV is defined as the visual area from which one captures visual information with a single glance without any eye movement (Sanders, 1970; Ball, Beard, Roenker, Miller, & Griggs, 1988; Ball, Owsley, Stalvey, Roenker, Sloane, & Graves, 1998; Ball, Wadley, & Edwards, 2002). It indicates attentional performance toward peripheral visual field while visual information was concurrently processed from fixation point. For effective visual processing, the spatial extent of efficient attention around any given fixation point determines the amount of information processed at any one time (Sanders, 1970). Therefore, a person with less attentional decline from his visual fixation point can be said to have a larger UFOV or a more effective visual processing for a given UFOV size (Ball, Beard, Roenker, Miller, & Griggs, 1988). The bigger the UFOV, the more information can be processed at any one time. The current UFOV test has been developed based on this second perspective as a screening tool for driver, especially to predict driving performance of elderly drivers

(Ball, Wadley, & Edwards, 2002). This computer-based UFOV test (UFOV®, Visual Awareness Research Group, Inc, Punta Gorda, USA) comprises of three subtests, namely, stimulus identification, divided attention and selective attention (See Figure 1). The description of the subtests are as follows:

1. *Stimulus Identification.* The participant has to identify if the target presented in the center of the computer screen is an image of a car or a truck (see Figure 1, top). The target will be presented for varying lengths of exposure time (starting at 500 ms).

2. *Divided Attention.* The participant has to identify the centrally presented target image as a car or a truck while localizing a simultaneously presented periphery target image (15° eccentricity from the screen centre. See Figure 1, middle). This subtest evaluates the attention allocated to the space between central and peripheral targets. Individuals who have reduced UFOV may not have the necessary "spatial processing bandwidth" to quickly localize the periphery target, hence will perform poorly for this subtest

3. *Selective Attention.* This task is the same as the divided attention subtest except for the triangular distracters that increased task difficulty (see Figure 1, bottom). This subset is to test if the participant can ignore the distractors and only selectively attend to the relevant central and peripheral targets.

Subtest 1

Subtest 2

Subtest 3

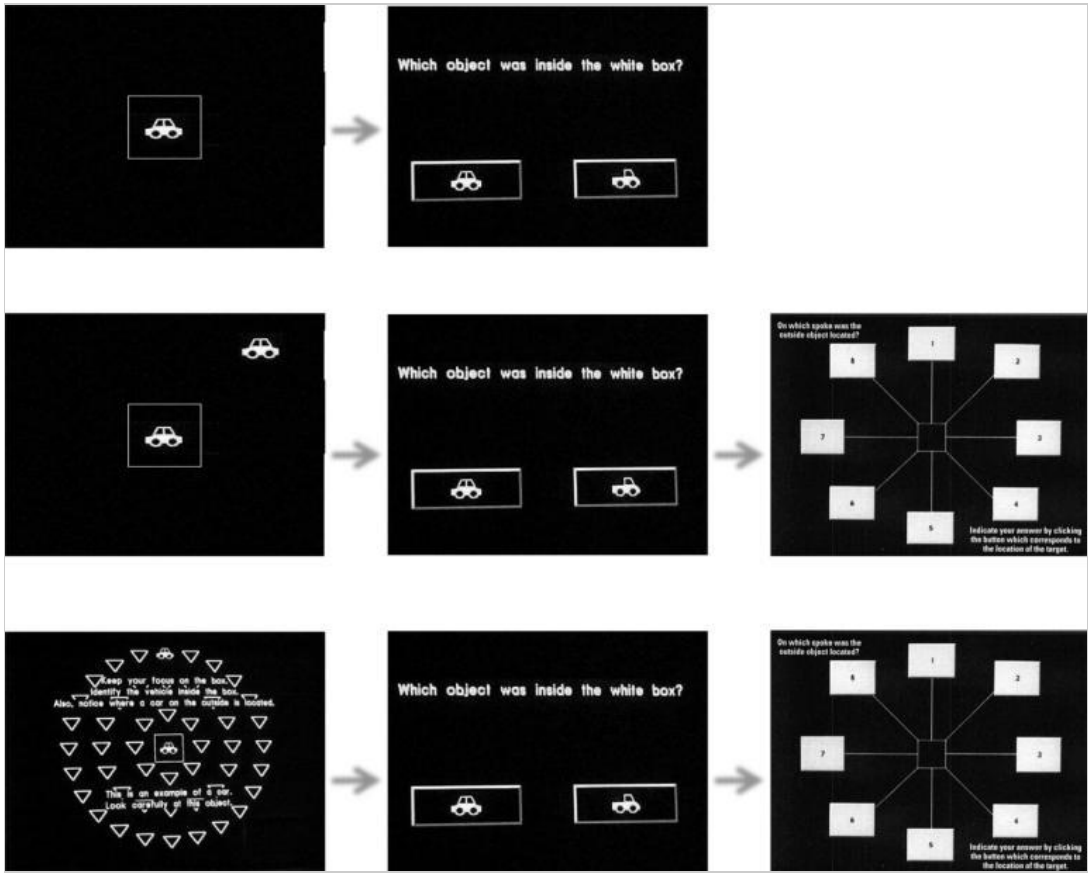

Figure 1: The UFOV® test which comprises of 3 subtests (Adapted from http://mecvswetenschap.wordpress.com/2013/05/26/abnormale-visuele-aandacht-bij-myalgische-encefalomyelitis/)

As UFOV is about visual information processing performance, it has a wide range of assessment application in perceptual science. The majority of the applications are in aging and driving performance assessment.

Aging. Normative data were collected in two studies. One for children and young adults age between 5 to 21 years old (Bennett, Gordon, & Dutton, 2009), the other for older adults age between 65 to 94 years old (Edwards, et al., 2006). In the first study, Bennett and his colleagues (2009) found that UFOV improves with age until it reaches stable adult level at the age of 14 approximately. In the second study, Edwards et al. (2006) found that UFOV is very much declined in his elderly group of participants. The mean reaction time for UFOV Subtest 3 was found to be 319.67 ms for Edward's elderly participants, which was at least 3 times slower than what was found in Bennett's young adult group (age 15 to 21, mean reaction time = 87.5 ms, an approximation from Figure 3 in Bennett, Gordon, & Dutton, 2009). Not surprisingly, the slower processing speed in older adult as shown by UFOV test was found to be associated with poorer attentional efficiency and slower conjunctional visual search (Cosman, Lees, Lee, Rizzo, & Vecera, 2012). This finding was also supported by studies in age-related learning difficulties (Richards, Bennett, & Sekuler, 2006) and eye movement analysis (Scialfa, Thomas, & Joffe, 1994).

Driving. This is one of the most common transportation activity throughout the world, and also one the of most risky activity for accidental death. Accident rate for elderly drivers is most likely the case of age-related declined in perceptual and attentional functions which are struggling to meet the high visual-response demands of driving (Ball, Owsley, Sloane, Roenker, & Bruni, 1993). As such, numerous studies have validated the strong relationship between elderly drivers' accident rate and UFOV(Owsley, Stalvey, Roenker, Sloane, & Graves, 1998; Ball, Wadley, & Edwards, 2002), and demonstrated that a healthy UFOV is required for driving (Ball,

Owsley, Sloane, Roenker, & Bruni, 1993; Isler, Parsonson, & Hansson, 1997; Rogé, Pébayle, Kiehn, & Muzet, 2002; Rogé, Pébayle, Hannachi, & Muzet, 2003; Rogé, Pébayle, Lambilliotte, Spitzenstetter , Giselbrecht, & Muzet, 2004; Clay, Wadley, Edwards, Roth, Roenker, & Ball, 2005; Wood J. M., Chaparro, Lacherez, & Hickson, 2012).

While poor UFOV is age-related in general, it is by no means a non-occurring in healthy young adult drivers. UFOV is a very dynamic phenomenon that also declines with increased auditory, visual and mobile-phone usage distraction (Wood, et al., 2006; Puell & Barrio, 2008). Sleep deprivation and reduced vigilance also contributes to poorer UFOV (Rogé, Pébayle, Kiehn, & Muzet, 2002; Rogé, Pébayle, Hannachi, & Muzet, 2003; Rogé, Pébayle, Lambilliotte, Spitzenstetter , Giselbrecht, & Muzet, 2004). Hence, the assessment of visual attention using UFOV may not be limited to age-related or driving studies. Due to UFOV's validated concept being increasingly accepted by the scientific community, with proper testing design improvement, it can be an attentional assessment parameter to differentiate attentional performance levels in normal healthy young individuals.

Steady-State Visual Evoked Potentials (SSVEPs)

SSVEP is the neuronal signal typically from the occipital brain region that oscillates at the same frequency as the flicker/flashing frequency of the visual stimulus presented, and this oscillation is modulated by how and where visual attention is deployed (Beverina, Palmas, Silvoni, Piccione, & Giove, 2003). The SSVEPs can be identified by recording brain signals using electroencephalography (EEG) and then transform its recorded data into its frequency domain where SSVEP is seen as an increase in amplitude or power in the same frequency as the stimulus presentation frequency rate (Beverina, Palmas, Silvoni, Piccione, & Giove, 2003; Herrmann, 2001) (See Figure 2).

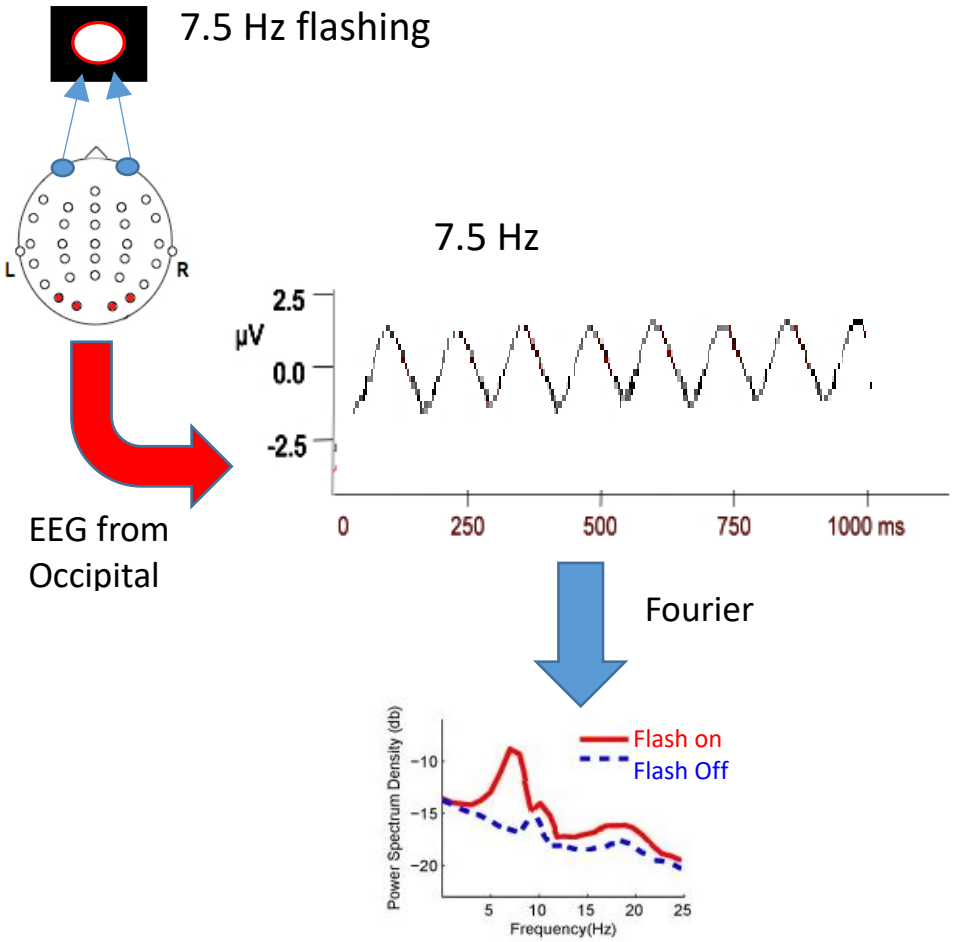

Figure 2: An illustration of SSVEP extraction from occipital region of the brain and its analysis process.

Relationships between SSVEP and psychophysical assessment of attention have often been studied. Mishra, Zinni, Bavelier, & Hillyard, (2011) found that action game players have increased suppression of SSVEP amplitudes to unattended peripheral stimuli. Many other effects of attention phenomena in modulating SSVEP has also been studied (Morgan, Hansen, & Hillyard, 1996; Müller, Teder-Sälejärvi, & Hillyard, 1998; Müller et al 1998; Belmonte, 1998; Kim, Grabowecky, Paller, Muthu, & Suzuki, 2007). Not surprisingly, objective feedback using SSVEP has become potential objective assessments for retinal functions (Herbik, Geringswald, Thieme,

Pollmann, & Hoffmann, 2014), visual acuity (Mackay, Bradnam, Hamilton, Elliot, & Dutton, 2008), amblyopia (Baker, Simard, Saint-Amour, & Hess, 2015), stereoscopic vision (Johansson, & Jakobsson, 2000), binocular rivalry (Zhang, Jamison, Engel, He, & He, 2011; Sutoyo, & Srinivasan, 2009; Jamison, Roy, He, Engel, & He, 2015;) and even fatigue (Cao, Wan, Wong, da Cruz, J& Hu, 2014). In the recent two decades, frequency-tagging technique for SSVEPs has been used to study localized attention (Ding, Sperling, & Srinivasan, 2006; Toffanin, de Jong, Johnson, & Martens, 2009; Müller, Malinowski, Gruber, & Hillyard, 2003; Malinowski, Fuchs, & Müller, 2007). This technique requires visual stimulus of interest to flash at a specific frequency; hence the stimulus is said to be "tagged" with a frequency. The amplitude of SSVEP is modulated by attention to the flashing stimulus regardless of whether eye gaze is directed to the stimulus or not (Müller, Malinowski, Gruber, & Hillyard, 2003; Malinowski, Fuchs, & Müller, 2007). Consequently, many studies have used changes in SSVEPs as the neuronal response during experiments in place of or to support the occurrence of specific subjective responses (Ding, Sperling, & Srinivasan, 2006; Toffanin, de Jong, Johnson, & Martens, 2009; Müller, Malinowski, Gruber, & Hillyard, 2003; Malinowski, Fuchs, & Müller, 2007).

1.3 Pupillary Oscillation

The pupil is the aperture in the human eye that modulates light entering the eye for optimal vision. It is controlled by both the sympathetic and parasympathetic nervous system for dilation and constriction respectively, in response to changes in brightness (Loewenfeld, 1999; Beatty, & Lucero-Wagoner 2000). Hence, the instantaneous antagonistic activity of both nervous systems determines the size of the pupil at any one time. In many previous studies, pupil responses have been used as evidences of

visual acquisition of information and activation of visual attention to specific stimuli (Hawkes, & Stow 1981; Privitera, Renninger, Carney, Klein, & Aguilar, 2008; Daniels, Nichols, Seifert, & Hock, 2012; Wierda, van Rijn, Taatgen, & Martens, 2012; Mathôt, Van der Linden, Grainger, & Vitu, 2013; Wang, & Munoz, 2014). Binda, Pereverzeva, & Murray, 2014; Mathôt, Dalmaijer, Grainger, J., & Van der Stigchel, 2014). These studies found strong association between initial pupil responses and the onset of attention to visual target located at eye fixation (overt attention) as well as peripheral of the fixation (covert attention). When attending to targets peripheral to the fixation point, pupil constricts when target is brighter than background and dilates when target is darker than background (Mathôt, Van der Linden, Grainger, & Vitu, 2013). The most logical explanation for the occurrence of appropriate selective pupil size modulation to selective attention is the need for optimal brightness to achieve best possible vision for the attended target anywhere within the visual field (Mathôt, & Van der Stigchel, 2015). Hence, attention-modulated pupil responses provide an objective means to assess attention anywhere within one's visual field, and can be easily measured by using an eye tracker (Klingner, Kumar, & Hanrahan, 2008).

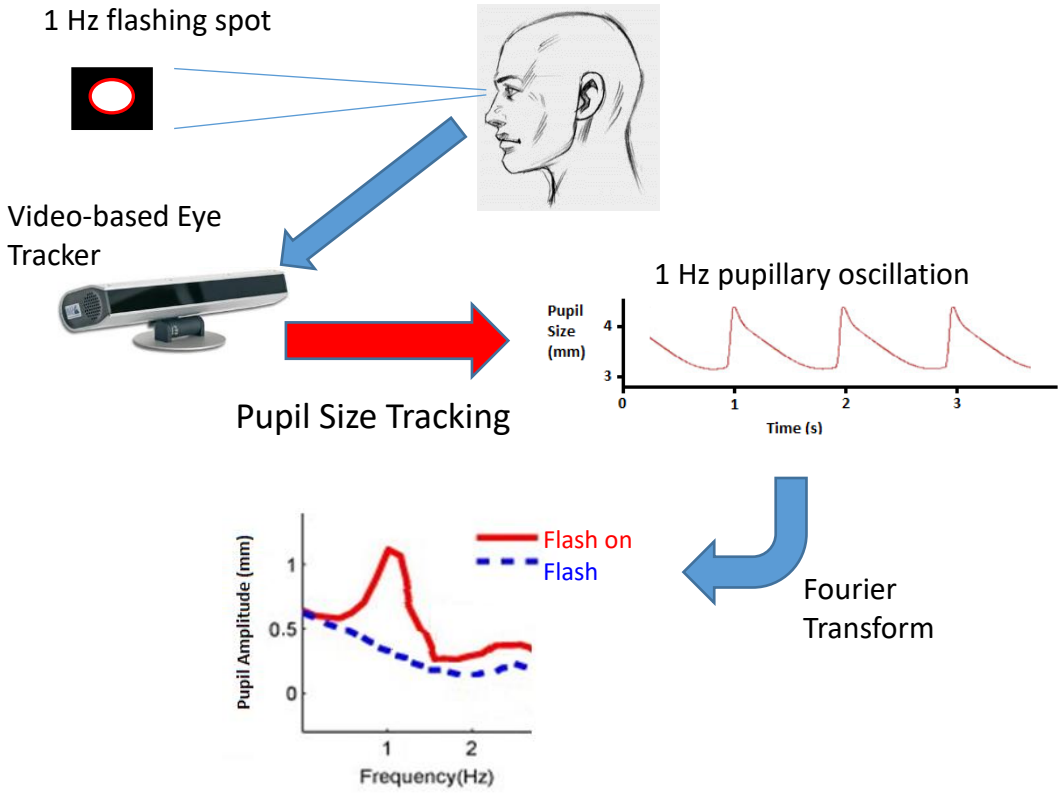

Figure 3: An illustration of pupillary oscillation analysis process

Recently, Pupil Frequency Tagging (PFT) method is used instead of analyzing event-related pupil response (Naber, Alvarez, & Nakayama, 2013). In PFT, the visual target onset occurs at a fixed frequency, and this elicited a corresponding pupil responses at the same frequency (See Figure 3). Such pupil size response occurring at any specific frequency is termed pupillary oscillation (PO). The beauty of PFT is similar to SSVEP where signals are analyzed in the frequency domain using Fourier transformation (Naber, Alvarez, & Nakayama, 2013). As such, errors in identifying correct event-related pupil response can be avoided. In our Experiment A in the next section, we deployed PFT techniques to our peripheral targets to verify the presence of selective attention for peripheral visual field that is indicative of UFOV.

1.4 Investigating SSVEP and Pupillary Oscillation for their potential role in UFOV assessment.

Given the literature discussion in the earlier subsection, there is a high possibility that combining both SSVEP and PO can offer an objective assessment and prediction of UFOV performance. There are three possible parameters to what defines UFOV performance of an individual;

i) response time (milliseconds) which is the visual processing speed measured for responding correctly to an UFOV stimuli,

ii) percentage accuracy of detecting peripheral targets while attention is also focused on central target, and

iii) peripheral field size (in visual angle degrees) of the UFOV in terms of eccentricity from centre fixation.

To avoid cross-interaction, studying the variation of any one of the three parameters above would require the other two parameters to be fixed and non-varying. Of the three parameters, the commercial UFOV® test only uses visual processing speed paradigm as the assessment of UFOV. However, the most important parameter is none other than the field size of the UFOV, which literally describes the general peripheral boundary between attended and unattended vision away from fixation centre, with the assumption that overt attention peaks at central fixation and generally declines towards peripheral vision. Hence, field size better describes the practical aspect of Useful-Field-Of-View. This dissertation describes two sets of experiments, namely, Experiment A and Experiment B. Experiment A fixed both the stimulus exposure time and field size to studied the UFOV performance in terms of central-peripheral target detection accuracy using a small number of human participants. The purpose was to use the accuracy parameter to quickly establish a general confidence

that SSVEP and pupillary oscillation has indeed a relationship with UFOV. Experiment A serves as a feasibility or preliminary study to swiftly confirm study design and effects. Note that the visual process speed parameter was not studied as it requires expensive high frame rate display monitors, graphic cards and software setup that could precisely control stimulus at less than 5ms which is not available at the time of the research work. The Experiment B was then designed, based on the success in Experiment A, using a typical psychophysical method to estimate the size of individuals' UFOV and to record their SSVEP and PO, the two key physiological signals in this study. The purpose was to analysed SSVEP and PO for their ability to predict UFOV sizes. The predicted sizes were benchmarked against the estimated UFOV sizes collected from psychophysical test.

Chapter 2: Experiment A

Experiment A was design to identify UFOV task(s) that can show differences in UFOV performance between individuals and at the same time contains stimuli that elicit SSVEP and PO effectively. The aim was to examine and confirm the fundamental hypothesis of the relationship between UFOV and the two physiological signals. To do so, we designed experimental paradigms with a pattern-reversal annulus ring covering only the peripheral visual field to collect peripheral field SSVEPs levels. Since SSVEPs are indicative of attentional resources and UFOV is about the extent of "spot-light" of attention, hypothetically, SSVEPs stimulated by pattern-reversal stimulus at or near the peripheral regions of this "spotlight" should carry information about the outer boundary of the attentional field, in a way similar to frequency-tagging. Hence, we distributed peripheral stimulus just outside this annulus to collect psychophysical performance data to verify if accuracy in detecting peripheral stimuli could be predicted by this peripheral field SSVEP. In addition, the peripheral stimulus was also designed to collect meaningful pupil response to study its relationship with UFOV as well; the PFT method will be implemented for the mentioned peripheral stimuli by presenting them at a fixed onset frequency to elicit the relevant pupillary oscillation. Hypothetically, larger amplitude of pupillary oscillation triggered by peripheral on-off targets indicates better attention towards the peripheral visual field, hence better UFOV performance.

2.1 Methods

Eight healthy participants (6 males, 2 females, ages 18–37) with vision correctable to 6/6 for both far and near in both eyes were recruited. The experiments were conducted using a 120-Hz light-emitting diode (LED) monitor (Asus VG278HR; ASUSTeK Computer, Inc., Taipei,Taiwan) with a typical computer equipped with a GTX 570 Nvidia (Santa Clara, CA, USA) graphics card. The monitor screen was positioned 70 cm from the participant's eyes. A commercial off-the-shelf EEG system (ASA LAB waveguard64; ANT-Neuro, Enschede, The Netherlands) was used to record brain signals noninvasively by placing the sensors on the scalp at electrode positions O1, O2, and Oz of the occipital region according to the international 20–20 system standard, referenced to M1 and M2 positions on the mastoid. These electrode positions have been previously demonstrated to collect strong SSVEPs (Pastor, Artieda, Arbizu, Valencia, & Masdeu, 2003; Zhang, Jin, Qing, Wang, & Wang, 2012; Störmer, Winther, Li, & Andersen, 2013). All electrodes attained an impedance level of 10 kΩ or less before the start of the experiments. An eye tracker (SMI RED 250; SensoMotoric Instruments Gmb, Teltow, Germany) was used in this study to collect pupil oscillation data as well as to ensure that participants' eyes were fixating on the central stimulus. All participants completed the following experiments, and each participant was familiarized using 10 trials of each experiment prior to the commencement of the experiment.

i) Experiment A1 – Baseline Peripheral Attentional Task

The purpose of this task was to ensure that participants had good covert attention to peripheral visual field to begin with. Each trial consisted of a baseline phase and an activity phase (See Figure 4). During the baseline phase, participant were asked to fixate on the 0.83Hz blinking cross (0.4° visual angle in size, 100ms on, 1100ms off) at the centre of a gray screen. Around the

blinking cross was an annulus ring of checkered pattern at 7.5 reversal/s (each checkered box is 1.5°). The mean illuminance of the checkered pattern was 150 cd/m^2. The thickness of the ring spans between 3.5° to 7° degrees from the fixation cross centre, leaving a centre gray zone extending from the fixating point to the inner edge of the ring. The baseline phase lasted for 10 seconds followed by the activity phase, which was the same as the baseline phase except for two aspects. Firstly, just outside and around the annulus ring were eight equally distributed small peripheral rings (1.4° visual angle in size). The centre of these rings are approximately 8° from the centre of the cross. Only one of these circles was randomized to be filled black for 100ms (onset of peripheral stimulus) every 1.2 seconds in synchrony with the fixation cross. Secondly, the activity phase was randomized to last for 16 to 32 seconds to allow sufficient time to adapt to the peripheral stimuli. The end of the activity phase is indicated by a white-noise screen which was presented for 2 seconds; then participant has to indicate which one of the peripheral circles last seen was filled black by pressing a response button corresponding to the peripheral circle position (e.g., numeric keypad number 1=bottom left circle, 9=top right circle). The purpose was to exclude anticipatory deployment of attention to the periphery. Participants were told to hold their blink during the baseline and activity phase but were encouraged to blink to their satisfaction during the time when they made their response for the peripheral target after the white noise. Participants were also told to take their time to make this response so as to have ample time for blinking and sufficient rewetting of their eyes. Scores were recorded as the percentage of correct responses for the peripheral stimulus that occurred just before the white-noise onset. There were a total of 20 trials per participant.

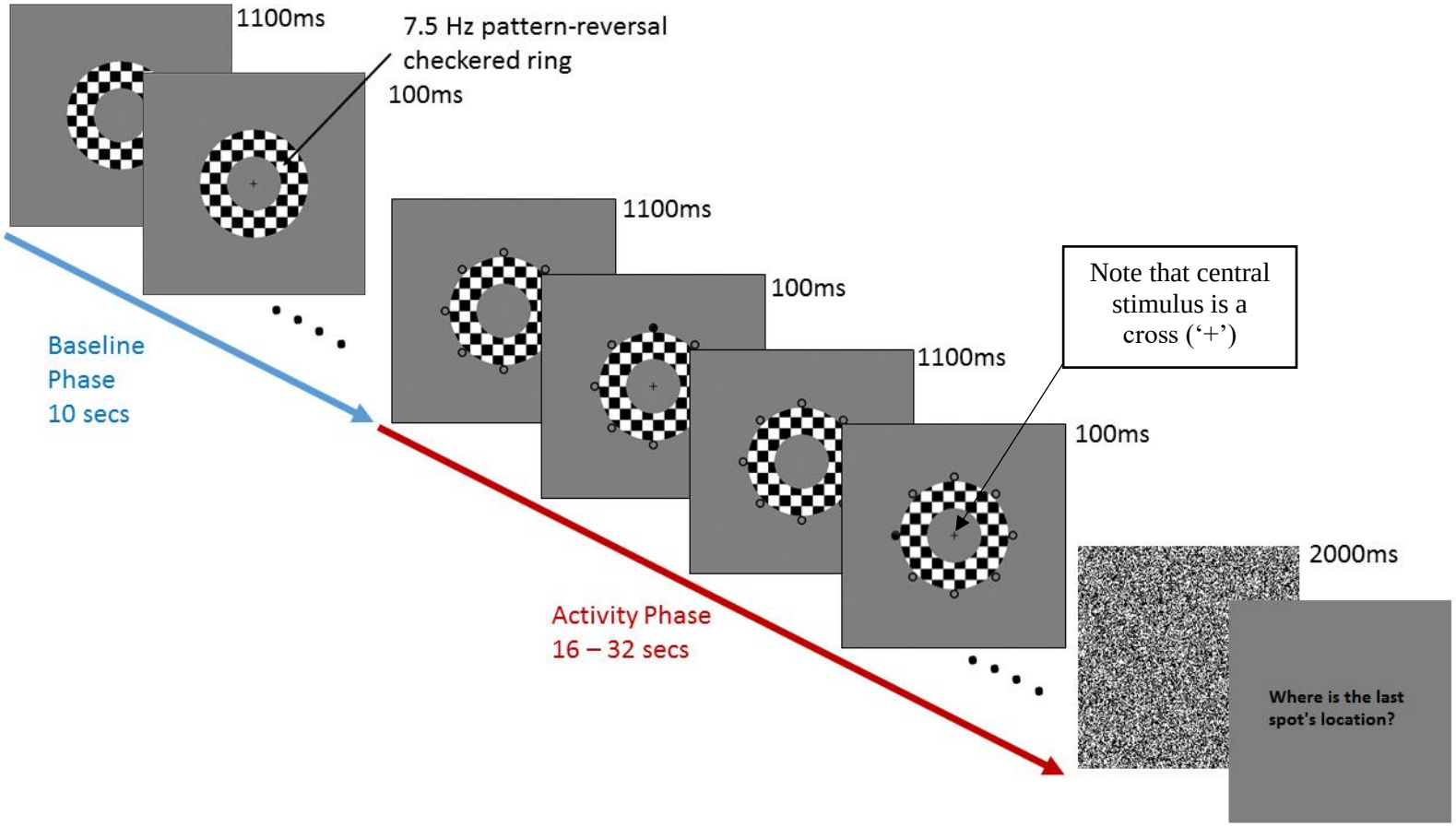

. Figure 4: An example of a single Experiment A1 trial.

Trial results were discarded if a subject was found to fixate beyond 1° away from the central stimulus during the entire trial or when a blink occurred during the last 5 seconds of the baseline or activity phase.

ii) Experiment A2 – Central-peripheral dual task:

The purpose of this task was to investigate the participant's ability to direct simultaneous attention to both central and peripheral stimulus. In other words, it measured the likelihood of detecting a target at a given eccentricity while attending to a central stimulus, thus assessing the breadth of allocated attention in space (i.e., UFOV performance). The trial design was the same as Experiment A1 except that during activity phase, the center fixating stimulus was a small circular ring, 0.167° (10 arcmin) in size (See Figure 5). The circular ring presented a 0.083° (5 arcmin) broken gap every 1.2 seconds in synchrony with the peripheral stimulus onset. The presentation of the gap was randomized to occur at either the up, down, left, or right part of the circular ring. The participant had to actively respond in real time to the gap direction using keyboard arrow buttons, while response to the peripheral stimulus occurred after the white noise when each trial ended. There were a total of 20 trials. The UFOV performance scores were recorded as the percentage of correct responses for the peripheral stimulus that occurred just before the white-noise onset. Note that trial results were excluded from score calculations if a participant did not make a correct response to the last central stimulus during its simultaneous onset with the last peripheral stimulus just before the white noise.

iii) Experiment A3 – Central-peripheral dual task with active distractors:

The purpose of this task was to investigate participant's ability to perform a central–peripheral attention task in the presence of peripheral distractors. The trial design was the same as Experiment A2 except that during the activity phase, extra distractors between the peripheral circles in the form of black spots (1.4° visual angle in size) were presented along with the onset of peripheral stimulus (See Figure 6).

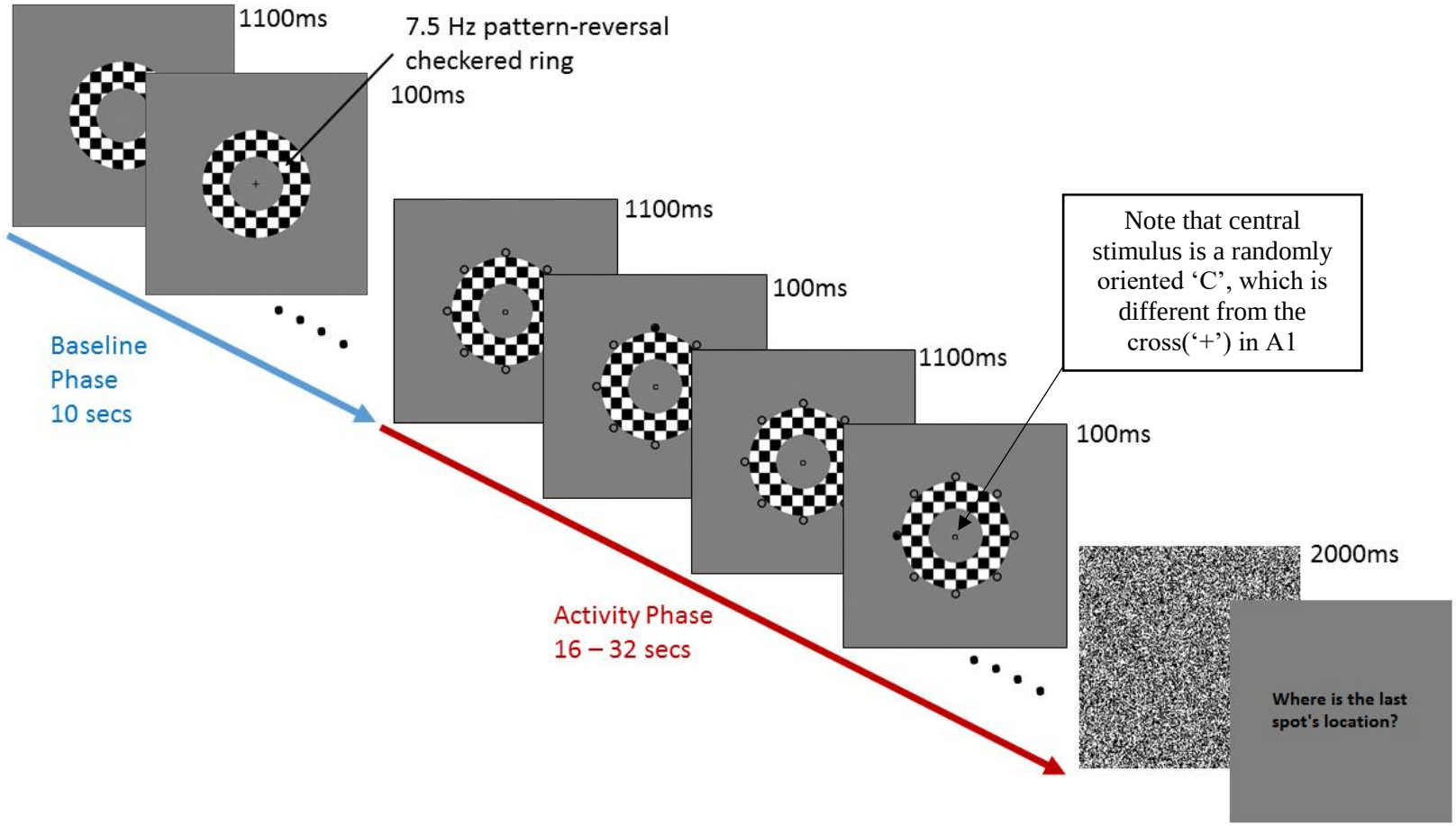

Figure 5: An example of a single Experiment A2 trial.

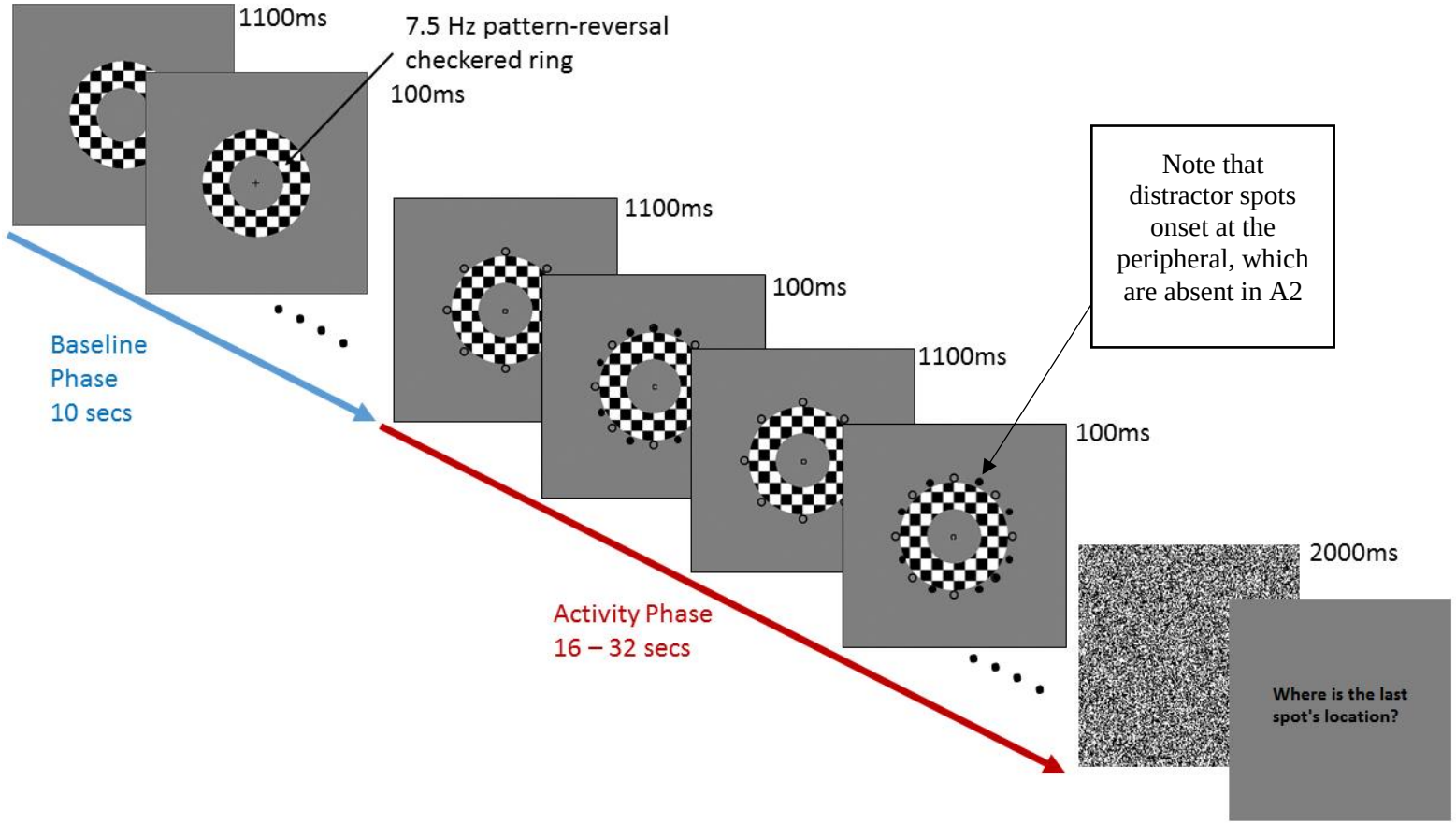

Figure 6: An example of a single Experiment A3 trial.

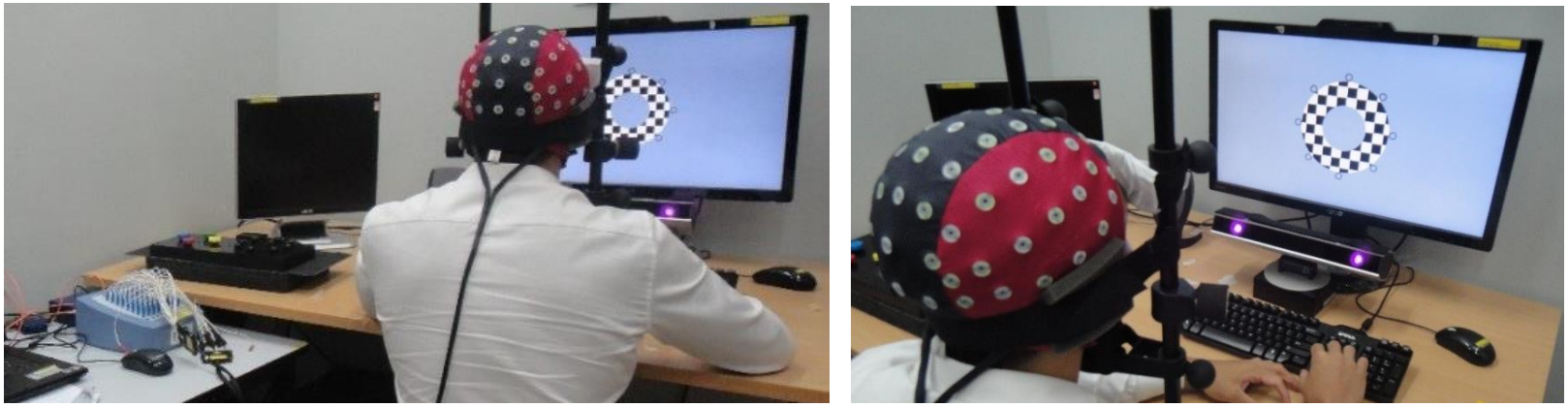

Illustration 1: A typical setup of the experiment

2.2 Data Processing & Analysis

Statistical analyses on were conducted using GraphPad Prism 7.0 (La Jolla, CA, USA) on the SSVEP and pupil oscillation data pre-processed using the following methods.

SSVEPs

The raw signal data from O1, O2 and Oz channels underwent noise-removal and band pass between 1 and 40 Hz using the zero-phase Hamming-windowed sinc Finite Impulse Response (FIR) filters (Widmann, Schröger, & Maess, 2014) from the EEGLAB toolbox (Version 13.1.1) for MATLAB R2013b (The MathWorks, Inc., Natick, MA, USA). For each channel and for each experiment, the last 5-second filtered data before the end of baseline phase were selected and transformed into frequency domain from which 7.5-Hz neural oscillation power (in dB = $10\text{Log}10[\mu V^2]$) was obtained. The same procedure was done for the activity phase in each experiment. Then the obtained power was averaged across all three channels in their respective phases and experiments. The normalized SSVEP (nSSVEP) power for each experiment was calculated by taking the average 7.5-Hz power of the accumulated activity phase minus its accumulated preceding baseline phase's power of the same frequency.

Pupillary Oscillation

Pupil sizes from both eyes underwent noise-removal and band-pass using the same technique in MATLAB. For each eye and for each experiment, the last 5-second data before the end of baseline phase was selected and transformed into frequency domain from which 0.83 Hz PO amplitude (in mm) was obtained. The same procedure was done for the activity phase in each experiment. Then the obtained PO amplitudes were averaged between the two eyes in their respective phases and experiments. The

normalised PO (nPO) amplitude was calculated by taking the averaged 0.83 Hz PO amplitude of the accumulated activity phase minus its accumulated preceding baseline phase's amplitude of the same frequency.

2.3 Psychophysical Behavioral Results

All participants fixated within 1° away from the stimulus center in all trials, and no blinks during the last 5-second window during the baseline and activity phases (where SSVEP and PO signals were used for processing) were detected by the eye tracker. All participants attained a perfect score for responses to the last central stimulus in Experiments A2 and A3 during their simultaneous onset with the last peripheral stimulus before the white noise; hence no trials were excluded. In each of Experiments A1 to A3, the activity phase lasted for an average of 24 seconds. Since responses to central stimuli were consistent with good central fixation behavior for all participants in the experiments, all correct responses here were simplified to consider only correct responses to peripheral stimulus. On the other hand, accuracy scores differed between different experiments for response to peripheral stimuli/targets.

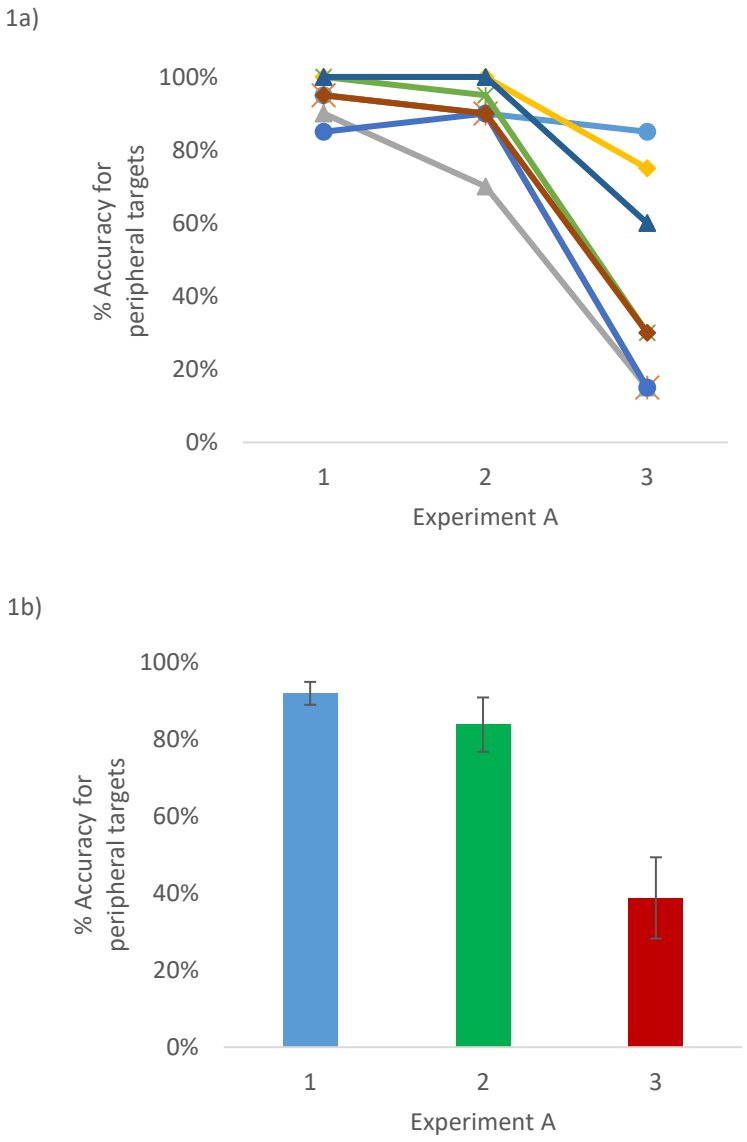

Figure 7: Percentage accuracy for peripheral targets in experiments A1 to A3 for a) Individual and b) group mean (Error bar = SE).

Figure 7 shows the percentage accuracy for peripheral targets for each experiment. All participants scored near perfect if not perfect for Experiments A1 and A2, except for one who scored 70% in Experiment A2. The accuracy scores started to spread within the participants in Experiment A3 where the task difficulty is the greatest with the peripheral distractors. Repeated measure ANOVA with Greenhouse-Geisser correction indicated a significant difference in percentage correct for peripheral

targets among the tasks($F(1.122,7.855) = 32.471$, $p < 0.01$). A post hoc test with Bonferroni correction revealed that there were significant differences only between A1 and A3 (mean differences = 0.544, 95% CI [0.257, 0.831], $p < 0.01$), and A2 and A3 (mean differences = 0.5, 95% CI [0.224, 0.776], $p < 0.01$). There was no significant differences between A1 and A2 (Mean differences = 0.044, 95% CI [-0.037, 0.124], $p = 0.4$). The analysis suggested that Experiment A1 and A2 were easily accomplished and exhibited near ceiling effects for all participants except one. Hence, these two experiments did not show difference in performance between the sampled normal individuals, in contrast to Experiment A3, which showed a spread of performance differences between individuals. It was also noted that the top three performers in this experiment were a semi-professional volleyball player, a competitive basketball player and a frequent video gamer (role-playing game [RPG] player) respectively in the descending order of top scores, while the rest of the participants are office workers with negligible engagements in sports and video games.

2.4 Regression Analysis Results

nSSVEPs versus performance

Repeated measure ANOVA indicated no significant difference in nSSVEPs between the experiments ($F(2,14) = 0.607$, $p = 0.559$). Figure 8 shows the mean values of nSSVEP for Experiments A1 to A3. However, looking at the small sample size here and the high variance observed in Figure 8, there is a possibility of decreasing nSSVEPs with increasing stimulus difficulties given a case of low statistical power. Nevertheless, until proven with a larger sample size, the difference in nSSVEPs between Experiments A2 and A3 seems to be small if even existent.

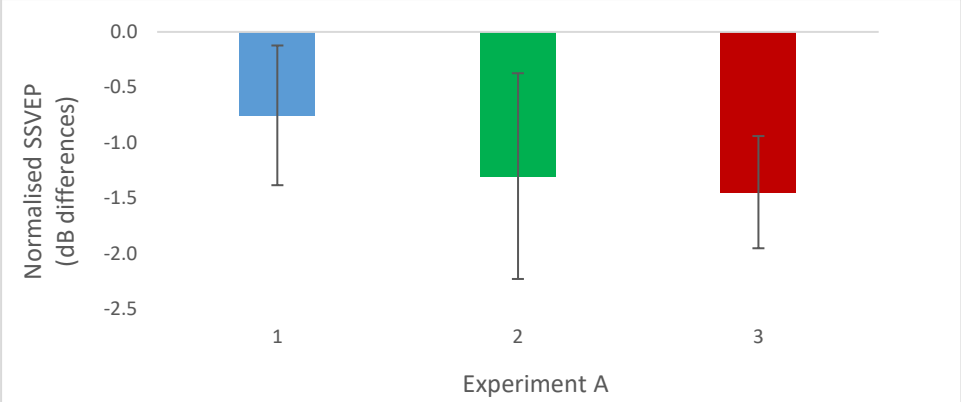

Figure 8: Normalised SSVEPs in experiments A1 to A3 (Error Bar = SE).

Orthogonal linear regression (Deming regression) and Pearson correlation analyses were done to study the relationship between peripheral target accuracies and the corresponding nSSVEPs for each of the experiment (See Figure 9). Regression analysis showed a significant relationship between target accuracies in Experiment A3 and its nSSVEPs ($F(1,6)=16.250$, $p < 0.01$), and their correlation coefficient, $r = 0.854$, indicates a strong positive relationship. There was no significant relationship and correlation found between the accuracy and nSSVEPs for Experiment A1 ($F(1,6) = 0.065$, $r = 0.103$, $p = 0.808$) and Experiment A2 ($F(1,6) = 0.397$, $r = 0.249$, $p = 0.552$). It was also noted that the previously mentioned top three performers had nSSVEPs larger than the rest of the participants.

9a) Experiment A1

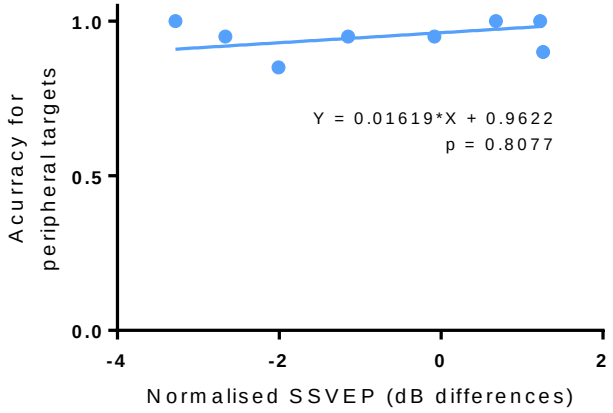

9b) Experiment A2

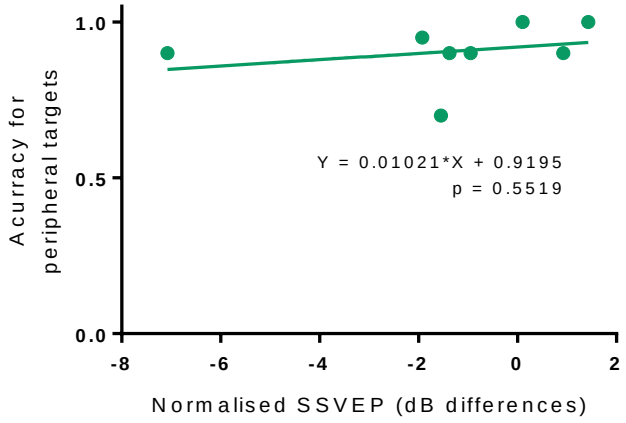

9c) Experiment A3

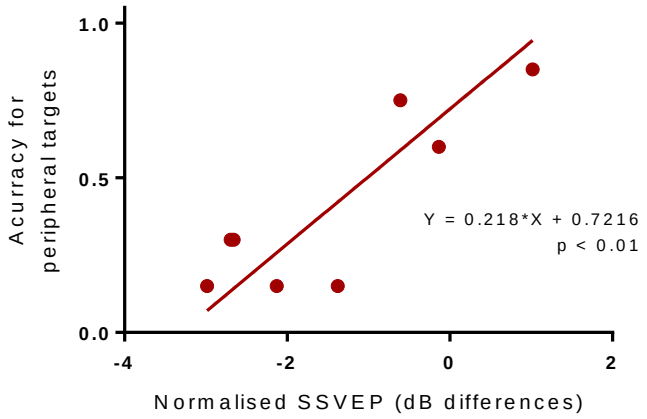

Figure 9: Percentage accuracy versus Normalised SSVEPs in Experiment A1 to A3.

nPO versus performance

Repeated measure ANOVA indicated no significant difference in pupillary oscillation between the experiments ($F(2,12) = 0.373$, $p = 0.696$). Note that one participant's pupil data was corrupted for Experiment A2, hence all her data across experiments was omitted in this ANOVA analysis. Figure 12 shows the mean values of nPO for Experiments A1 to A3. However, looking at the small sample size here and the high variance observed in Figure 10, there is a possibility of decreasing nPO with increasing stimulus difficulties given a case of low statistical power. The difference in nPO between Experiments A2 and A3 seems to be small even if proven to be significant.

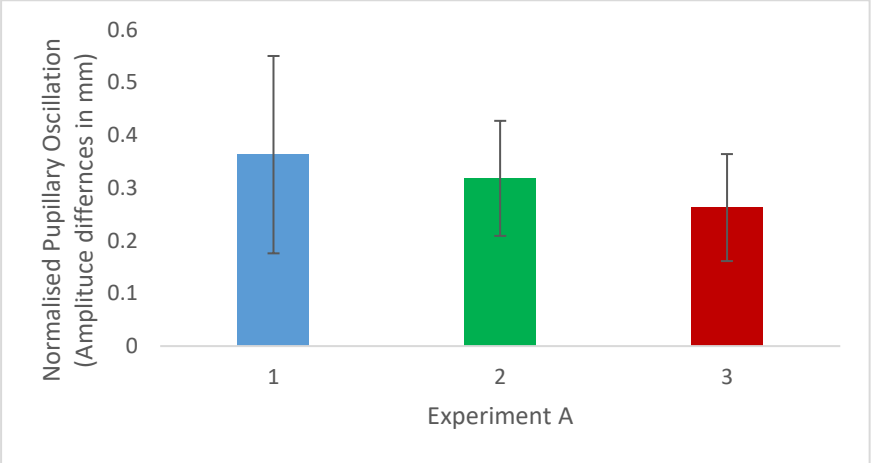

Figure 10: Normalised Pupillary Oscillation in Experiment A1 to A3 (Error Bar = SE).

Regression analysis similar to those for nSSVEPs was done to study the relationship between peripheral target accuracies and its corresponding nPO for each of the Experiment A1 to A3 (See Figure 11). Deming regression analysis showed a significant relationship between target accuracies in Experiment A3 and its nPO ($F(1,6)=20.13$, $p < 0.01$), and their correlation coefficient, $r = 0.878$, indicates a

strong positive relationship. There was no significant relationship and correlation found between the accuracy and nPO for Experiment A1 ($F(1,6) = 1.514$, r = 0.449, p = 0.265) and Experiment A2 ($F(1,6) = 0.567$, r = 0.319, p = 0.485). It was also noted that the previously mentioned top three performers had nPO larger than the rest of the participants. The results here is very similar to the findings for nSSVEPs.

13a) Experiment A1

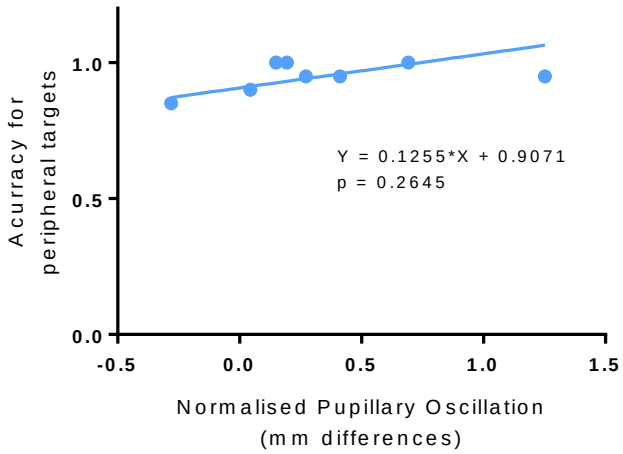

13b) Experiment A2

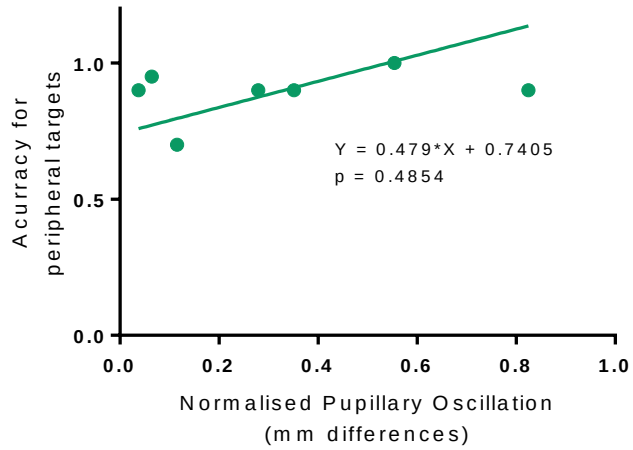

Figure 11: Percentage accuracy versus Normalised Pupillary Oscillation in Experiment A. Also note that Experiment A2 only have 7 participants' data point)

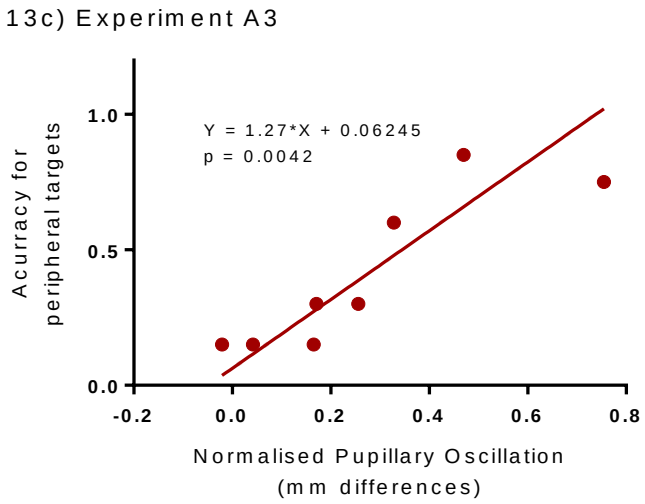

Figure 11(Continue): Percentage accuracy versus Normalised Pupillary Oscillation in Experiment A. Also note that Experiment 2 only have 7 participants' data point)

2.5 Discussion

Experiment A1 demonstrated that all participants have good peripheral vision to start with. Experiment A2 demonstrated that all participants can perform the central-peripheral task well. Experiment A3 threw in peripheral distractors on top of a central-peripheral dual attention task to examine how individuals handle multiple information closer to the boundaries of UFOV. The peripheral distractors in A3 have shown to be the effective in increasing task difficulty, providing a wider spread of performance differences between participants.

nSSVEPs

The peripheral distractors in Experiment A3 were shown to be effective in increasing peripheral task difficulty, providing a wider spread of performance differences

between participants. Noticeably, the relationship between UFOV performance and nSSVEP in Experiment A3 is driven by two clusters of data in the current small sample size. Hence, at the moment, implementing peripheral distractors in Experiment A3 could differentiate the participants' performance into only two different levels. Interestingly, peripheral task difficulty was not accompanied by a corresponding significant difference in nSSVEPs when comparing Experiments A3 and A2 (with and without peripheral distractor comparison, probably partly due to small sample size. Even if there is sufficient sample size, this small difference is likely to have little practical meaning. Hence, nSSVEPs here is likely to reflect an individual's inherent neuronal states of attention level when engaging a central task rather than a dependent variable of task difficulty. Another strong contributing factor is how the baseline was designed. Both SSVEPs were stimulated and acquired during baseline phase (no task) and activity phase (task). Taking the signal differences between them to associate with effects arising from the corresponding task performance is more meaningful than purely having an SSVEP extracted and baselined to a controlled condition without any checkered stimulus.

Another observation in Experiment A3 was that most nSSVEPs in this study were negative in value, and those with good UFOV had positive nSSVEP values. This may be attributed to the fact that good UFOV performers in Experiment A3 maintained their attention better under the stress of a difficult peripheral task, hence suffered less peripheral field SSVEP attrition when executing central–periphery dual detection during the activity phase. Given that SSVEP strength is relatively stronger for attended stimuli (Beverina, Palmas, Silvoni, Piccione, & Giove, 2003; Herrmann, C. S., 2001), this explanation is plausible.

The last observation worth noting concerns the top three performers in Experiment A3 (mentioned earlier) who included two sportsmen and a video gamer. The effect of

video gaming has previously been demonstrated, with specific differences in the SSVEPs of video gamers compared to normal individuals (Mishra, Zinni, Bavelier, & Hillyard, 2011; Krishnan, Kang, Sperling, & Srinivasan, 2013). Krishnan et al (2013) found that Role Playing Game (RPG) players have increased SSVEPs for attended flashing stimuli accompanied by an increased detection accuracy in a multi-region visual search task. Hence, they are thought to be deploying some form of attention enhancement. Findings for the participant in Experiment A3 who was a frequent RPG player seem to concur with the findings of Krishnan et al (2013) as her relatively higher nSSVEP is accompanied by better peripheral detection accuracy than most of the other participants. Unfortunately, Experiment A here did not have participants who were active/frequent action video game players. It was known that action video gamers performed better in UFOV task (Hubert-Wallander, Green, & Bavelier, 2011; Green, & Bavelier, 2003), and they probably ignore distractors better using a unique neural strategy revealed by the suppression of SSVEPs from irrelevant flashing stimuli ((Mishra, Zinni, Bavelier, & Hillyard, 2011).

On the other hand, the influence of sports training on SSVEPs is less studied. Also, the findings in the literature regarding better UFOV for ball sport athletes are rather mixed. Matos & Godinho (2005) and Memmert, Simons & Grimme (2009) highlighted that UFOV for these sportsmen is not significantly better than non-sportsmen. Memmert, Simons & Grimme (2009) suggested that the commercial version of UFOV test is designed for screening elderly persons for risk of driving accidents and may not have the sensitivity to find the differences between sportsmen and non-sportsmen among healthy young individuals. However, Schwab & Memmert (2012) found that sports vision training improves UFOV for hockey players but did not report sports performance to suggest any corresponding improvement in actual sports activity. Study done by Störmer, Winther, Li, & Andersen (2013) suggested

that individuals who are better at tracking multiple flashing moving targets within their visual field exhibits higher SSVEPs elicited by the frequency-tagged targets. If these individuals are analogous to ball game sportsmen, then there is a good possibility that better UFOV in sportsmen could be accompanied by higher levels of SSVEPs.

Normalised Pupil Oscillation

The findings for nPO are very similar to those of the nSSVEPs, especially for the results from regression analysis. In general, the results from pupil oscillation here strongly supported the differences in UFOV performances among the participants and provides strong physiological evidence that different performer has different neural-physiological characteristics. Just like the nSSVEPs, since there was no significant differences between pupillary oscillation findings between the first three experiments despite differences in UFOV performance. Even if there is a larger sample size for a significant difference, the difference is likely to be small and of little practical meaning. Hence, the normalised pupil oscillation here is likely to reflect an individual's inherent neuronal states of attention level when engaging a central task rather than a dependent variable of task difficulty. The top 3 performers in Experiment A3 mentioned earlier who are sportsmen and video gamers have larger amplitudes of normalised pupil oscillation in Experiment A3 than the rest of the participants, which supports the nSSVEP results. The pupillary oscillation results provide further physiological evidence along with the nSSVEP results in explaining the UFOV performance in Experiment A3. On top of that, it was also observed that the gradient (beta value) of the Experiment A3's regression line in Figure 13c for nPO was larger compared to the one in Figure 9c for nSSVEP of the same

experiment. This indicates the nPO varies wider with UFOV performances compared to nSSVEP, hence may be the stronger indictor of UFOV performance.

2.6 Chapter Conclusion

It was demonstrated that the peripheral stimuli designed in Experiment A can elicit different pupil and SSVEP response for different individuals. Experiment A shown that changes in peripheral field SSVEP and pupil oscillation can potentially be used to identify an individual with good UFOV performance in the presence of distractors. Experiment A serve as a preliminary study to ascertain the feasibility of using SSVEP and PO as the objective predictors for UFOV performance. While percentage accuracy reflects individuals with different UFOV capabilities, it is not informative in providing an estimation of the extent of the actively-attended peripheral field (i.e. the size of UFOV). The same issue occurs also for the commercial version of UFOV test which only relies on the fastest response time to peripheral stimulus for a fixed eccentricity peripheral targets; hence, UFOV® does not actually provide any quantitative estimation of UFOV size. The size of UFOV is important as it literally describes what the term UFOV's practical meaning, and helped to differentiate attended and unattended peripheral vision. The boundary between attended and unattended peripheral vision have more practical use compared to performance in accuracy or response time within a fixed-eccentricity field of vision. Experiment A3 setup will be modified for the next set of experiment, Experiment B, for the purpose of field size estimation of UFOV, by testing various eccentricities of peripheral stimulus to estimate the distribution of attentional performance toward the periphery using a much larger sample size. It will also be worthwhile to recruit sportsmen, video gamers and office workers to stretch performance distribution.

[Note that the portion of the research on SSVEP was published in 2016 by the candidate in *Investigative Ophthalmology & Visual Science, 57(7), 3248-3256,* titled "A Preliminary Study on Normalized Pattern-Reversal Peripheral Field SSVEPs as a Potential Objective Indicator of Useful Field of View Performance - A Potential Neural Indicator of UFOV."]

Chapter 3: Experiment B

Experiment B was designed to estimate the UFOV size performance of human participants and record their SSVEP and PO. The aim was to study the relationship between the two physiological signals and UFOV size performance. The secondary aim is to provide the foundation findings and grounds to guide the development of a neural network model which could predict UFOV size performance from these signals.

3.1 Design overview

The findings from Experiment A indicate that experiment A3 paradigm using peripheral distractors is able to differentiate UFOV performance between individuals. Therefore, stimulus design from experiment A3 was adopted in Experiment B. However, to repeat Experiment A3 for various peripheral target eccentricities is impractical due to the enormous testing time which can induce fatigue in participants and confound the results. The typical solution is to adopt a typical psychophysical staircase testing procedure (Ehrenstein & Ehrenstein, 1999) to adaptively vary the target eccentricities for the estimation of UFOV size performance. The term *eccentricity size* which is the angular distance in degree from the central stimulus to the peripheral target will be used as the quantitation unit to describe UFOV performance throughout this dissertation. The larger the eccentricity size which participant can manage, the better is his/her UFOV performance. For a correct response to the presented stimulus, the staircase procedure increases the peripheral target eccentricity size for the next stimulus. For an incorrect response, the eccentricity size decreases for the next stimulus. During the sequence of response,

any change in responses from correct to incorrect or incorrect to correct for any two adjacent response are defined as reversals (See Figure 12). Typically, the average of 3, 6 or 9 reversal points defines the score for an individual.

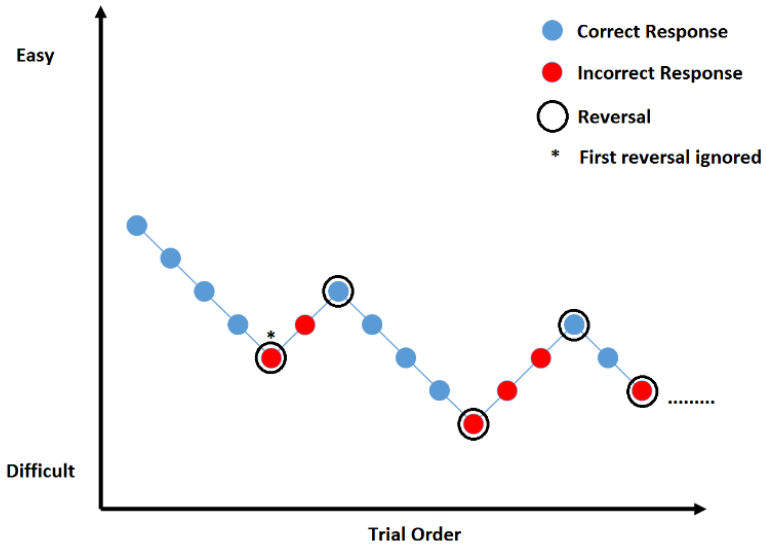

Figure 12: A typical psychophysical staircase procedure

To optimise the procedure for shorter testing time, the first stimulus will not start at the smallest eccentricity size, so as to avoid having individual to laboriously plough through most of the sizes to reach his/her best eccentricity size. Thus, the first stimulus starts at with 8° eccentricity size. This is the same size as that was used in Experiment A3. While this method helps to quickly measure the eccentricity size for UFOV performance, it has a drawback. The SSVEP and PO data are not homogenous across participants for this method. The number of signal recordings for each eccentricity size varied among individuals, as most average performers may not reach the biggest eccentricity size and excellent performers may not have a chance to see the smallest eccentricity size stimulus. Hence, simultaneous physiological signal recording during the task will not yield SSVEP and PO data that corresponds to those eccentricity sizes not exposed to the participant. The important point here is that

different eccentricity size means different sizes of checkered-pattern annulus ring and different distances of the peripheral targets from central fixation which may affect SSVEP and PO respectively. To solve this problem, a separate Experiment B2 was implemented to expose participants to all available sizes of the stimulus once, to gather a complete set of SSVEP and PO recordings from all eccentricity sizes. In short, Experiment B1 is designed mainly to assess the eccentricity size of the participant and Experiment B2 is designed to collect SSVEP and PO data from each eccentricity size. The data in B2 will be analysed for their ability to correlate UFOV size performance in B1, and subsequently will also be used to produce predictions of eccentricity sizes which will be benchmarked against those eccentricity results from B1's psychophysical UFOV estimation.

3.2 Methods

Fifty-three healthy male participants (ages 18–36) with vision correctable to 6/6 for both far and near in both eyes were recruited. Participants were divided into 4 groups based on their activeness in game (first person shooting game or RPG) and sports(ball or racket sports). Group 1 participants were those who have less than 6 hours of games and sports per week. Group 2 participants were those who have more than 6 hours of sports per week. Group 3 participants were those who have more than 6 hours of games per week. Group 4 participants were those who have more than 6 hours for both sports and games per week. There are 14, 11, 16 and 12 participants for Group 1 to 4 respectively. The experiments were conducted using the same instruments as in Experiment A. All participants underwent a screening task to ensure that they had healthy covert attention to peripheral visual field to begin with. The screening task comprises of only the activity phase of Experiment A2 trial stimulus

design for four eccentricity sizes of 6°, 8°, 10° and 12° without distractors. The minimum and maximum eccentricity of peripheral targets tested in this experiment is limited by the monitor display screen size to 6° and 12° respectively. In this screening task, eye tracker was used purely for the sake of ensuring participant's eyes are always on the central target, and therefore no recording was made. Each eccentricity size was trial 8 times, one time for each of the eight peripheral target position. Any participant who missed more than 1 peripheral target for any one of the eccentricities will be excluded from the rest of the experiment, which none of the participants committed fortunately. All participants underwent the following 2 experiments.

i) Experiment B1 – eccentricity size estimation using central-peripheral dual task with active distractors

The purpose of this experiment is to determine the differences in eccentricity sizes in different individuals as their UFOV performance indicator. Each trial in this experiment was the same as the one in Experiment A3 except that

a) instead of a fixed 20 trials of randomly assigned peripheral targets at a fixed eccentricity, a psychophysical staircase approach is adopted to manipulate the eccentricity of the peripheral targets between 6° to 12° in steps of 0.5°(A total of 13 eccentricity sizes).

b) a 3-second countdown break is implemented between the baseline phase and activity phase, to allow participant to blink to their satisfaction between the two phases (See Figure 13). This break measure is taking the heed from some of the participants in Experiment A who highlighted that holding blink continuously for more than 30 seconds was somewhat uncomfortable.

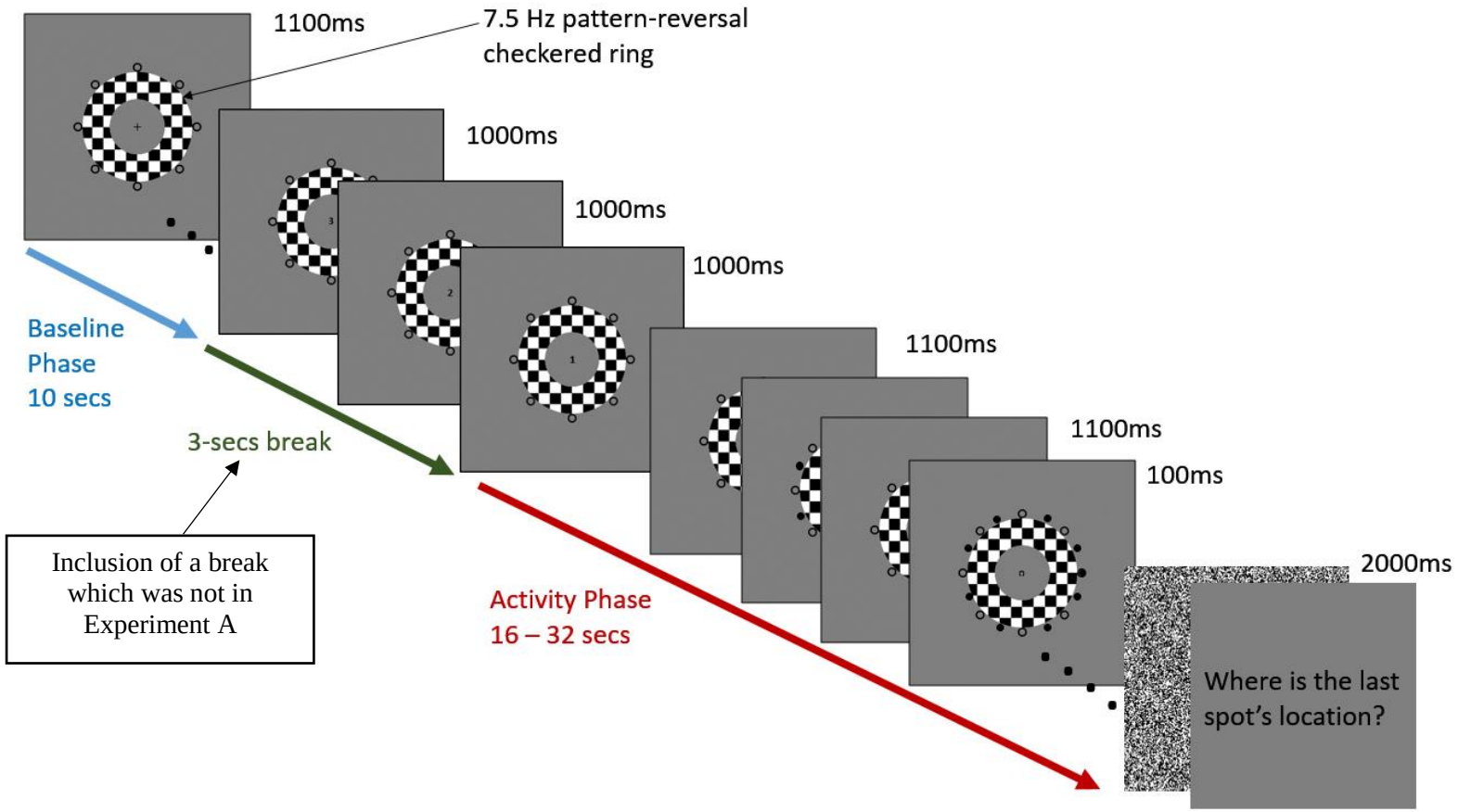

Figure 13: An example of a single Experiment B1. Note the insertion of the 3-second break along the green arrow.

c) the procedure has an improvement in computerised control to allow researcher to repeat any trial should the participant exhibits bad central fixation.

There are 3 sessions of trials in Experiment B1. For each session, the first trial always starts with 8° peripheral target eccentricity, and an incorrect response to the randomly assigned peripheral targets in this trial will reduce the eccentricity by 0.5° for the next trial. Likewise, a correct response will increase eccentricity by 0.5° for the next trial. The changes in eccentricity is limited to within 6° to 12° due to screen size. The same adaptive procedure goes for the subsequent trials. A reversal point is defined as either a correct response followed by an incorrect one or vice versa (See Figure 12 for illustrative explanation). The session ends when four reversals are committed, or when more than three consecutive incorrect responses are committed for the minimum 6° eccentricity (lower ceiling), or when more than three correct response was committed for the maximum 12° eccentricity (upper ceiling). The eccentricity size score here is the average eccentricity of all reversal points excluding the first one; hence only the eccentricity size from 3 reversal points was averaged. Note that as eccentricity of peripheral targets/distractor changes, the outer and inner ring diameter of the annulus ring will change by the same proportion (See Figure 14 for illustrative explanation). Table 1 describes the dimension of the stimulus's features in detail. Note that all the stimulus feature changes in the same proportion as eccentricity size changes. This is to address the issue of decrease sensitivity to stimulus size as eccentricity increases, due to reduced cone photoreceptors (Curio et al, 1990) and larger receptive fields towards the peripheral retina (Ransom-Hogg, & Spillmann, 1980), and the relationship between visual resolution and eccentricity is approximately linear

between 6° to 12° eccentricity (Chui et al, 2005). All participants went through the 3 sessions of trials in Experiment B1 and the average scores from these sessions is recorded as the UFOV performance for Experiment B1. The purpose of having 3 sessions is to gather averages from a total of 9 reversals (3 reversals in each session) while allowing participants to rest between sessions. Implementing a single session to capture 9 reversals will require longer testing session and participant will not be given the opportunity to rest. Fatigue may accumulate to a point where the quality of data collected may be affected.

ii) Experiment B2 – SSVEP and pupillary oscillation recording for each eccentricity size during central-peripheral dual task with active distractors

The stimulus setup is exactly the same as in B1 except that no psychophysical methods are used and every eccentricity's stimulus was shown once to the participant. The purpose of this task was to collect SSVEP and PO for stimulus starting with peripheral targets from 6° to 12° eccentricity in steps of 0.5°. Therefore, there are 13 trials in this experiment. Experiment B2 is designed for two purpose:

1) to take signals from each of the eccentricity size to complement the issue of B1 not able to gather a complete set of signals from all eccentricity sizes. The reason for doing so is to gather relevant stimulus sizes that would illicit the best signals for predicting UFOV and eliminate those which are not.
2) to counter check if physiological signals gathered not during the estimation of UFOV (hence, defined here as offline SSVEP and PO signals) can still be a valid predictor of UFOV sizes estimated on a different occasion.

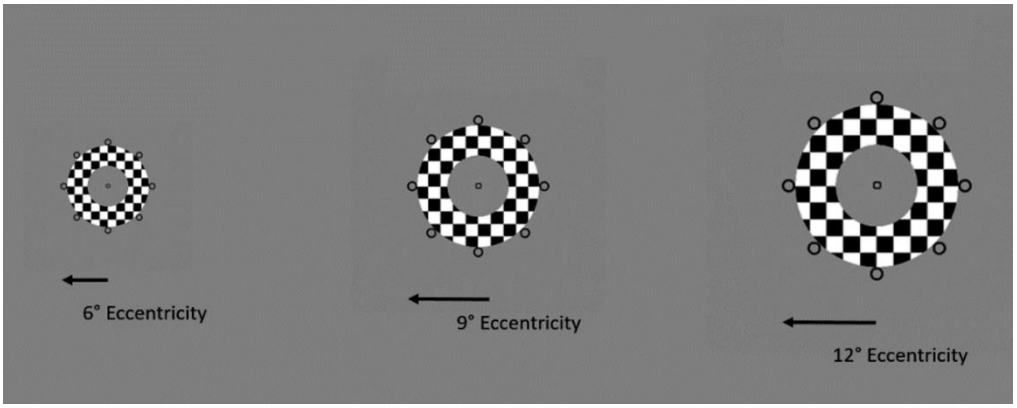

Figure 14: Typical illustration of peripheral target eccentricities and UFOV sizes.

Table 1: Dimension of each stimulus eccentricity size in degrees subtend to the eye.

Eccentricity Size	size of box-pattern of checkerboard	Peripheral circle size	Size of checkerboard inner radius	Size of checkerboard external radius
6.0°	1.23°	0.90°	2.8°	5.5°
6.5°	1.31°	0.98°	3.0°	6.0°
7.0°	1.39°	1.06°	3.3°	6.4°
7.5°	1.55°	1.15°	3.5°	6.9°
8.1°	1.64°	1.23°	3.8°	7.5°
8.5°	1.72°	1.31°	3.9°	7.9°
9.0°	1.80°	1.39°	4.2°	8.4°
9.5°	1.88°	1.47°	4.4°	8.8°
10.0°	2.05°	1.55°	4.7°	9.2°
10.5°	2.13°	1.55°	4.9°	9.7°
11.0°	2.21°	1.64°	5.1°	10.2°
11.5°	2.29°	1.72°	5.4°	10.7°
12.0°	2.45°	1.80°	5.6°	11.2°

3.3 Data Analysis

Given that Experiment A revealed a potential linear relationship between percentage accuracy performance on fixed eccentricity size and the physiological signals, some form of linearity relationship should continue to exist between eccentricity sizes and the physiological signals as well. This section examines the relationship between Experiment B1's UFOV sizes performance and the physiological signals collected

from Experiment B1 and B2. All Deming regression and Pearson correlation analyses were conducted using GraphPad Prism 7.0 (La Jolla, CA, USA) in this section. The outcome of the analysis will help to determine the approach towards building the model for predicting eccentricity sizes based on these signals. Normalised SSVEP and PO were calculated the same way as in Experiment A.

3.4 Results

Eccentricity sizes and physiological signals in Experiment B1

As explained in earlier sections, due to the nature of the psychophysical staircase to quickly estimate the eccentricity size for each participant, not all participants were engaged with stimulus from all 13 different eccentricity sizes. Participants who performed relatively well would never need to be given smaller eccentricity size stimuli. Vice versa for those who performed relatively worse than average would not have the opportunity to be shown big eccentricity size stimuli. Nevertheless, considering the findings in Experiment A3 that physiological signals can reflect performance in fixed eccentricity size (fixed checkered-pattern annulus ring stimulus) condition, one would expect signals averaged from various annulus ring stimulus sizes in Experiment B1 should still be able to provide some evidence that physiological signals do vary according to eccentricity sizes to a certain degree. Deming regression shown in Figure 15 confirmed such evidence from the data in Experiment B1.

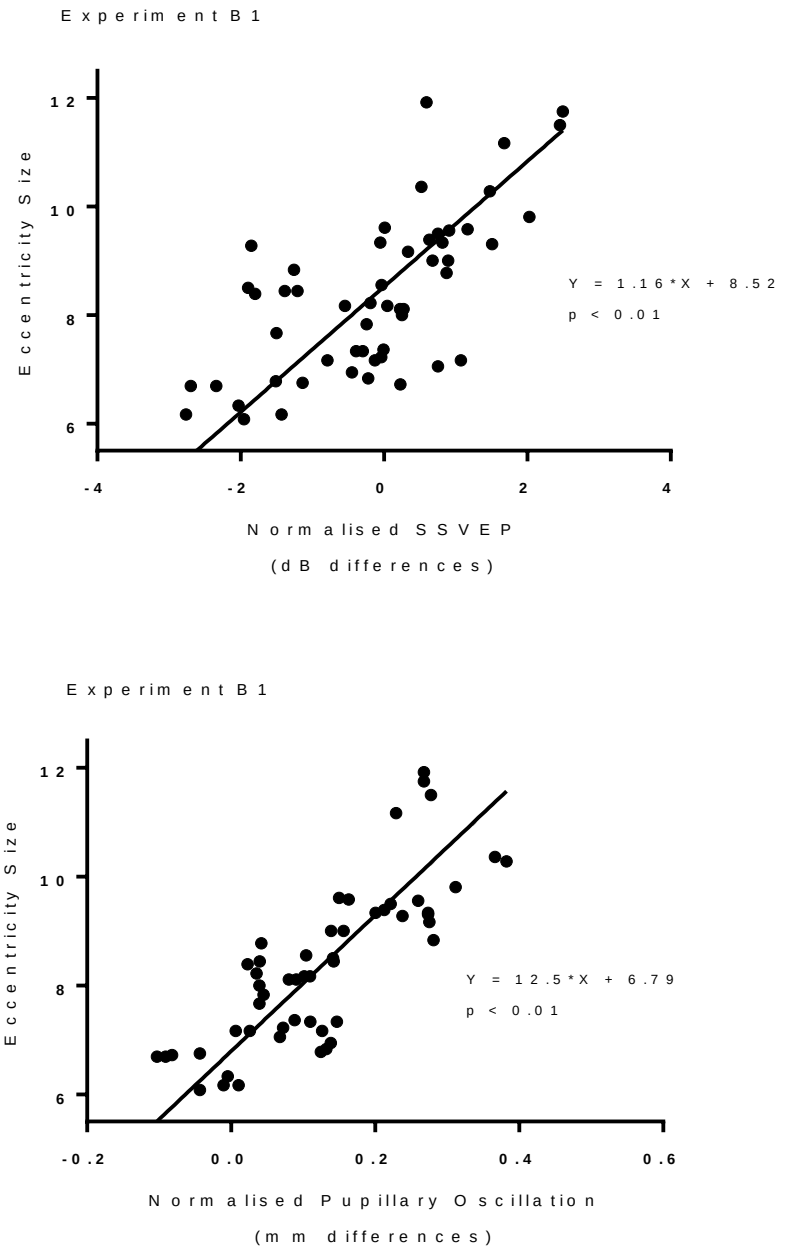

Figure 15: Relationship between physiological signals and eccentricity sizes.

Regression analysis showed a significant relationship between UFOV size and its nSSVEP ($F(1,51)=44.86$, $p < 0.01$), and their correlation coefficient, $r = 0.684$, indicates a moderate positive relationship. Noted that the correlations here was much weaker than the nSSVEP in Experiment A3 where $r = 0.854$. Results also revealed

strong relationship between eccentricity size and its nPO ($F(1,51)=91.73$, $p < 0.01$), and their correlation coefficient, r = 0.802. The correlation of nPO here was slightly weaker compared to the nPO in Experiment A3 where r = 0.878. Between Experiment A3 and B1, the differences in correlation is larger in the case of nSSVEP. Nevertheless, in Experiment B1, nPO seems to be the stronger predictor of UFOV performance over nSSVEP, and this agrees with the findings in Experiment A3.

Eccentricity sizes in Experiment B1 and physiological signals in Experiment B2

With evidence of relationship between physiological signals and UFOV sizes in Experiment B1, the analysis moved on to investigate the relationship between eccentricity sizes in B1 and physiological signals in B2.

Pearson correlation analysis revealed that correlation between signals and UFOV varies across sizes (See Table 2 and 3). In general, the correlations between nSSVEP and UFOV raised to a maximum at 9° UFOV size from the smallest size and drops gradually thereafter. The statistical significant changes accordingly as well. The trend is even more prominent in the case of nPO where the correlation coefficients are generally larger than those corresponding ones in nSSVEP, and peaks at the 10° eccentricity size. This concurs with the earlier observation that nPO is the stronger predictor of UFOV compared to nSSVEP.

Table 2: Correlation between eccentricity size and nSSVEP across various eccentricities

Peripheral Target Eccentricity	6.0	6.5	7.0	7.5	8.0	8.5	9.0	9.5	10.0	10.5	11.0	11.5	12.0
Pearson Correlation, r	0.27	0.24	0.44	0.02	0.60	0.54	0.64	0.32	0.49	0.27	0.12	0.27	0.21
p-Value	0.05	0.09	<0.01	0.91	<0.01	<0.01	<0.01	0.02	<0.01	0.05	0.38	0.05	0.14

Table 3: Correlation between eccentricity size and nPO across various eccentricities

Peripheral Target Eccentricity	6.0	6.5	7.0	7.5	8.0	8.5	9.0	9.5	10.0	10.5	11.0	11.5	12.0
Pearson Correlation, r	0.51	0.48	0.52	0.76	0.67	0.60	0.68	0.62	0.71	0.54	0.38	0.47	0.59
p-Value	<0.01	<0.01	<0.01	<0.01	<0.01	<0.01	<0.01	<0.01	<0.01	<0.01	0.01	<0.01	<0.01

Performance differences between gamer, sports-active and inactive participants

One-way ANOVA indicated no significant difference between the groups in nSSVEP ($F(3,49) = 0.7283$, $p = 0.540$), nPO ($F(3,49) = 0.9112$, $p = 0.442$) and UFOV eccentricity size ($F(3,49) = 0.482$, $p = 0.6963$). Figure 16 shown the averages in each group for nSSVEP, nPO and UFOV eccentricity size performance. Although there is no statistically significance, there is a trend of lower physiological signals and eccentricity sizes for Group 1 compared to the other groups. Surprisingly, those who spend more than 6 hours in both games and sports (Group 4) do not seem to show trends of be better than Group 2 and 3. The insignificant differences are likely due to small sample size in each group and the 6-hour criteria may not necessary reflects the capability level in games and sports.

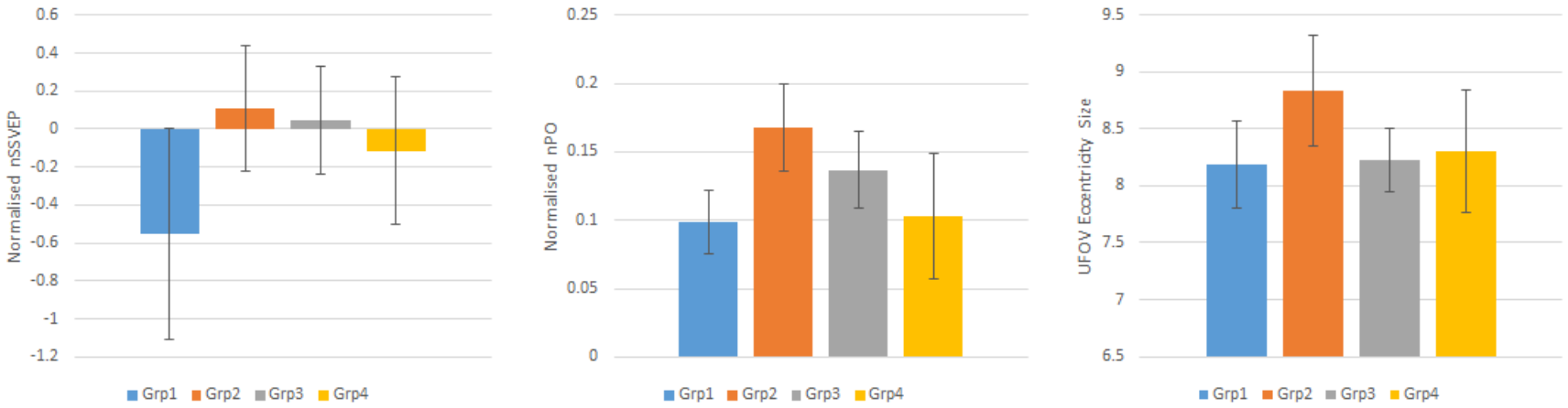

Grp 1:	Non-active
Grp 2:	> 6 hours of sports/wk
Grp 3:	> 6 hours of games/wk
Grp 4:	> 6 hours of games and sports/wk

Figure 16: Averages across groups for nSSVEP, nPO and UFOV eccentricity size performance

3.5 Chapter Conclusion

The findings provide the valuable first-cut information that UFOV can be predicted using physiological signals gathered from eccentricity sizes that are largely between 7° to 10.5° UFOV. While statistical analysis provides evidence of relationship, it does not deal with the unknown non-linearity aspect of the data to accurately predict the eccentricity size value from nSSVEP and nPO. As such, modelling is required to apply the knowledge into application. In the next Chapter, neural network modelling is implemented to deal with the unknown non-linearity part of the physiological data to provide a more accurate prediction of UFOV.

Chapter 4: Predictive Model for UFOV

The collected data from Experiment B2 will be used to train and develop a neural network model that takes in nSSVEP and nPO as input vectors to predict and estimate the eccentricity size (i.e. output vector). Given the good linear correlation results, the non-linearity component of the data is likely to be small and can be easily dealt with modelling techniques. The strength in correlation also provides strong indications for the selection of the appropriate physiological signals stimulated by the optimal annulus stimulus ring size and peripheral target position (determined by eccentricity sizes) for developing the predictive model. Essentially, good modelling results can be achieved by isolating the weakly-related or non-related signals from those stronger ones. The following sections describes how neural network models were trained to achieve predictions of UFOV eccentricity sizes using the physiological markers.

4.1 Neural network model approach

While this section does not provide a holistic understanding of neural networks, it highlights the important features of a typical feedforward neural network modelling (Bebis &Georgiopoulos, 1994), sufficient enough to explain for the work done in this research. Neural networks (also known as Artificial Neural Network) is first defined in the late 80s in “Neural Network Primer: Part I” (Caudill, 1987) as:

> *"...a computing system made up of a number of simple, highly interconnected processing elements, which process information by their dynamic state response to external inputs.”*

The idea of neural network was motivated by neurons in the biological brain. The fundamental processing elements in the statement above is know as neurons (Gurney, 1997; Haykin, 2009). These neurons are associated with transfer functions, allowing them to process and pass on information to the next node. Figure 17 below illustrated the typical 1-hidden layer feedforward network structure. The key components of the neural network to transform data lies in the weights and transfer functions. For example in Figure 17, there are 100 sets of inputs 1 to 3. The first set is first multiplied by the weights when fed into the hidden layer. Bias inputs are thresholds implemented to improves the efficiency of the network. The weighted set of inputs and bias are then summated at the node and the outcome underwent a transformation by the transfer function before passing on to the next layer which essentially does the same thing before finally end up as the output. This output value is compared against a known target value for differences.

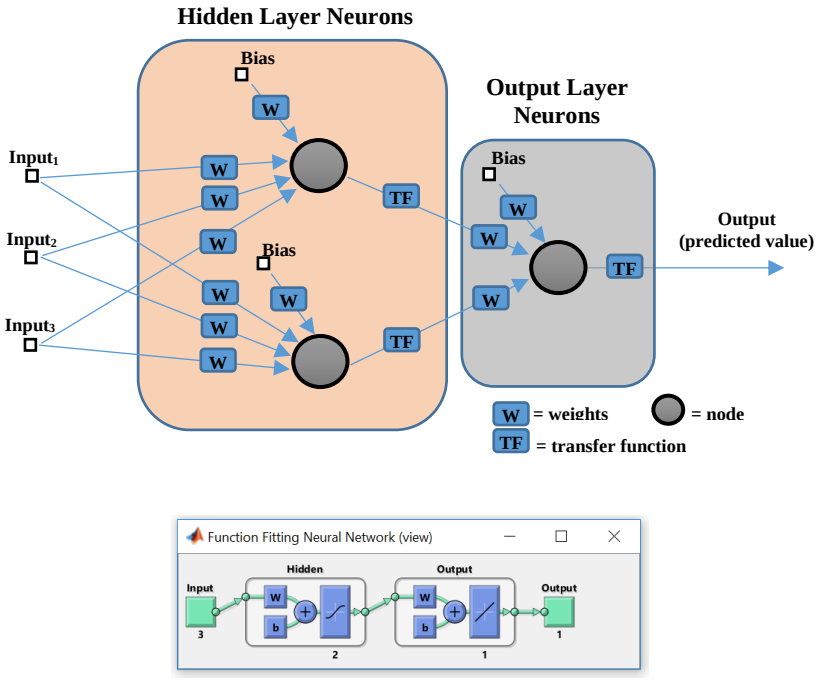

Figure 17: Examples of feedforward neural networks: a single-hidden layer neural network with a 3-2-1 configuration. The diagram below is an equivalent representation from MATLAB Neural Network Toolbox.

Every set of inputs went through the same process and end up with 100 set of differences. These 100 sets of differences determine how the weights are being adjusted before the same sets of inputs are fed into neural network again. The adjustment of weights is known as learning. In the case where there is a known target value for comparison and learning, the learning process is also known as supervised learning. A typical training function for learning, which will be used in the work here, is the Levenberg-Marquardt backpropagation training function (Yu, & Wilamowski, 2011). The learning process will continue until the training goal was reached or when the maximum training iterations was reached. Training goal here refers to the minimum differences between predicted value and known target value. To check the model's predictive performance, a set of input data with known target values which are not used for training is fed into the network, and the predicted values are benchmarked against the corresponding known target values. The mean of the differences between the two values across the set defines the performance of the trained network model, usually in the form of Mean Squared Error (MSE). Neural network can also be designed for more than 1 hidden layer. Figure 18 illustrated a typical example of a 2-hidden layer feedforward neural network and the information processing in each layer is identical to the one described in the 1-hidden layer structure. Feedforward network structures with more than 1-hidden layer is also known as multilayer feedforward networks.

Due to the potentially low non-linearity of data in this research, a simple 1-hidden or 2-hidden layer feedforward network should be sufficient. There are altogether 26 input vectors in this study, first 13 vectors correspond to nSSVEP signal readings from 6° to 12° peripheral target eccentricities, the next 13 vectors correspond to nPO signal readings from size 6 to 12° peripheral target eccentricities. The different

eccentricities indicates different checkboard annulus size The input vectors are detailed in Table 4.

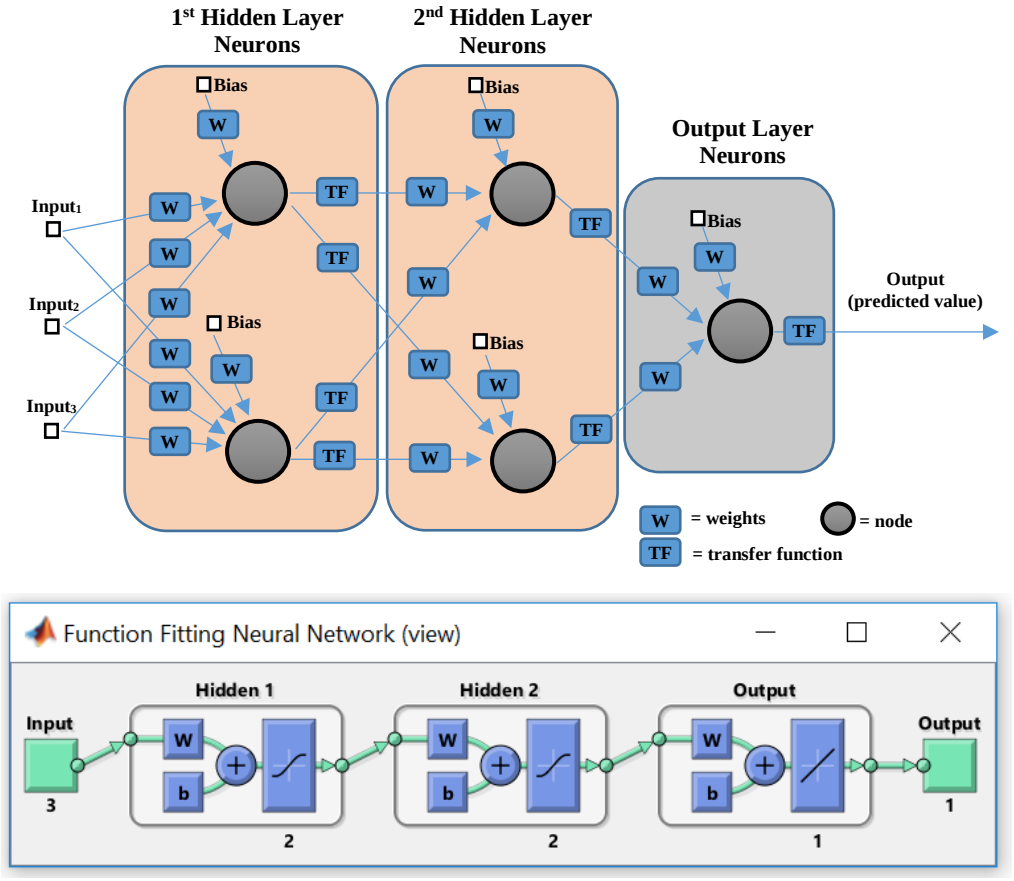

Figure 18: Examples of feedforward neural networks: a single-hidden layer neural network with a 3-2-2-1 configuration. The diagram below is an equivalent representation from MATLAB Neural Network Toolbox.

Table 4: Input vectors for neural network training

Input vector No:	1	2	3	4	5	6	7	8	9	10	11	12	13
Eccentricity size where nSSVEP signals are collected	6.0	6.5	7.0	7.5	8.0	8.5	9.0	9.5	10.0	10.5	11.0	11.5	12.0
Input vector No:	14	15	16	17	18	19	20	21	22	23	24	25	26
Eccentricity size where nPO signals are collected	6.0	6.5	7.0	7.5	8.0	8.5	9.0	9.5	10.0	10.5	11.0	11.5	12.0

Multiple top-performing input vectors that are highly correlated with eccentricity size performance always produce better predictive model then a single best-performing

input vector. The question is here: **What is the least number of top-performing input vectors that will produce the best network model to predict UFOV?** The motivation for making such a predictive model stems from the fact that input vectors are essentially physiology signals that requires time and effort to collect. Reducing the number of vector data to be collected means reducing testing time. On the hind side, reduction in vectors must also be accompanied by either an improvement or negligible reduction in predictive performance. In another words, the removal of vectors must be of those which do not contribute or has little influence to the predictive performance. From these considerations, the process of model development here involves the following 3 steps:

1) Initial modelling with all input vectors.

   This is to ascertain that the group of input vectors are generally capable of predicting UFOV to a certain degree.

2) Elimination of vectors with no statistical significance

   The assumption here is that vectors produces no correlation significant with eccentricity sizes (See Chapter 3, Section 4) will reduce the predictive performance of the model. Hence, by eliminating these non-predictive vectors, the model could potentially perform better.

3) Step-wise elimination of least predictive vector

   When step 2 is successful, this part of the work eliminates the least predictive vector and then evaluated for its performance before eliminating the next least predictive vector. This process continues until only one vector is left for the final evaluation.

4.2 Initial modelling with all input vectors

All the modelling work from this section onwards uses the commercially available standard Neural Network Toolbox that is well implemented in MATLAB. All 26 vectors were used as input vectors where each vector is a column of 53 rows of physiological signal data from the 53 participants in Experiment B2. Hence, the input matrix is a collection of vectors in the form of 53 rows X 26 columns. The data structure for modelling consists of the input matrix concatenated with a single label vector column of 53 rows. This label vector (27^{th} Vector) is the corresponding eccentricity sizes in Experiment B1 for each participant's row of physiological signal, and is defined as the target value which training and validation seek to get as close as possible to. Therefore, the data structure is a 53 row X 27 columns matrix altogether. In this development of neural network model, supervised training methods were implemented with the labelled data in the 27^{th} column vector. The parameters of the training were set according to Table 5.

Table 5: Neural network settings

Parameter	Type	Settings	Remarks
Neural Network Model	Function fitting (Feedforward networks)	26-N_1-1 (1-hidden layer) and 26-N_1-N_2-1 (2-hidden layer)	
Training function	Levenberg-Marquardt backpropagation	-	
Input Layer	Number of input vectors	26	
Hidden Layer 1 (N_1)	Number of neurons	1 to 20	Hyperbolic tangent sigmoid transfer function (tansig)
Hidden Layer 2 (N_2)	Number of neurons	1 to 5 only for 26-N_1-N_2-1	Hyperbolic tangent sigmoid transfer function (tansig)
Output Layer	Number of output vectors	1	Linear transfer function (purelin)
Epoch	Maximum number of epochs to train	10000	
Learning rate	Step size to update weights and bias to the neurons	0.01	
Iterations	Number of repeats for each network model	10	
Goal	Training goal	0	

All the parameters are implemented in a set of MATLAB codes (See Appendix A) which was executed in a computer. Upon the execution of the codes, neural network model was trained using Levenberg-Marquardt backpropagation training function (Yu, & Wilamowski, 2011) on feedforward neural networks (Bebis &Georgiopoulos, 1994). As per any typical development of model, the data collected is always divided into training sets and testing sets. The testing sets are data not involved in training of the model and used to validate if the predictive model works for data that does not influence the training. It is analogous to a policeman training a guard dog with images of several types of gun, for the dog to recognise guns as threats. Following this, the dog was shown a gun it never seen before and see if the dog can still recognise it is as a threat. To implement such a validation method, a k-fold cross-validation approach (Kohavi,1995) is adopted to avoid bias interpretation of the training results while involving all data for training. For the k-fold cross-validation to work, the 53 participants' data were divided into 11 groups (where k = 11) with 5 data in each group and the last group is a wrap-around form consisted of 51^{st}, 52^{nd}, 53^{rd}, 1^{st} and 2^{nd} data. The first group was isolated from the dataset as the testing set and the rest of the groups were used for training the model. The trained model was then feed with the testing data set and the predicted values produced was compared to the corresponding target values. The performance of a model was determined by how close these predicted values were to the target values, and, as mentioned earlier, was mathematically defined as the mean square error (average squared of the differences) between the predicted values and the target values. The process was repeated again with the second group of data as the testing set and so on until all groups has been trial once as the testing set, and this was defined as one iteration of training completed. The average of all MSEs in an iteration was computed as the estimated performance of the model as if it was trained with all data. As training results will

defer slightly when repeated, 10 iterations of training and validation was introduced here for an overall average over the already k-fold averaged MSE to ensure a better estimation of performance. This 10-iteration 11-fold cross-validation was implemented for the permutations of 1 to 30 neurons in a single hidden layer neural network (26-N_1-1), as well as for permutations of first-hidden layer size (1 – 30 neurons) X second-hidden layer size (1 – 5 neurons) for a 2-hidden layer setting (26-N_1-N_2-1). Figure 19 illustrated the examples of the diagram of the model design for single-hidden layer and 2-hidden layer design respectively. Note that hidden layers are implemented with the hyperbolic tangent sigmoid transfer function while the output layer has linear transfer functions.

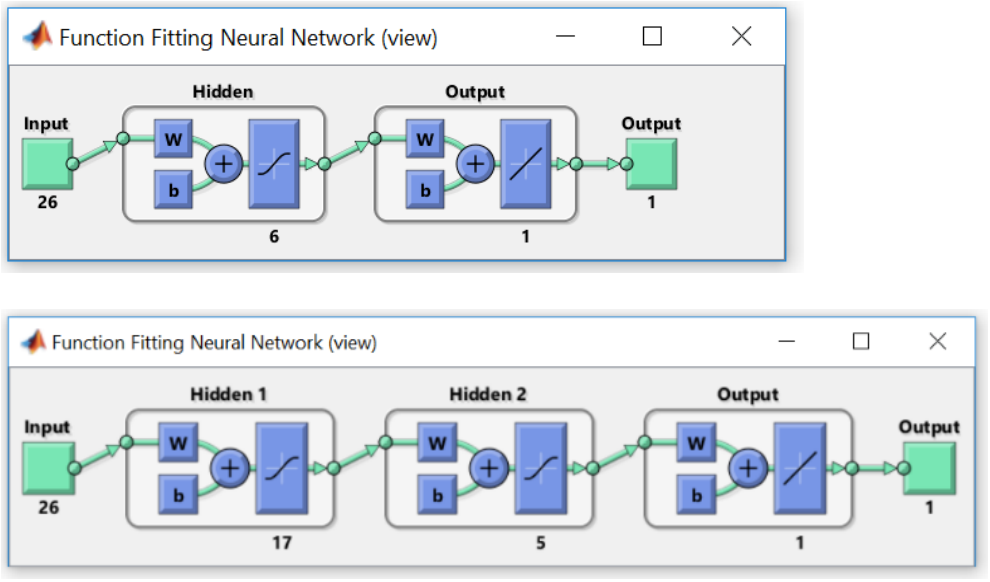

Figure 19: Examples of feedforward neural networks: a single-hidden layer neural network with a 26-6-1 configuration(top) and a 2-hidden layer network with a 26-17-5-1 configuration (bottom)

The results of the cross-validation are shown in Figure 20. Lower MSE means better prediction performance. Note that one can estimate the accuracy of the prediction by looking at the square root of the MSE. For example, the first chart (most left side) in Figure 20 has an average MSE of 0.57562 with 5 hidden neurons. Hence, the average prediction accuracy is estimated to be $\pm\sqrt{0.57562} = \pm 0.7587°$ from the eccentricity size target value. For a more conservative estimation using upper limit of 95% CI as the accuracy index, one can read off the top of the black error bar in Figure 20 as the possible "worst case" prediction accuracy. Nevertheless, MSE has been the standard performance indicator in the literature, thus will be used throughout this dissertation.

Several observations can be seen from this training and validation session. Firstly, for a l-hidden layer model, the performance network model improves gradually from 1 to 5 hidden neurons before it starts to worsen, leaving the best performing network as 26-5-1. Secondly, by introducing the 2-hidden layer models, the best performance of the model improves with the introduction of 1 and 2 neurons in the second-hidden layer, but for subsequent addition of neurons, performance started to degrade. The best performing 2-hidden layer model is 26-24-3-1, where 24 neurons in the first layer produces the best results. Overall, the 2-hidden layer network model also seems to perform better than a 1-hidden layer one.

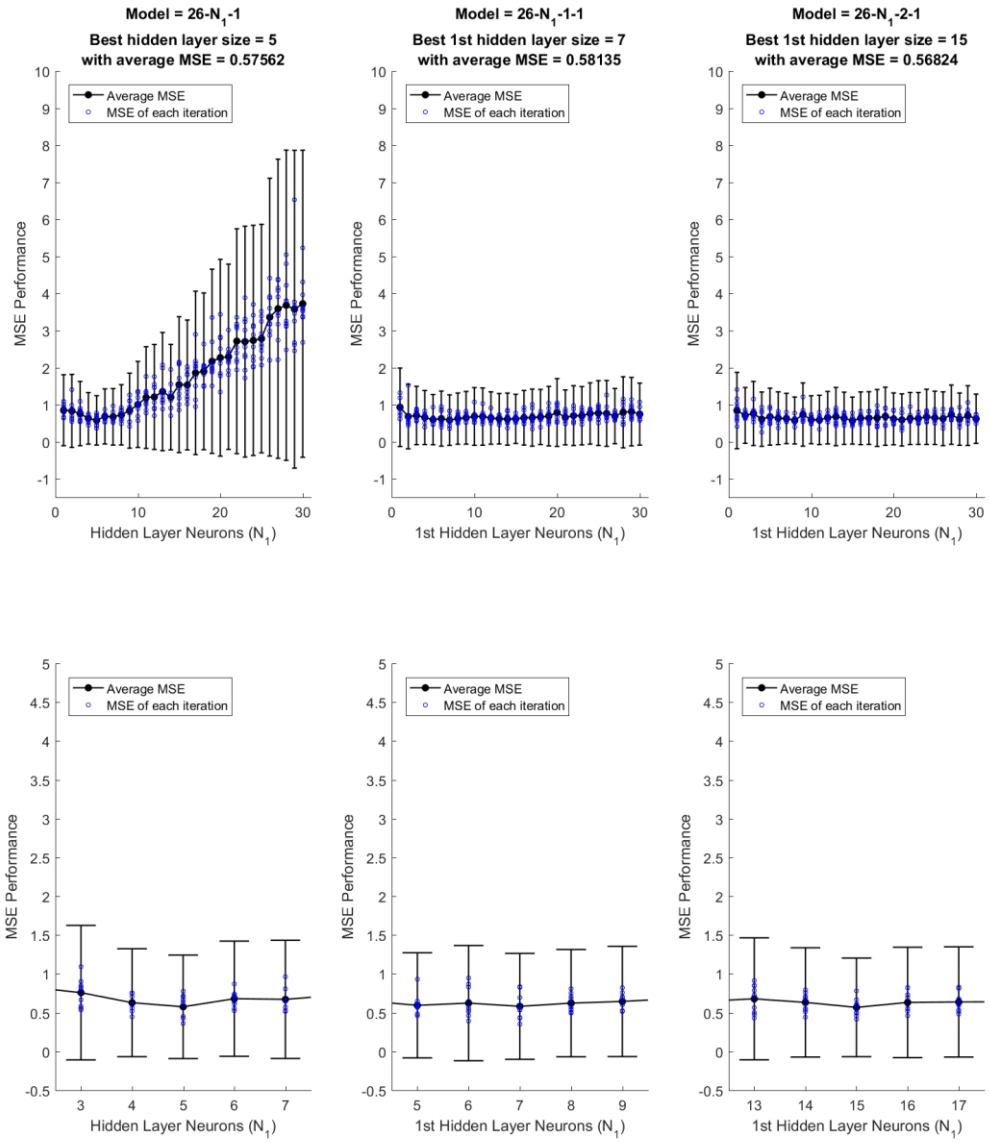

Figure 20: Average MSE performance across all neural network configurations with all 26 input vectors. Error bar indicates 95% CI. Top row of graphs displays all hidden layer neurons, bottom row of graphs zoomed in to the best hidden layer neurons.

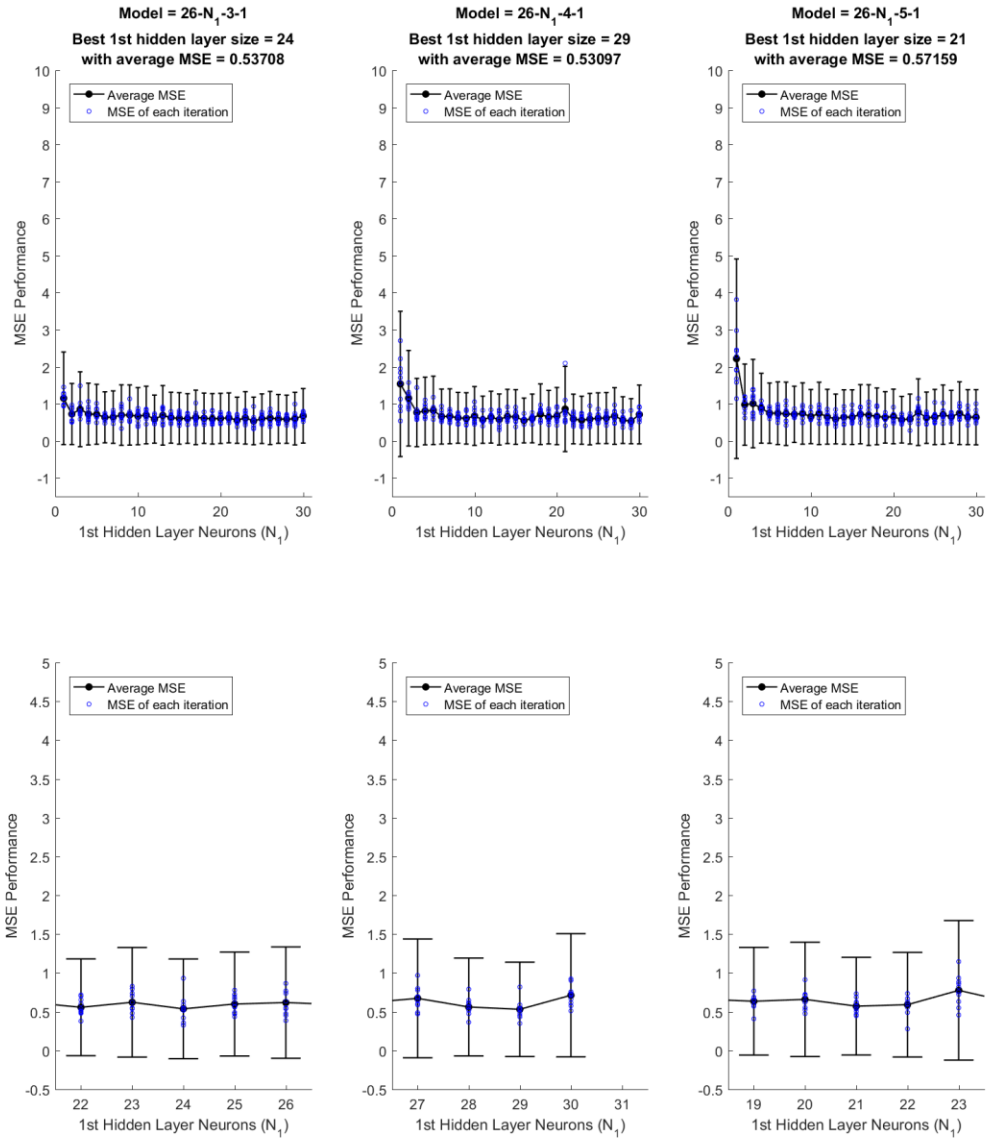

Figure 20(Continue): Average MSE performance across all neural network configurations with all 26 input vectors. Error bar indicates 95% CI. Top row of graphs displays all hidden layer neurons, bottom row of graphs zoomed in to the best hidden layer neurons.

4.3 Elimination of vectors with no statistical significance

The cross-validation process described in the previous subsection was repeated in this stage with only the 19 statistically significant input vectors. Table 6 describes the distribution of statistically significant vectors.

Table 6: Statistically significant input vectors for neural network training (highlighted cell indicates statistical significant value)

Input vector No:	1	2	3	4	5	6	7	8	9	10	11	12	13
Peripheral target eccentricity where nSSVEP signals are collected	6.0	6.5	7.0	7.5	8.0	8.5	9.0	9.5	10.0	10.5	11.0	11.5	12.0
Pearson Correlation, r	0.27	0.24	0.44	0.02	0.60	0.54	0.64	0.32	0.49	0.27	0.12	0.27	0.21
Input vector No:	14	15	16	17	18	19	20	21	22	23	24	25	26
Peripheral target eccentricity where nPO signals are collected	6.0	6.5	7.0	7.5	8.0	8.5	9.0	9.5	10.0	10.5	11.0	11.5	12.0
Pearson Correlation, r	0.51	0.48	0.52	0.76	0.67	0.60	0.68	0.62	0.71	0.54	0.38	0.47	0.59

The results of the cross-validation are shown in Figure 21. With the exclusion of statistically insignificant vectors, the performance of the model generally improves across all configurations of hidden neuron layers dropping below 0.5 MSE. It was also noted that the variation between iterations of model training was also reduced slightly based on the error bars. Hence, the effect of eliminating unnecessary vectors has shown to work towards better performance.

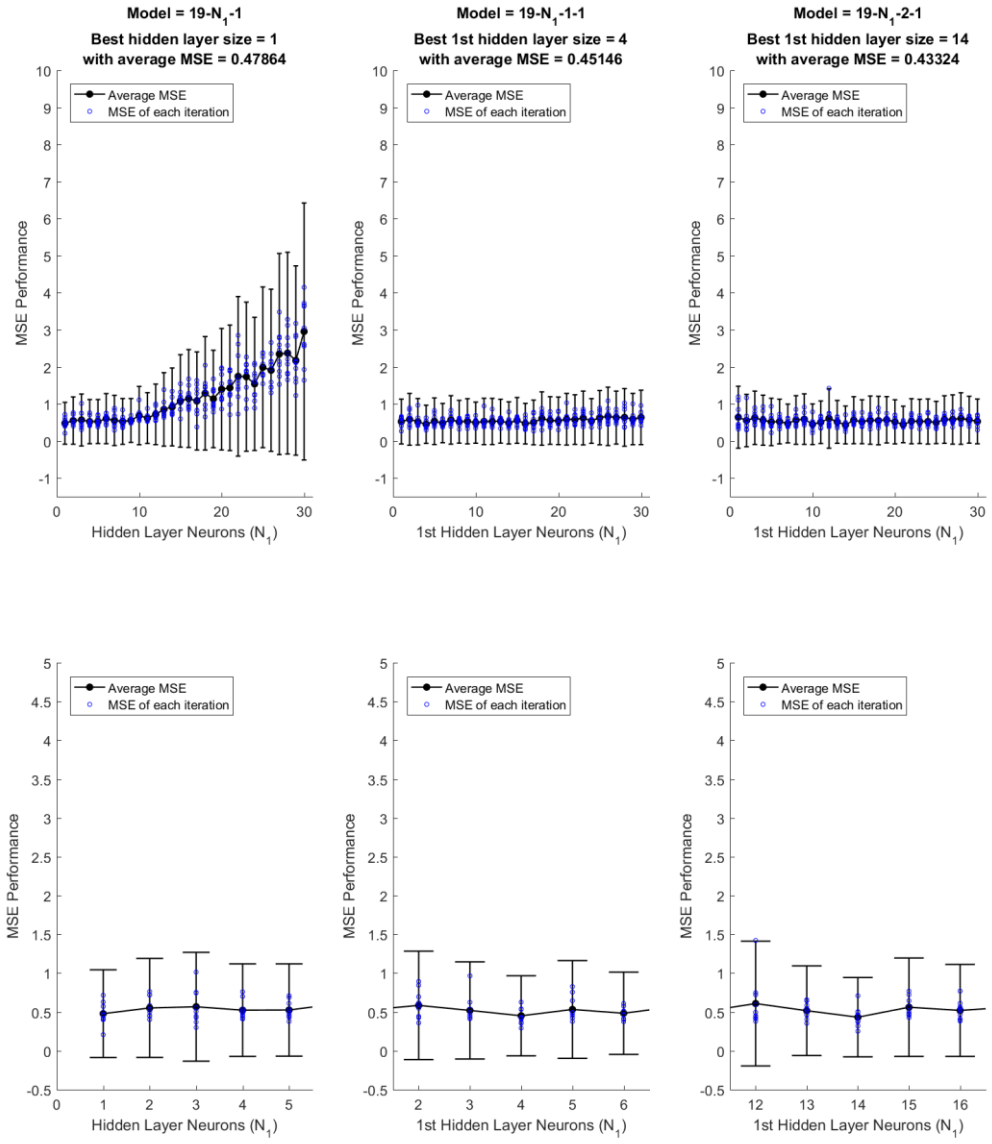

Figure 21: Average MSE performance across all neural network configurations with 19 significant input vectors. Error bar indicates 95% CI. Top row of graphs displays all hidden layer neurons, bottom row of graphs zoomed in to the best hidden layer neurons.

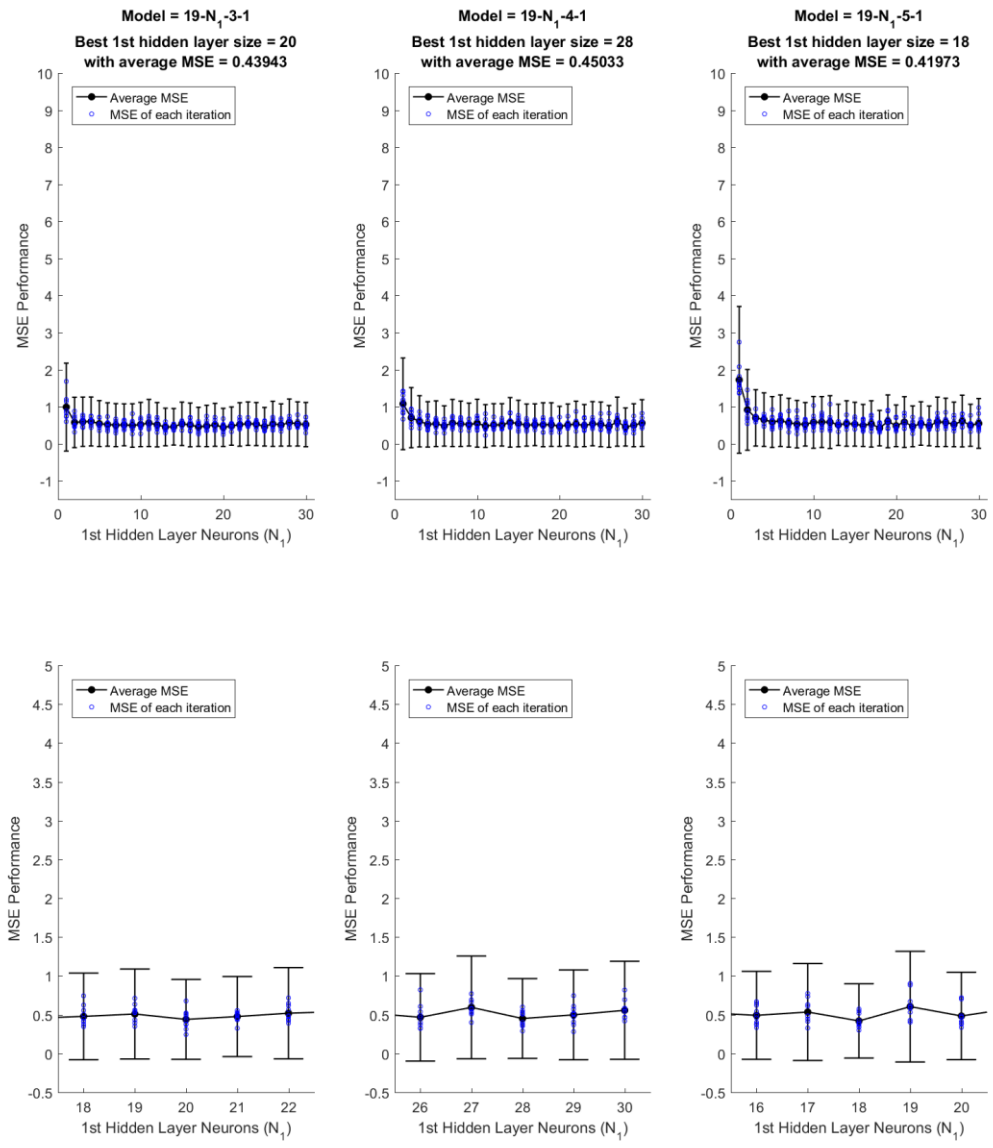

Figure 21(Continue): Average MSE performance across all neural network configurations with 19 significant input vectors. Error bar indicates 95% CI. Top row of graphs displays all hidden layer neurons, bottom row of graphs zoomed in to the best hidden layer neurons.

4.4 Step-wise elimination of least predictive vector

With the evidence that exclusion of non-predictive vectors improves prediction performance, the aim of the subsequent training sessions is to find out what are the least number of critical vectors to produce the model with the best predictive performance. To accomplish that, the cross-validation process was repeated again in a step-wise fashion with the least predictive input vector in each step removed. Predictive power is determined by the input vector's correlation coefficient, r, values in Table 6. Table 7 illustrated the survival trend of the input vectors into each repeats of cross-validation sessions here. The settings used for the cross validation is exactly the same as the previous subsection except for the reduction in input vectors.

Table 7: Survival trend of the input vectors into each repeats of cross-validation session

Training/ Cross validation Sessions	nSSVEP Vectors													nPO Vectors											
	1	2	3	4	5	6	7	8	9	10	11	12	13	14	15	16	17	18	19	20	21	22	23	24	25	26
0	■	■	■	■	■	■	■	■	■	■	■	■	■	■	■	■	■	■	■	■	■	■	■	■	■	■
1			■		■	■	■	■	■					■	■	■	■	■	■	■	■	■	■	■	■	■
2			■		■	■	■		■					■	■	■	■	■	■	■	■	■	■	■	■	■
3			■		■	■	■		■					■	■	■	■	■	■	■	■	■	■		■	■
4					■	■	■		■					■	■	■	■	■	■	■	■	■	■		■	■
5					■	■	■		■					■	■	■	■	■	■	■	■	■	■			■
6					■	■	■		■					■		■	■	■	■	■	■	■	■			■
7					■	■	■							■		■	■	■	■	■	■	■	■			■
8					■	■	■									■	■	■	■	■	■	■	■			■
9					■	■	■										■	■	■	■	■	■	■			■
10					■		■										■	■	■	■	■	■	■			■
11					■		■										■	■	■	■	■	■				■
12					■		■										■	■	■	■	■	■				
13							■										■	■	■	■	■	■				
14							■										■	■		■	■	■				
15							■										■	■		■		■				
16																	■	■		■		■				
17																	■			■		■				
18																	■					■				
19																										

Note that session 0 refers to the cross-validation session for Figure 20 with the full 26 input vectors and session 1 refers to the cross-validation session for Figure 21 with the 19 significant input vectors

The results of the average MSE performance across step-wise elimination cross-validation are shown in Table 8, Figure 24 and Figure 25 (All the detailed results can be found in Appendix B). The results suggested that the model with the network 7-1-2-1 seems to provide the best predictive performance (MSE = 0.0775, Accuracy ≈ ± 0.278°) in Train Session 13 with only 7 input vectors 7, 17,18,19,20,21 and 22 (7.5° to 10° eccentricity size). For a more conservative estimation using the 95% CI, the worse possible accuracy is approximately ± 0.429° (MSE = 0.184). The MSE results in Table 8 is represented in Figure 22 and Figure 23. There are a few observations that can be drawn from the results. Firstly, there is an inverted 'U' relationship between the number of top-performing vectors and MSE performance (See Figure 22), where MSE started to improve with each round of least predictive vector eliminated, but the improvements started to reverse after Session 13 with top 7 predictive vectors, and this happens for 1-hidden layer model and all five 2-hidden layer models. Secondly, the same trend was also observed for the variation between iterations (See Appendix B, compare error bars between Session 1, Session 13 and Session 19). Thirdly, MSE also improves with the introduction of 1 and 2 neurons in the 2nd hidden layer, but degrades for 3 to 5 neurons in that layer (See Table 8).

4.5 Chapter Conclusion

In this section, it is shown that feedforward neural network modelling has a moderate accuracy in determining UFOV performance, in terms of eccentricity sizes, based on SSVEP and Pupillary Oscillation gathered during a demanding central-peripheral attention task. A large part of the success is due to the low non-linearity in the relationship between input vectors and UFOV.

Table 8: Best network configuration for each network structure. (First value in each row indicates the average MSE)

Sessions	1-Hidden Layer input-N_b-1	2-Hidden Layers input-N_b-1-1	2-Hidden Layers input-N_b-2-1	2-Hidden Layers input-N_b-3-1	2-Hidden Layers input-N_b-4-1	2-Hidden Layers input-N_b-5-1
0	0.576, 26-5-1	0.581, 26-7-1-1	0.568, 26-15-2-1	0.537, 26-24-3-1	0.531, 26-29-4-1	0.572, 26-21-5-1
1	0.479, 19-1-1	0.451, 19-4-1-1	0.433, 19-14-2-1	0.439, 19-20-3-1	0.450, 19-28-4-1	0.420, 19-18-5-1
2	0.469, 18-1-1	0.465, 18-5-1-1	0.425, 18-8-2-1	0.457, 18-16-3-1	0.441, 18-14-4-1	0.473, 18-24-5-1
3	0.476, 17-4-1	0.469, 17-1-1-1	0.438, 17-12-2-1	0.463, 17-10-3-1	0.447, 17-20-4-1	0.468, 17-7-5-1
4	0.390, 16-1-1	0.455, 16-1-1-1	0.443, 16-22-2-1	0.426, 16-17-3-1	0.443, 16-17-4-1	0.428, 16-9-5-1
5	0.411, 15-1-1	0.357, 15-1-1-1	0.346, 15-1-2-1	0.443, 15-7-3-1	0.418, 15-18-4-1	0.447, 15-20-5-1
6	0.346, 14-2-1	0.353, 14-1-1-1	0.259, 14-1-2-1	0.449, 14-23-3-1	0.417, 14-17-4-1	0.453, 14-13-5-1
7	0.333, 13-1-1	0.222, 13-1-1-1	0.228, 13-1-2-1	0.402, 13-9-3-1	0.450, 13-2-4-1	0.464, 13-6-5-1
8	0.277, 12-1-1	0.269, 12-1-1-1	0.215, 12-1-2-1	0.395, 12-2-3-1	0.465, 12-16-4-1	0.469, 12-12-5-1
9	0.271, 11-1-1	0.312, 11-1-1-1	0.231, 11-1-2-1	0.369, 11-1-3-1	0.417, 11-3-4-1	0.469, 11-11-5-1
10	0.192, 10-1-1	0.243, 10-1-1-1	0.155, 10-1-2-1	0.313, 10-2-3-1	0.281, 10-2-4-1	0.423, 10-13-5-1
11	0.181, 9-1-1	0.187, 9-1-1-1	0.165, 9-1-2-1	0.224, 9-1-3-1	0.284, 9-2-4-1	0.339, 9-5-5-1
12	0.168, 8-1-1	0.171, 8-1-1-1	0.148, 8-1-2-1	0.166, 8-1-3-1	0.296, 8-2-4-1	0.328, 8-3-5-1
13	0.170, 7-2-1	0.197, 7-1-1-1	0.077, 7-1-2-1	0.109, 7-1-3-1	0.216, 7-2-4-1	0.265, 7-2-5-1
14	0.304, 6-1-1	0.315, 6-1-1-1	0.362, 6-2-2-1	0.434, 6-2-3-1	0.495, 6-2-4-1	0.510, 6-5-5-1
15	0.279, 5-1-1	0.265, 5-1-1-1	0.319, 5-1-2-1	0.371, 5-3-3-1	0.489, 5-7-4-1	0.435, 5-2-5-1
16	0.312, 4-1-1	0.297, 4-1-1-1	0.344, 4-1-2-1	0.320, 4-1-3-1	0.372, 4-2-4-1	0.345, 4-2-5-1
17	0.573, 3-1-1	0.587, 3-1-1-1	0.680, 3-3-2-1	0.683, 3-2-3-1	0.711, 3-2-4-1	0.711, 3-2-5-1
18	0.724, 2-1-1	0.679, 2-1-1-1	0.738, 2-1-2-1	0.769, 2-2-3-1	0.784, 2-1-4-1	0.832, 2-2-5-1
19	1.041, 1-1-1	1.049, 1-1-1-1	1.119, 1-1-2-1	1.125, 1-1-3-1	1.107, 1-1-4-1	1.191, 1-3-5-1

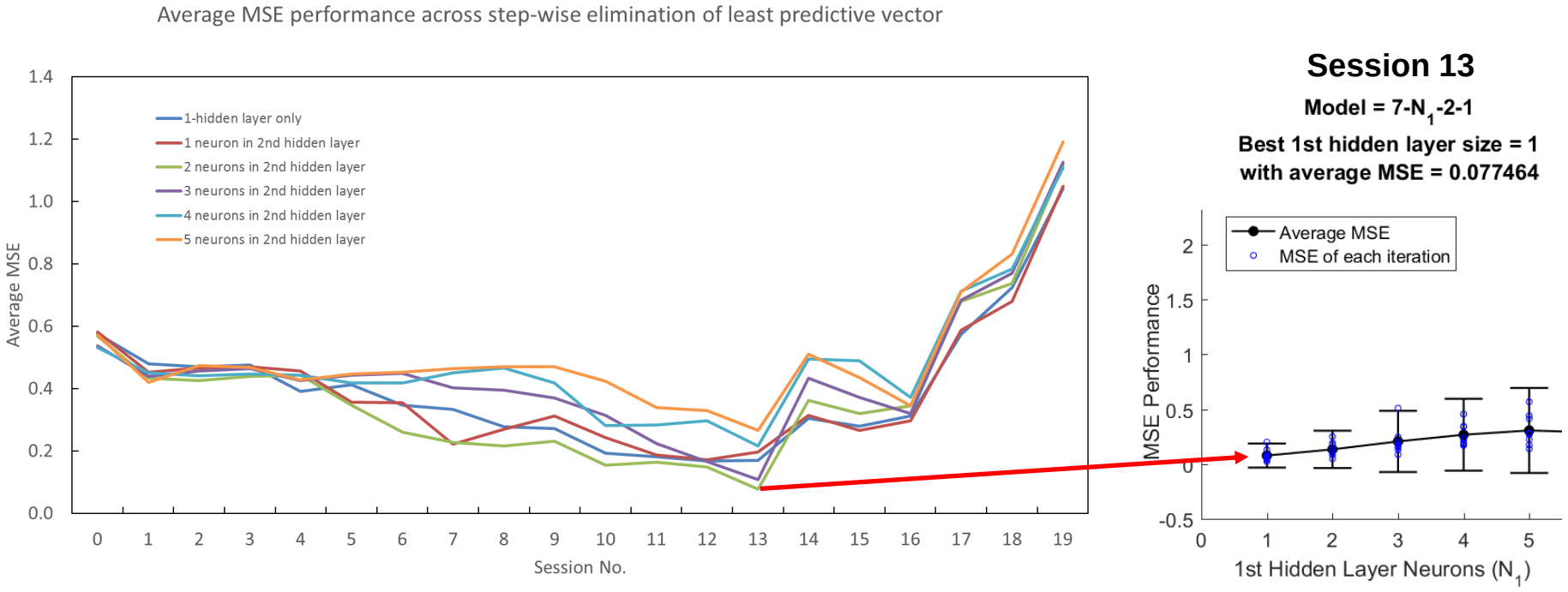

Figure 22: Average MSE performance of the best network configuration in each sessions following a step-wise least significant input vector elimination(left) and the details of MSE performance for Session 13(right). Note that Session 0 and 1 reflects a summary of Figure 20 and 21 respectively. Also, note that the best 1st hidden layer neuron number is not included for the graph on the left. See Table 7, 8 and Appendix B for information on best 1st hidden layer neuron number.

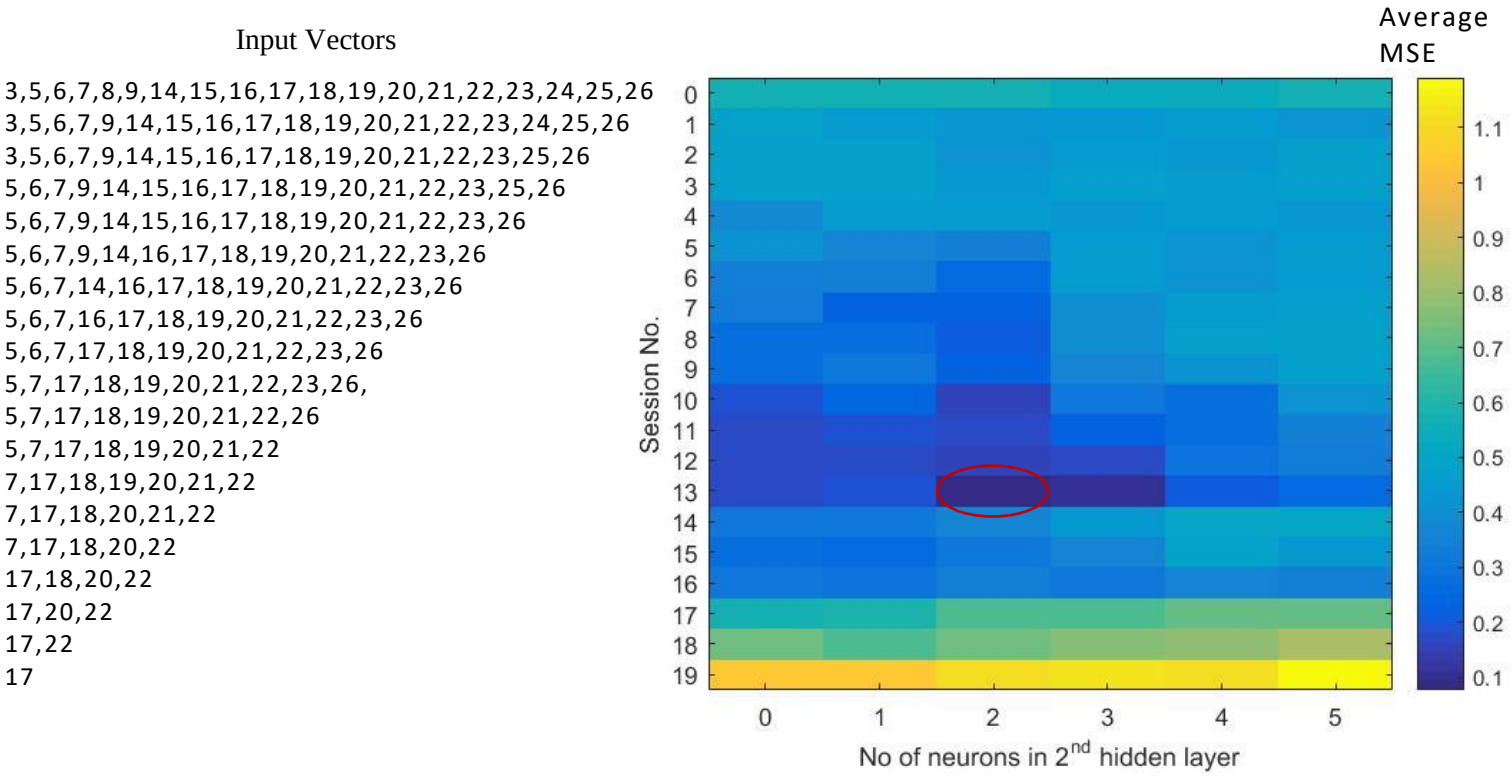

Figure 23: Colour map analysis showing the optimal combination of 2nd hidden layer neurons and input vectors. Also, note that the best 1st hidden layer neuron number is not included for the graph on the left. See Table 7, 8 and Appendix B for information on best 1st hidden layer neuron number.

Chapter 5: Discussion and Final Conclusion

There are many aspects to human vision capabilities. One of the least explored aspect of vision is UFOV. The focus on this aspect for research is largely motivated by the challenging unknowns of UFOV's characteristics in human. To summaries the work here towards discovering a new method for the objective assessment of UFOV ability, there are four major steps demonstrated in this dissertation. Firstly, Chapter 1 unveils the importance of UFOV and the two human physiological markers, SSVEP and pupil oscillation, which are well published in the literature to have phenomenal association with UFOV. Secondly, Chapter 2 investigated different tasks and examine the relationship between their UFOV accuracy performance results and these markers using a small number of human observers. Through the results, the task paradigm with the potential to produce UFOV results that is highly correlated to the markers is selected. Thirdly, Chapter 3 expands the concept of the selected task paradigm into UFOV eccentricity size performance measurement and test it on a larger sample size of human observers, to ascertain the relationship between UFOV size and the physiological markers. The work in Chapter 3 also aimed to collect data points for training a neural network model that can predict UFOV performance using SSVEP and pupillary oscillation markers. Finally, Chapter 4 describes the process of designing the neural network model and how 11-fold cross-validation was implemented to test the accuracy and reliability of the train model in using these markers to predict UFOV performance.

While much of the scientific discussion of SSVEP and PO has been presented towards the end of Chapter 2, there are four points regarding the future potentials of the model to be discussed in the following sections.

5.1 The predictive model as a performance verifier.

Experiment A and B demonstrates a data collection paradigm which allows SSVEP, OP and psychophysical-derived UFOV performance to be collected concurrently. The UFOV performance collected through subjective psychophysical responses can be verified by comparing them to the UFOV values predicted by the physiological markers. Hence, the predictive model in this case is particularly useful in confirming the UFOV capability of an individual, providing an extra supportive evidence over the subjective response results. This could be important for the selection of potential elite sportsmen or soldiers.

5.2 The predictive model as a screening tool

Where mass screening of UFOV is desired, current methods in Experiment B2 provides the quick solution for estimating UFOV. For each trial of checkboard stimulus, the maximum duration is around 45 seconds (baseline phase + activity phase). Hence, the question here is what is the least number of trials to provide a good estimate of UFOV eccentricity size. In the case of psychophysical methods, a session in Experiment B1 will take about an average of 9 trials which is a maximum of 9 x 45 seconds = 6.75 minutes to output an estimated UFOV reading. Of course, this is also assuming that a quick estimation does not require multiple sessions of B1 task for an average score like in Experiment B1. Similarly, for screening purposes, a small compromise in UFOV prediction accuracy can be made for a shorter testing time by having lesser trials and using only eye tracker (nOP input vectors only). This option is possible based on the supporting result in network training session 16 (See Table 8 and Figure 24), where input vectors 17,18, 20 and 22 can potentially provide an average accuracy of about ±0.545° (MSE =0.344) and “worse case” accuracy of

±0.74° for the best network model 4-1-1-1. The compromise in accuracy is tolerable as it is within ±1°. These 4 input vectors, which corresponds to eccentricity 7.5°, 8°, 9° and 10°, are all nPO inputs from the eye tracker. This option is favourable as SSVEP is not as predictive as OP in estimating UFOV sizes and it takes some time to setup the SSVEP which requires 5 minutes as oppose to the 1-min calibration for eye tracking; therefore, one can leave out the troublesome and less predictive part. Hence, the total time required to implement the model prediction with eye tracker only is 1 minute + (4 x 45 seconds) = 4 minutes only. This is a time saving of more than 2 minutes from the psychophysical method.

5.3 Verifying the relationship between UFOV and elite gamers/sportsmen

While there are no statistically significant results to suggest the UFOV superiority of gamers and sportsmen over those who does not involved in games and sports, the descriptive data suggest a trend that non-active group seems to perform worse than those involved in games and sports. In view of the possible case of insufficient sample size in the activity groupings and it is worthwhile to investigate such traits. As mentioned in previous Chapter 3, the case of using 6-hour criteria as the selection for groupings may not be ideal as it does not necessary indicates an individual's ability in sports or game. Hence, for future studies, the best solution is to identify a specific game and recruit participants to play the game for scores and take part in Experiment B. The participants can be divided into several groups according to how well they score in the game, and then their UFOV performances are compared between these groups. The same can be applied to sports.

5.4 Improving the model

The moderate success in prediction is largely due to good linearity relationship between the physiological signals and UFOV which therefore reduces the need for the network model to train for the non-linear behaviour of the data. This is probably the reason that allows network to achieve moderate accuracy with 53 participant's data which is considered small for most modelling work. Nevertheless, the typical way to further improve the prediction accuracy is still to increase the human sample size for more input vectors and target/testing values. Given enough resources and time, another improvement for consideration is to have 5 or more sessions for both Experiment B1 and B2. This study assumes the subjective-based psychophysical UFOV performance as the reliable subjective-evidence-based performance indicator. Hence, improving the prediction of the model should also consider ways to increase the reliability of the target/testing values by minimising the errors arising from the variation of the subjective-based UFOV performance. By repeating more sessions of psychophysical measurement of UFOV in Experiment B1, the averaged score can be more accurate. Along the same tune, by repeating more sessions in Experiment B2, more data in each vector can be fed into the model for training and more target/testing values are available for learning.

In conclusion, physiological data, SSVEP and Pupillary Oscillation, gathered during a demanding central-peripheral attention task can be used to assess UFOV by using the appropriately-trained neural network model that takes in physiological inputs (nSSVEP and nPO).

Bibliography

Baker, D. H., Simard, M., Saint-Amour, D., & Hess, R. F. (2015). Steady-State Contrast Response Functions Provide a Sensitive and Objective Index of Amblyopic. *Investigative ophthalmology & visual science*, 56(2), 1208-1216.

Ball, K. K., & Owsley, C. (1993). The useful field of view: a new technique for evaluating age-related declines in visual function. *Journal of the Amercian Optometric Association*, 64, 71-79.

Ball, K. K., Roenker, D., Cissell, G., Graves, M., Edwards, J., & Whorley, K. (1994). Visual attention analyzer: technology to evaluate and train drivers' visual performance. *SPIE* 2102, 126.

Ball, K. K., Wadley, V. G., & Edwards, J. D. (2002). Advances in Technology Used to Assess and Retrain Older Drivers. *Gerontechnology*, 1(4), 251-261.

Ball, K., Beard, B., Roenker, D., Miller, R., & Griggs, D. (1988). Age and visual search: Expanding the useful field of view. *Journal of the Optical Society of America*, 5, 2210-2219.

Ball, K., Owsley, C., Sloane, M. S., Roenker, D. L., & Bruni, J. R. (1993). Visual attention problems as a predictor of vehicle crashes in older drivers. *Investigative Ophthalmology & Visual Science*, 34(11), 3110-3123.

Ball, K., Owsley, C., Stalvey, B., Roenker, D. L., Sloane, M. E., & Graves, M. (1998). Driving avoidance and functional impairment in older drivers. *Accident Analysis & Prevention*, 30(3), 313-322.

Beatty, J., & Lucero-Wagoner, B. (2000). The pupillary system. *Handbook of Psychophysiology*, 2, 142-162.

Bebis, G., & Georgiopoulos, M. (1994). Feed-forward neural networks. *IEEE Potentials*, 13(4), 27-31.

Belmonte, M. (1998). Shifts of visual spatial attention modulate a steady-state visual evoked potential. *Cognitive Brain Research*, 6(4), 295-307.

Bennett, D. M., Gordon, G., & Dutton, G. N. (2009). The useful field of view test, normative data in children of school age. *Optometry and Vision Science*, 86(6), 717-721.

Beverina, F., Palmas, G., Silvoni, S., Piccione, F., & Giove, S. (2003). User adaptive BCIs: SSVEP and P300 based interfaces. *PsychNology Journal*, 1(4), 331-354.

Binda, P., Pereverzeva, M., & Murray, S. O. (2014). Pupil size reflects the focus of feature-based attention. *Journal of neurophysiology*, 112(12), 3046-3052.

Cao, T., Wan, F., Wong, C. M., da Cruz, J. N., & Hu, Y. (2014). Objective evaluation of fatigue by EEG spectral analysis in steady-state visual evoked potential-based brain-computer interfaces. *Biomedical engineering online*, 13(1), 28.

Caudill, M. (1987). Neural networks primer, part I. *AI expert*, 2(12), 46-52.

Chan, A. H., & So, D. K. (2007). Shape characteristics of useful field of view and visual search time. *Le travail humain*, 70, 343-367.

Chui, T. Y., Yap, M. K., Chan, H. H., & Thibos, L. N. (2005). Retinal stretching limits peripheral visual acuity in myopia. *Vision Research*, 45(5), 593-605.

Clay, O. J., Wadley, V. G., Edwards, J. D., Roth, D. L., Roenker, D. L., & Ball, K. K. (2005). Cumulative meta-analysis of the relationship between useful field of view and driving performance in older adults: Current and future implications. *Optometry and Vision Science*, 82(8), 724-731.

Coffey, B., & Reichow, A. W. (1987). Guidelines for screening and testing the athlete's visual system:part III. *Curriculum II (OEPF)*, 59, 355-368.

Cosman, J. D., Lees, M. N., Lee, J. D., Rizzo, M., & Vecera, S. P. (2012). Visual search for features and conjunctions following declines in the useful field of view. *Experimental Aging Research*, 38, 411-421.

Crundall, D., Underwood, G., & Chapman, P. (1999). Driving experience and the functional field of view. *Perception*, 28, 1075-1087.

Curcio, C. A., Sloan, K. R., Kalina, R. E., & Hendrickson, A. E. (1990). Human photoreceptor topography. *Journal of comparative neurology*, *292*(4), 497-523.

Daniels, L. B., Nichols, D. F., Seifert, M. S., & Hock, H. S. (2012). Changes in pupil diameter entrained by cortically initiated changes in attention. *Visual neuroscience*, 29(02), 131-142.

Ding, J., Sperling, G., & Srinivasan, R. (2006). Attentional modulation of SSVEP power depends on the network tagged by the flicker frequency. *Cerebral cortex*, 16(7), 1016-1029.

Edwards, J. D., Ross, L. A., Wadley, V. G., Clay, O. J., Crowe, M., Roenker, D. L., et al. (2006). The useful field of view test: Normative data for older adults. *Archives of Clinical Neuropsychology*, 21, 275-286.

Ehrenstein, W. H., & Ehrenstein, A. (1999). Psychophysical methods. In *Modern techniques in neuroscience research* (pp. 1211-1241). Springer Berlin Heidelberg.

Green, C. S., & Bavelier, D. (2003). Action video game modifies visual selective attention. *Nature*, 423(6939), 534-537.

Gurney, K. (1997). An introduction to neural networks. *CRC press*.

Hawkes, C. H., & Stow, B. (1981). Pupil size and the pattern evoked visual response. *Journal of Neurology, Neurosurgery & Psychiatry*, 44(1), 90-91.

Haykin, S. S. (2009). Neural networks and learning machines (3rd Edition). Upper Saddle River, NJ, USA: *Pearson*.

Heinrich, S. P., & Bach, M. (2001). Adaptation dynamics in pattern-reversal visual evoked potentials. *Documenta Ophthalmologica*, 102(2), 141-156.

Herbik, A., Geringswald, F., Thieme, H., Pollmann, S., & Hoffmann, M. B. (2014). Prediction of higher visual function in macular degeneration with multifocal electroretinogram and multifocal visual evoked potential. *Ophthalmic and Physiological Optics*, 34(5), 540-551.

Herrmann, C. S. (2001). Human EEG responses to 1–100 Hz flicker: resonance phenomena in visual cortex and their potential correlation to cognitive phenomena. *Experimental brain research*, 137(3-4), 346-353.

Hubert-Wallander, B., Green, C. S., & Bavelier, D. (2011). Stretching the limits of visual attention: the case of action video games. *Wiley interdisciplinary reviews: cognitive science*, 2(2), 222-230.

Isler, R. B., Parsonson, B. S., & Hansson, G. J. (1997). Age related effects of restricted head movements on the useful field of view of drivers. *Accident, Analysis and Prevention*, 29(6), 793-801.

Jamison, K. W., Roy, A. V., He, S., Engel, S. A., & He, B. (2015). SSVEP signatures of binocular rivalry during simultaneous EEG and fMRI. *Journal of neuroscience methods*, 243, 53-62.

Johansson, B., & Jakobsson, P. (2000). Fourier analysis of steady-state visual evoked potentials in subjects with normal and defective stereo vision. *Documenta ophthalmologica*, 101(3), 233-246.

Kim, Y. J., Grabowecky, M., Paller, K. A., Muthu, K., & Suzuki, S. (2007). Attention induces synchronization-based response gain in steady-state visual evoked potentials. *Nature neuroscience*, 10(1), 117-125.

Klingner, J., Kumar, R., & Hanrahan, P. (2008, March). Measuring the task-evoked pupillary response with a remote eye tracker. In *Proceedings of the 2008 symposium on Eye tracking research & applications* (pp. 69-72). ACM.

Kohavi, R. (1995, August). A study of cross-validation and bootstrap for accuracy estimation and model selection. In *IJCAI* (Vol. 14, No. 2, pp. 1137-1145).

Krishnan, L., Kang, A., Sperling, G., & Srinivasan, R. (2013). Neural strategies for selective attention distinguish fast-action video game players. *Brain topography*, 26(1), 83-97.

Latham, A. J., Patston, L. L. M., & Tippett, L. J. (2013). The virtual brain: 30 years of video-game play and cognitive abilities. *Frontiers in Psychology*, 4, 629. doi:10.3389/fpsyg.2013.00629

Lin, S. T., & Tey, L. K. (2016). A Preliminary Study on Normalized Pattern-Reversal Peripheral Field SSVEPs as a Potential Objective Indicator of Useful Field of View PerformanceA Potential Neural Indicator of UFOV. *Investigative Ophthalmology & Visual Science*, 57(7), 3248-3256.

Loewenfeld IE (1999) The Pupil: Anatomy, physiology, and clinical applications. Boston: *Butterworth-Heinemann*.

Mackay, A. M., Bradnam, M. S., Hamilton, R., Elliot, A. T., & Dutton, G. N. (2008). Real-time rapid acuity assessment using VEPs: development and validation of the step VEP technique. *Investigative Ophthalmology and Visual Science*, 49(1), 438.

Malinowski, P., Fuchs, S., & Müller, M. M. (2007). Sustained division of spatial attention to multiple locations within one hemifield. *Neuroscience letters*, 414(1), 65-70.

Mathôt S, van der Linden L, Grainger J, Vitu F (2013) The Pupillary Light Response Reveals the Focus of Covert Visual Attention. PLoS ONE 8(10): e78168.doi: 10.1371/journal.pone.0078168

Mathôt, S., & Van der Stigchel, S. (2015). New Light on the Mind's Eye: The Pupillary Light Response as Active Vision. *Current Directions in Psychological Scienc*e, 24(5), 374-378.

Mathôt, S., Dalmaijer, E., Grainger, J., & Van der Stigchel, S. (2014). The pupillary light response reflects exogenous attention and inhibition of return. *Journal of vision*, 14(14), 7.

Matos, R., & Godinho, M. (2005). Influence of sports practice in the useful field of vision in a simulated driving test. In *Active lifestyles: the impact of education and sport, book of abstracts of AIESEP 2005 World Conference*. Lissabon (Vol. 262).

Memmert, D., Simons, D. J., & Grimme, T. (2009). The relationship between visual attention and expertise in sports. *Psychology of Sport and Exercise*, 10(1), 146-151.

Mishra, J., Zinni, M., Bavelier, D., & Hillyard, S. A. (2011). Neural basis of superior performance of action videogame players in an attention-demanding task. *The Journal of Neuroscience*, 31(3), 992-998.

Morgan, S. T., Hansen, J. C., & Hillyard, S. A. (1996). Selective attention to stimulus location modulates the steady-state visual evoked potential. *Proceedings of the National Academy of Sciences*, 93(10), 4770-4774.

Müller, M. M., Malinowski, P., Gruber, T., & Hillyard, S. A. (2003). Sustained division of the attentional spotlight. *Nature*, 424(6946), 309-312.

Müller, M. M., Picton, T. W., Valdes-Sosa, P., Riera, J., Teder-Sälejärvi, W. A., & Hillyard, S. A. (1998). Effects of spatial selective attention on the steady-state visual evoked potential in the 20–28 Hz range. *Cognitive Brain Research*, 6(4), 249-261.

Müller, M. M., Teder-Sälejärvi, W., & Hillyard, S. A. (1998). The time course of cortical facilitation during cued shifts of spatial attention. *Nature neuroscience*, 1(7), 631-634.

Naber, M., Alvarez, G. A., & Nakayama, K. (2013). Tracking the allocation of attention using human pupillary oscillations. *Frontiers in psychology*, 4.

Nakauchi Shigeki and Tetsuto Minami (2015). Extracting the attentional status via SSVEPs: The cases of tracking the multiple moving objects and estimating the useful field of view. In *11th Asia-Pacific Conference on Vision*, Singapore. Symposium: Attention & the Brain.

Pastor, M. A., Artieda, J., Arbizu, J., Valencia, M., & Masdeu, J. C. (2003). Human cerebral activation during steady-state visual-evoked responses. *The journal of neuroscience*, 23(37), 11621-11627.

Privetera C. M., Renninger L. w., Carney T., Klien S., Auilar M. (2010). Pupil dilation during visual target detection. *Journal of vision*, 10(10):3, 1-14.

Privitera, C. M., Renninger, L. W., Carney, T., Klein, S., & Aguilar, M. (2008, February). The pupil dilation response to visual detection. In Electronic Imaging 2008 (pp. 68060T-68060T). *International Society for Optics and Photonics*.

Puell, m. C., & Barrio, A. (2008). Effect of driver distraction and low alcohol concentrations on useful field of view and frequency-doubling technology perimetry. *Acta Ophthalmologica*, 86, 634-641.

Ransom-Hogg, A., & Spillmann, L. (1980). Perceptive field size in fovea and periphery of the light-and dark-adapted retina. *Vision Research, 20*(3), 221-228.

Richards, E., Bennett, P. J., & Sekuler, A. B. (2006). Age related differences in learning with the useful field of view. *Vision Research*, 46, 4217-4231.

Rogé, J., Pébayle, T., Hannachi, S. E., & Muzet, A. (2003). Effect of sleep deprivation and driving duration on the useful visual field in younger and older subjects during simulator driving. *Vision Research*, 43, 1465-1472.

Rogé, J., Pébayle, T., Kiehn, L., & Muzet, A. (2002). Alternation of the useful visual field as a function of state of vigilance in simulated car driving. *Transportation Research Part F*, 5, 189-200.

Rogé, J., Pébayle, T., Lambilliotte, E., Spitzenstetter , F., Giselbrecht, D., & Muzet, A. (2004). Influence of age, speed and duration of monotonous driving task in traffic on the driver's useful visual field. *Vision Research*, 44, 2737-2744.

Sanders, A. F. (1970). Some aspects of the selective process in the functional visual field. *Ergonomics*, 13(1), 101-117.

Scialfa, C., Thomas, D. M., & Joffe, K. M. (1994). Age differences in the useful field of view: An eye movement analysis. *Optometry and Visual Science*, 71(12), 736-742.

Störmer, V. S., Winther, G. N., Li, S. C., & Andersen, S. K. (2013). Sustained multifocal attentional enhancement of stimulus processing in early visual areas predicts tracking performance. *The Journal of Neuroscience*, 33(12), 5346-5351.

Sutoyo, D., & Srinivasan, R. (2009). Nonlinear SSVEP responses are sensitive to the perceptual binding of visual hemifields during conventional ‘eye’ rivalry and interocular ‘percept’ rivalry. *Brain research*, 1251, 245-255.

Thurtell, M. J., Black, R. A., Halmagyi, G. M., Curthoys, I. S., & Aw, S. T. (1999). Vertical eye position–dependence of the human vestibuloocular reflex during passive and active yaw head rotations. *Journal of neurophysiology*, 81(5), 2415-2428.

Toffanin, P., de Jong, R., Johnson, A., & Martens, S. (2009). Using frequency tagging to quantify attentional deployment in a visual divided attention task. *International Journal of Psychophysiology*, 72(3), 289-298.

Visual Awareness Research Group, Inc. (1999). Retrieved Sep 20, 2013, from Visual Awareness: http://www.visualawareness.com

Von Grünau, M. W., Faubert, J., Iordanova, M., & Rajska, D. (1999). Flicker and the efficiency of cues for capturing attention. *Vision research*, 39(19), 3241-3252.

Wang, C. A., & Munoz, D. P. (2014). Modulation of stimulus contrast on the human pupil orienting response. *European Journal of Neuroscience*, 40(5), 2822-2832.

Widmann, A., Schröger, E., & Maess, B. (2015). Digital filter design for electrophysiological data–a practical approach. *Journal of neuroscience methods*, 250, 34-46

Wierda, S. M., van Rijn, H., Taatgen, N. A., & Martens, S. (2012). Pupil dilation deconvolution reveals the dynamics of attention at high temporal resolution. *Proceedings of the National Academy of Sciences*, 109(22), 8456-8460.

Wood, J. M., Chaparro, A., Lacherez, P., & Hickson, L. (2012). Useful field of view predicts driving in the presence of distracters. *Optometry and Vision Science*, 89(4), 373-381.

Wood, J. W., & Abernethy, B. (1997). An assessment of the efficacy of sports vision training programs. *Optometry and Vision Science*, 74(8), 646-659.

Wood, J., Chaparro, A., Hickson, L., Thyer, N., Carter, P., Hancock, J., et al. (2006). The effect of auditory and visual distracters on the useful field of view: implications for the driving task. *Investigative Ophthalmology & Visual Science*, 47(10), 4046-4650.

Yu, H., & Wilamowski, B. M. (2011). Levenberg–marquardt training. *Industrial Electronics Handbook*, 5(12), 1.

Zhang, P., Jamison, K., Engel, S., He, B., & He, S. (2011). Binocular rivalry requires visual attention. *Neuron*, 71(2), 362-369.

Zhang, Y., Jin, J., Qing, X., Wang, B., & Wang, X. (2012). LASSO based stimulus frequency recognition model for SSVEP BCIs. *Biomedical Signal Processing and Control*, 7(2), 104-111.

Appendix A

FFN_SSVEPPO.mat

```
% Put both SSVEPPO_03102016.mat and FFN_SSVEPPO.mat into a folder and
% execute the latter FFN_SSVEPPO.mat file from that folder.
% SSVEPPO_03102016.mat contains the variable "data" which is a variable in the
% form of 53 x 27 matrix variable described in Chapter 4, Section 4.2.
% Data in "data" variable is obtained from Experiment B
% 1) column 1 -13  = nSSVEP data input column vectors,
% 2) column 14 - 26  = nPO data input column vectors,
% 3) column 27 = target eccentricity size value vector.

% load input column vectors 1 - 26 and target value vector as 27th column
load('SSVEPPO_03102016.mat');tic;

 % set training method as Levenberg-Marquardt backpropagation.
trainFcn = 'trainlm';

adata = data; % backup copy of data for debugging and review purposes

thiddenLayersize1 = 30;
thiddenLayerSize2 = 5;
stszi = 1;
szisz = 5; %fixed to cluster of 5 for 11-fold cross validation
endszi = size(adata,1);

out1 = [];out = [];bm2 = [];

% select cross validation session based on Table 6 in dissertation
vec = input('Cross-validation Session =');

% option to plot data after training sessions ended
plt = 'Y';

if vec == 0
    vn = [1:26];
elseif vec == 1
    vn = [3 5:9 14:26];
elseif vec == 2
    vn = [3 5:7 9 14:26];
elseif vec == 3
    vn = [3 5:7 9 14:23 25 26];
elseif vec == 4
    vn = [5:7 9 14:23 25 26];
elseif vec == 5
    vn = [5:7 9 14:23 26];
elseif vec == 6
    vn = [5:7 9 14 16:23 26];
elseif vec == 7
    vn = [5:7 14 16:23 26];
elseif vec == 8
    vn = [5:7 16:23 26];
elseif vec == 9
    vn = [5:7 17:23 26];
elseif vec == 10
    vn = [5 7 17:23 26];
elseif vec == 11
    vn = [5 7 17:22 26];
elseif vec == 12
    vn = [5 7 17:22 ];
elseif vec == 13
    vn = [7 17:22 ];
elseif vec == 14
    vn = [7 17 18 20:22 ];
elseif vec == 15
    vn = [7 17 18 20 22 ];
elseif vec == 16
    vn = [17 18 20 22 ];
```

```
elseif vec == 17
    vn = [17 20 22 ];
elseif vec == 18
    vn = [17 22 ];
elseif vec == 19
    vn = [17];
end


sf = 'vectors-'; % string description of input vectors
for w = 1:size(vn,2)
    sf = char(strcat(sf,{' '},num2str(vn(w))));
    if w == 26
        sf ='vectors-all';
    end
end

% create folder to sort the process data, change variable folderin
folderin = strcat(cd,'\Output_S',num2str(vec),'_',sf,'_',trainFcn,'_',...
    num2str(yyyymmdd(datetime)),'_',datestr(now,'HHMMSS'));
mkdir(folderin);

% loop thru second hidden layer size
for hiddenLayerSize2 = 0:thiddenLayerSize2

% loop thru second hidden layer size
 for hiddenLayerSize1 = 1:thiddenLayersize1
    out = [];

  disp('########################################');
  % create variable results to store training outcome
  % for each network model
  results = cell(1,1);
  results{1,1} = '1st hiddenlayer;2nd hiddenlayer;vec;iter;k-fold-startpoint';
  results{1,2} = 'networks';
  results{1,3} = '1st hidden layer size';
  results{1,4} = 'iter';
  results{1,5} = 'mean network Performance';
  results{1,6} = 'std network Performance';
  results{1,7} = 'mean*std network Performance';


for iter = 1:10 %number of iteration


    disp(strcat(sf, ', Iteration =',num2str(iter),...
        ', 1st layer hidden size =',...
        num2str(hiddenLayerSize1),', 2nd layer hidden size =',...
        num2str(hiddenLayerSize2)));

    gnet = cell(1,1); %sub level results to go into the variable "results"
    gnet{1,1} = '1st hiddenlayer;2nd hiddenlayer;vec;iter;k-fold-startpoint';
    gnet{1,2} = 'NNetwork';
    gnet{1,3} = 'tr';
    gnet{1,4} = 'trainoutput';
    gnet{1,5} = 'gsubtract';
    gnet{1,6} = 'Perf-nntool';
    gnet{1,7} = 'testoutput';
    gnet{1,8} = 'Perf-test';
    c = 2;
for szi = stszi:szisz:endszi % validation process

    data = adata;
    if (endszi - szi) < 4 % isolate the testing data from the training data
     dta = data(1:(4 - (endszi - szi)),:); % wrap around for testing data
     tedata = [data(szi:endszi,:);dta];
     data(szi:endszi,:) = [];
     data(1:(4 - (endszi - szi)),:) = [];
     fo = strcat('Fold =',num2str(szi),'-',num2str(endszi),',1,2');
    else
    tedata = data(szi:szi+4,:);
    data(szi:szi+4,:) = [];
    fo = strcat('Fold =',num2str(szi),'-',num2str(endszi));
    end
```

```
    xc = tedata(:,[vn])';%reassign variables
    zc = tedata(:,27)';

    dataX = data(:,1);dataY = data(:,2);
    dataZ = data(:,27);dataIn = data(:,[vn]);


    x = dataIn(1:end,:)';
    t = dataZ(1:end,1)';


    % Create Network

    if hiddenLayerSize2 > 0
        %set the transfer function for 2-hiddenlayer netork
        net = fitnet([hiddenLayerSize1,hiddenLayerSize2],trainFcn);
        k1 = 'tansig';
        k2 ='tansig';
        k3='purelin';
        net.layers{1}.transferFcn = k1;
        net.layers{2}.transferFcn = k2;
        net.layers{3}.transferFcn = k3;
    else
        %set the transfer function for 1-hiddenlayer netork
        net = fitnet(hiddenLayerSize1,trainFcn);
        k1 ='tansig';
        k2='purelin';
        net.layers{1}.transferFcn = k1;
        net.layers{2}.transferFcn = k2;
    end

    % Setup configurations for Training, Validation, Testing
    net.divideParam.trainRatio = 100/100;
    net.divideParam.valRatio = 100/100;
    net.divideParam.testRatio = 0;
    net.trainParam.showWIndow = false;
    net.performParam.normalization = 'percent';
    net.trainparam.lr=0.01;
    net.trainparam.epochs=10000;
    net.trainparam.goal=0;

    % Train the Network
    [net,tr] = train(net,x,t);

    % Internal testing of the Network with training data
    % contains biases, but just to log anormalities in training for review
    y = net(x);
    e = gsubtract(t,y);
    performance = mse(t,y);
    % Actual Testing of the Network with testing data isolated earlier on
    testnet = net(xc);
    testp = mse(zc,testnet);

    %store subresults
    gnet{c,1} = [hiddenLayerSize1;hiddenLayerSize2;vec;iter;szi];
    gnet{c,2} = net;
    gnet{c,3} = tr;
    gnet{c,4} = y;
    gnet{c,5} = e;
    gnet{c,6} = performance;
    gnet{c,7} = testnet;
    gnet{c,8} = testp;

    c = c + 1;
    disp(strcat(fo,', MSE =',num2str(testp)));

end
     %store results
     results{iter+1,1} = [hiddenLayerSize1;hiddenLayerSize2;iter;vec];
     results{iter+1,2} = gnet;
     results{iter+1,3} = hiddenLayerSize1;
     results{iter+1,4} = iter;
     results{iter+1,5} = mean(cell2mat(gnet(2:end,8)));
     results{iter+1,6} = std(cell2mat(gnet(2:end,8)));
     results{iter+1,7} = results{iter+1,5}*results{iter+1,6};
```

```
    disp(strcat('Average MSE =',num2str(results{iter+1,5}),...
        ', Average std MSE =',...
        num2str(results{iter+1,6}),', Average mean*std MSE =',...
        num2str(results{iter+1,7})));
     toc;
    disp('============================================================');

end
   gj = cell2mat(results(2:end,3:7));
   mp = mean(gj(:,3));
   stdp = mean(gj(:,4));
   out(1,:)=[vec hiddenLayerSize1 hiddenLayerSize2 mp gj(:,3)' stdp gj(:,4)'];
   out1(:,:,hiddenLayerSize1) = out;

    % As the data is very big due to network size, save all variables for
    % every neuron change instead of saving everything at the end
    save(char(strcat(folderin,'\outp_1_',trainFcn,'_',...
        '_',sf,...
        '_1hl_',num2str(hiddenLayerSize1),...
        '_2hl_',num2str(hiddenLayerSize2),'_',...
        num2str(yyyymmdd(datetime)),'_',...
        datestr(now,'HHMMSS'),'.mat')),'-v7.3');

 end

 % building variables for plotting later
 for er = 1:size(out1,3)
 bm(er,:) = out1(:,:,er);
 end

 Ya = [1:size(bm,1)]';%Neuron axis in Y
 bm2(:,:,hiddenLayerSize2+1) = bm;
 pmatr(1:size(bm(:,4),1),hiddenLayerSize2+1) = bm(:,4);

 end%


% Option to plot and save the plot
if strcmp(plt,'Y') || strcmp(plt,'y')
    %plottimg of the results

         Ya = [1:size(bm,1)]';%Neuron axis in Y

         warning off;

         sf = 'Vectors-';
        for w = 1:size(vn,2)
            sf = char(strcat(sf,{' '},num2str(vn(w))));
        end

         for hiddenLayerSize1 = 0:size(bm2,3)-1
             bm = bm2(:,:,hiddenLayerSize1+1);

        figure(vec);
        minp = min(bm(:,4));
        minpt = find(bm(:,4) == minp);
        pmatr(1:size(bm(:,4),1),hiddenLayerSize1+1) = bm(:,4);

        if hiddenLayerSize1 == 0;
        x0=100;
        y0=100;
        width=1800;
        height=900;
        set(gcf,'units','points','position',[x0,y0,width,height]);
        end
        % plot the top row
        subplot(2,size(bm2,3),hiddenLayerSize1+1);

        if hiddenLayerSize1 > 0
        title({char(strcat({'Model = '},num2str(size(vn,2)),'-N_1-',...
            num2str(hiddenLayerSize1),'-1'));...
            char(strcat('Best 1st hidden layer size =',...
            {' '},num2str(minpt)));char(strcat('with average MSE =',...
            {' '},num2str(minp)))});
```

```
        xlabel('1st Hidden Layer Neurons (N_1)');
        ylabel('MSE Performance');
        else
        title({char(strcat({'Model = '},num2str(size(vn,2)),'-N_1-1'));...
            char(strcat('Best hidden layer size =',{' '},num2str(minpt)));...
            char(strcat('with average MSE =',{' '},num2str(minp)))});
        xlabel('Hidden Layer Neurons (N_1)');
        ylabel('MSE Performance');
        end

        set(gcf,'name',char(sf));
         for d = 4:4+((size(bm2,2)-5)/2)
            hold on;
             if d == 4
             sd = std(bm(:,d+1:d+(size(bm2,2)-5)/2),0,2);
             se = sd./sqrt(size(bm(:,d+1:d+(size(bm2,2)-5)/2),2));
             CI = bm(:,d)+(se*1.96);
             errorbar(Ya,bm(:,d),CI,'-k.','LineWidth',1,'MarkerSize',18);

             else
             plot(Ya,bm(:,d),'ob','MarkerSize',3);
             end
            legend('Average MSE','MSE of each iteration',...
                'Location','NorthWest');

        end
        axis([0 size(bm2,1)+1 -1.5 10]);
        hold off

        % plot the bottom row
        subplot(2,size(bm2,3),hiddenLayerSize1+2+thiddenLayerSize2);

         if hiddenLayerSize1 > 0
          xlabel('1st Hidden Layer Neurons (N_1)');ylabel('MSE Performance');
         else
          xlabel('Hidden Layer Neurons (N_1)');ylabel('MSE Performance');
         end

        set(gcf,'name',char(sf));
         for d = 4:4+((size(bm2,2)-5)/2)
            hold on;
             if d == 4
             sd = std(bm(:,d+1:d+(size(bm2,2)-5)/2),0,2);
             se = sd./sqrt(size(bm(:,d+1:d+(size(bm2,2)-5)/2),2));
             CI = bm(:,d)+(se*1.96);
             errorbar(Ya,bm(:,d),CI,'-k.','LineWidth',1,'MarkerSize',18);

             else
             plot(Ya,bm(:,d),'ob','MarkerSize',3);
             end
            legend('Average MSE','MSE of each iteration',...
                'Location','NorthWest');

         end

         if minpt < 4
          axis([0 5.5 -0.5 5]);
         else
          axis([minpt-2.5 minpt+2.5 -0.5 5]);
         end
        hold off

         end
    savefig(figure(vec),char(strcat(folderin,'\outp_fig_',trainFcn,'_S',...
        num2str(vec),'_',sf,num2str(yyyymmdd(datetime)),'_',...
        datestr(now,'HHMMSS'),'.fig')));
end

%Save only the files needed for plotting
save(char(strcat(folderin,'\outp_all_',trainFcn,'_S',...
    num2str(vec),'_',sf,'_',...
    num2str(yyyymmdd(datetime)),'_',...
    datestr(now,'HHMMSS'),'.mat')),...
    'out1','bm','pmatr','vn','trainFcn','bm2');
```

Appendix B

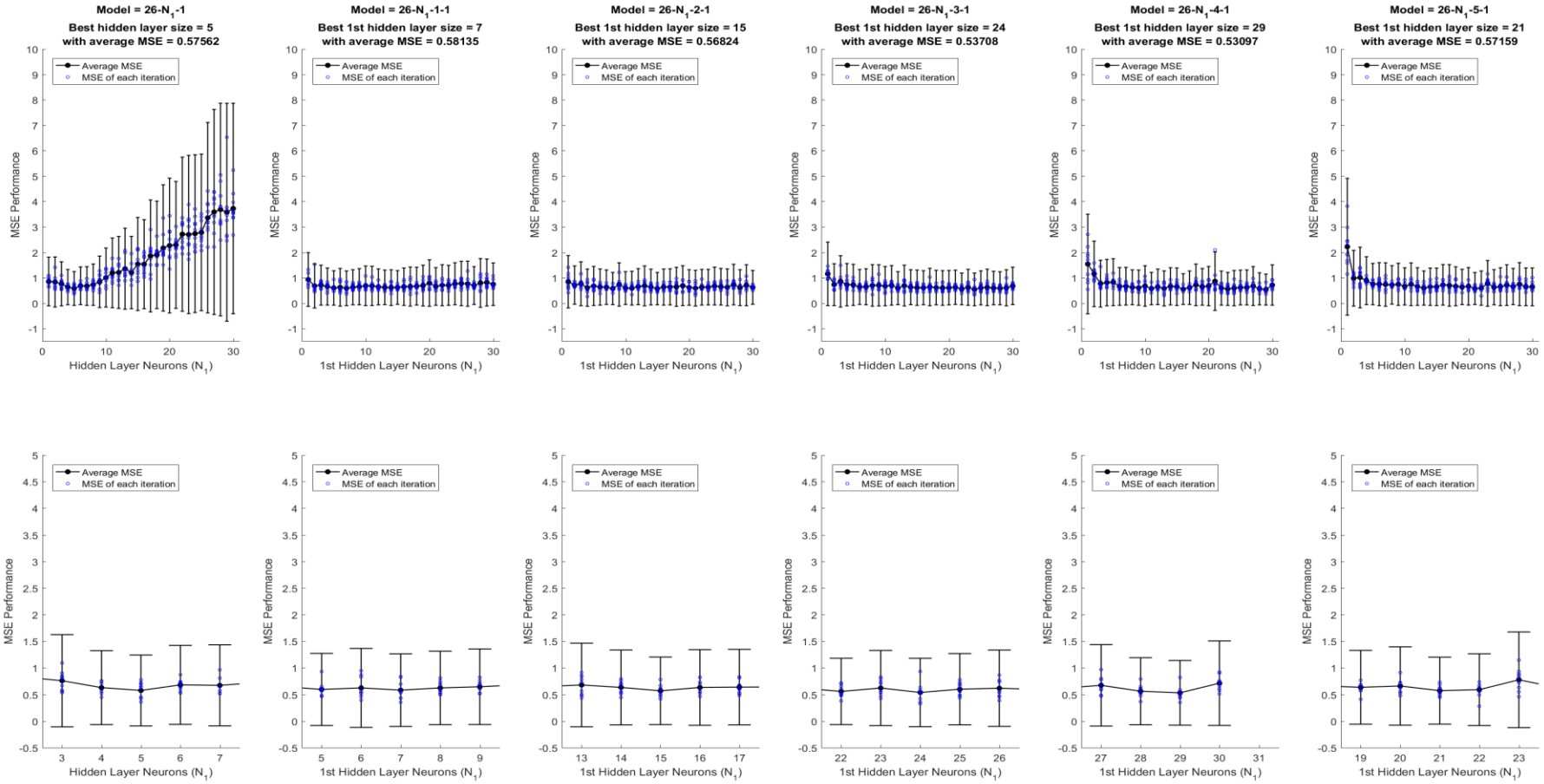

SESSION 0: Average MSE performance across all neural network configurations with all 26 significant input vectors. Error bar indicates 95% CI. Top row of graphs displays all hidden layer neurons, bottom row of graphs zoomed in to the best hidden layer neurons

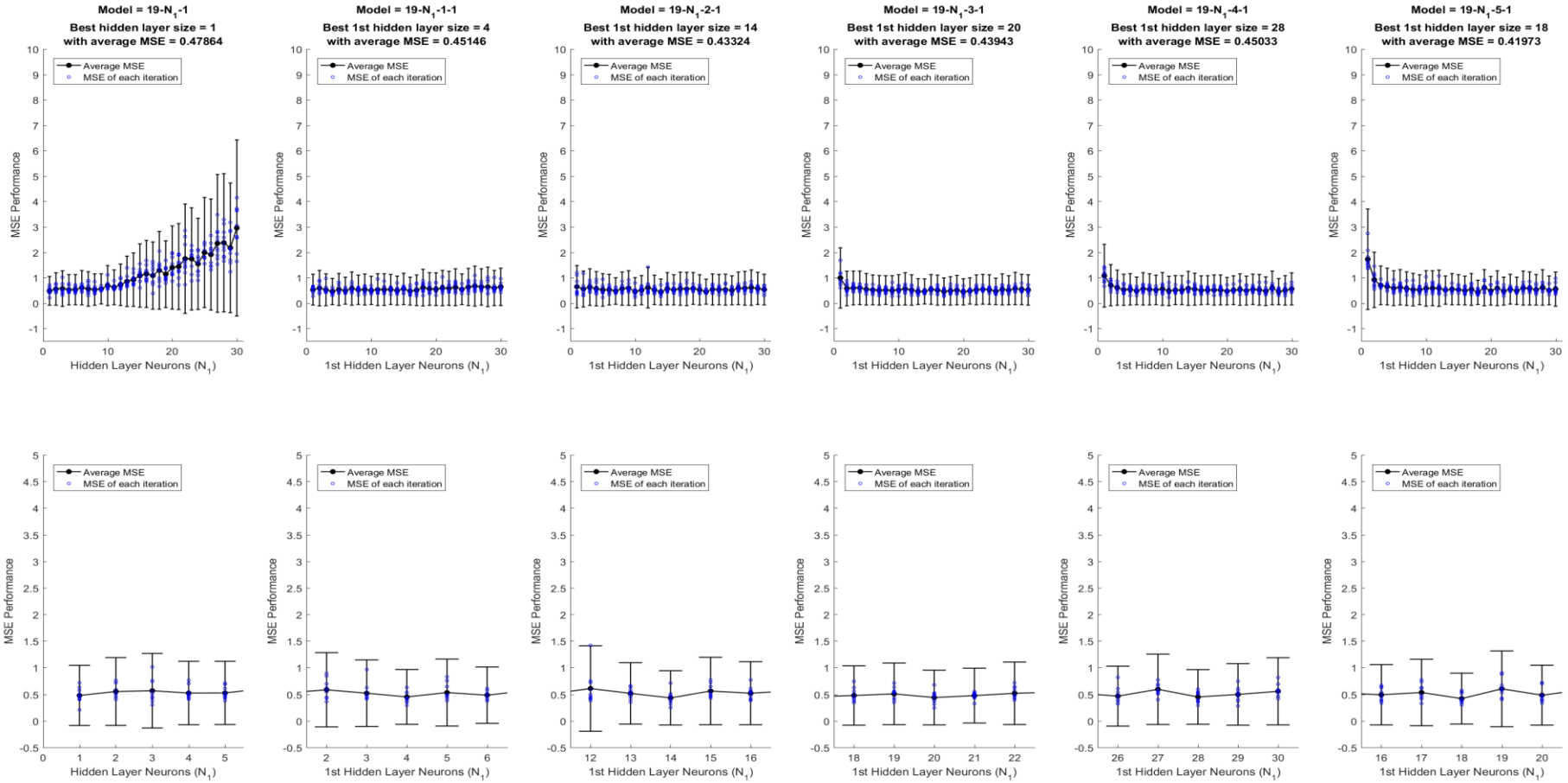

SESSION 1: Average MSE performance across all neural network configurations with top 19 significant input vectors. Error bar indicates 95% CI. Top row of graphs displays all hidden layer neurons, bottom row of graphs zoomed in to the best hidden layer neurons

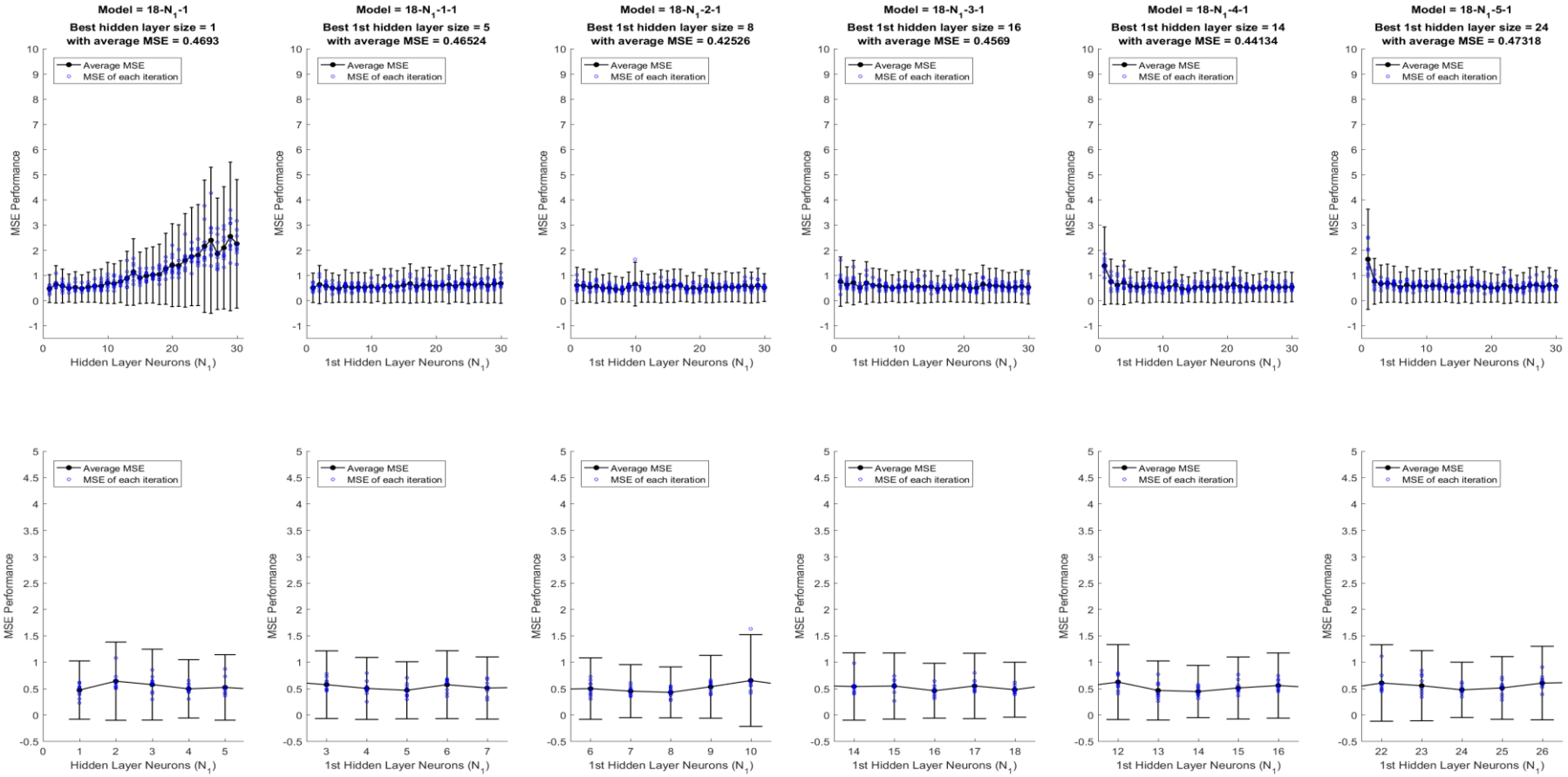

SESSION 2: Average MSE performance across all neural network configurations with top 18 significant input vectors. Error bar indicates 95% CI. Top row of graphs displays all hidden layer neurons, bottom row of graphs zoomed in to the best hidden layer neurons

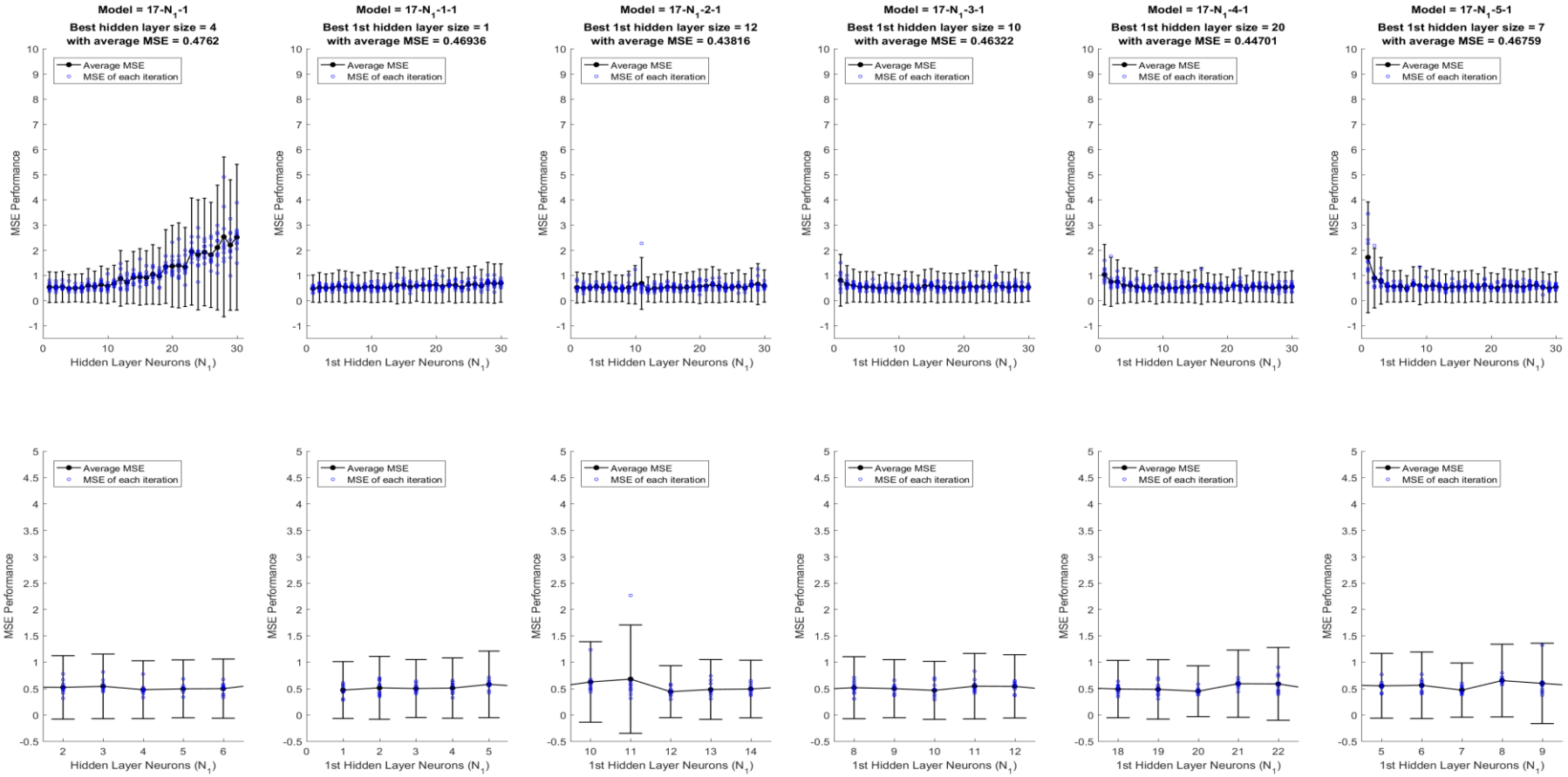

SESSION 3: Average MSE performance across all neural network configurations with top 17 significant input vectors. Error bar indicates 95% CI. Top row of graphs displays all hidden layer neurons, bottom row of graphs zoomed in to the best hidden layer neurons

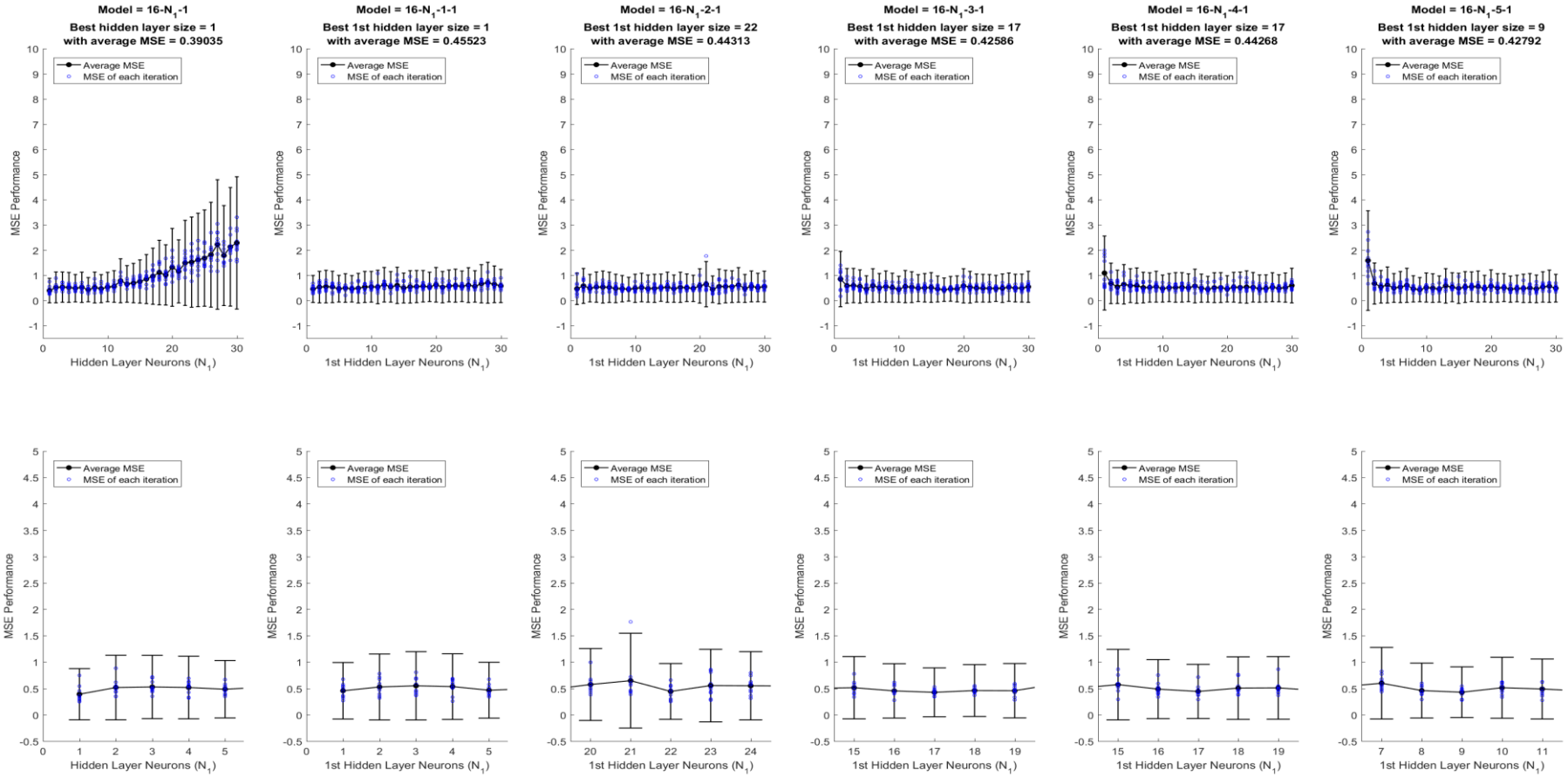

SESSION 4: Average MSE performance across all neural network configurations with top 16 significant input vectors. Error bar indicates 95% CI. Top row of graphs displays all hidden layer neurons, bottom row of graphs zoomed in to the best hidden layer neurons

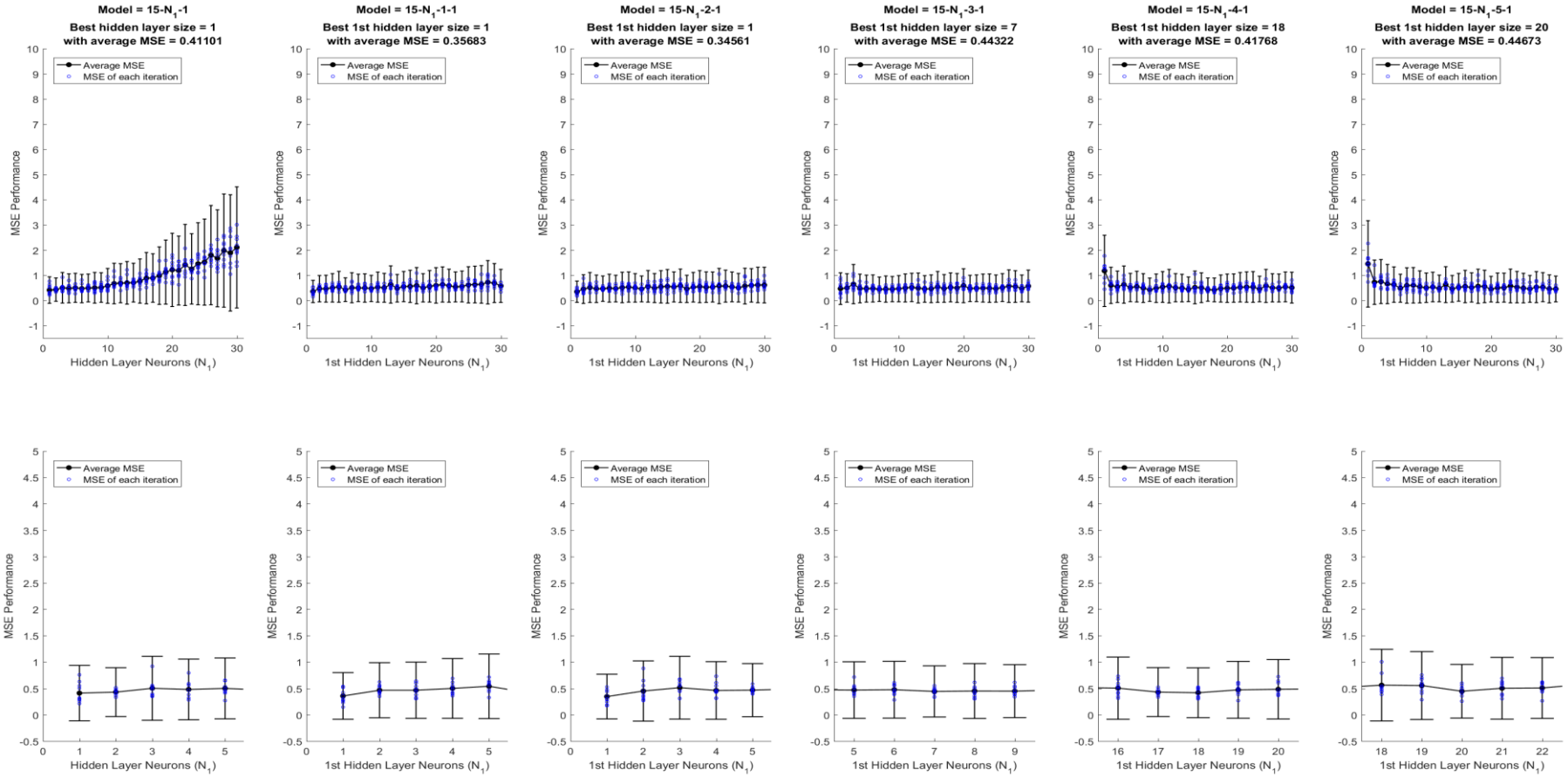

SESSION 5: Average MSE performance across all neural network configurations with top 15 significant input vectors. Error bar indicates 95% CI. Top row of graphs displays all hidden layer neurons, bottom row of graphs zoomed in to the best hidden layer neurons

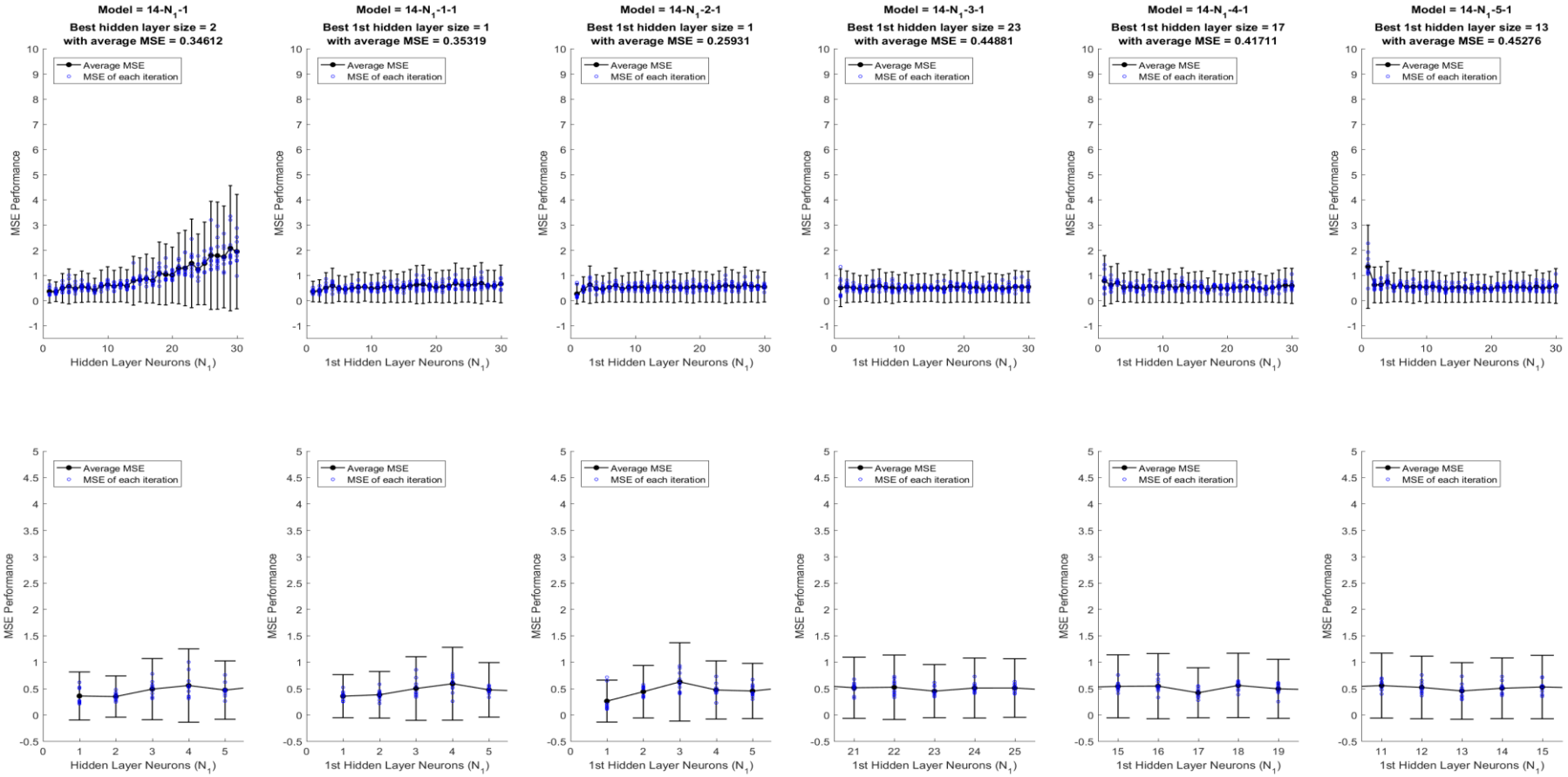

SESSION 6: Average MSE performance across all neural network configurations with top 14 significant input vectors. Error bar indicates 95% CI. Top row of graphs displays all hidden layer neurons, bottom row of graphs zoomed in to the best hidden layer neurons

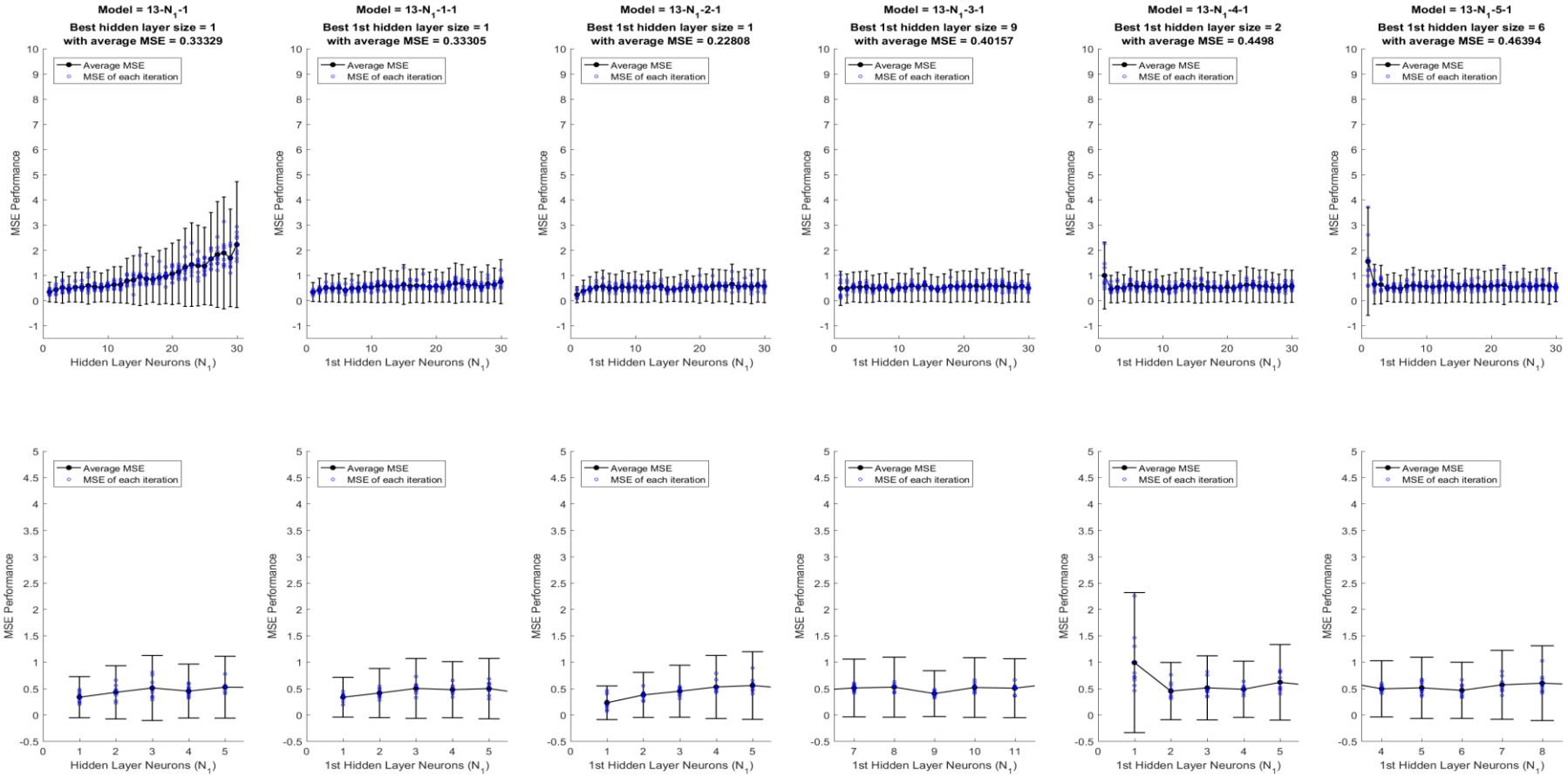

SESSION 7: Average MSE performance across all neural network configurations with top 13 significant input vectors. Error bar indicates 95% CI. Top row of graphs displays all hidden layer neurons, bottom row of graphs zoomed in to the best hidden layer neurons

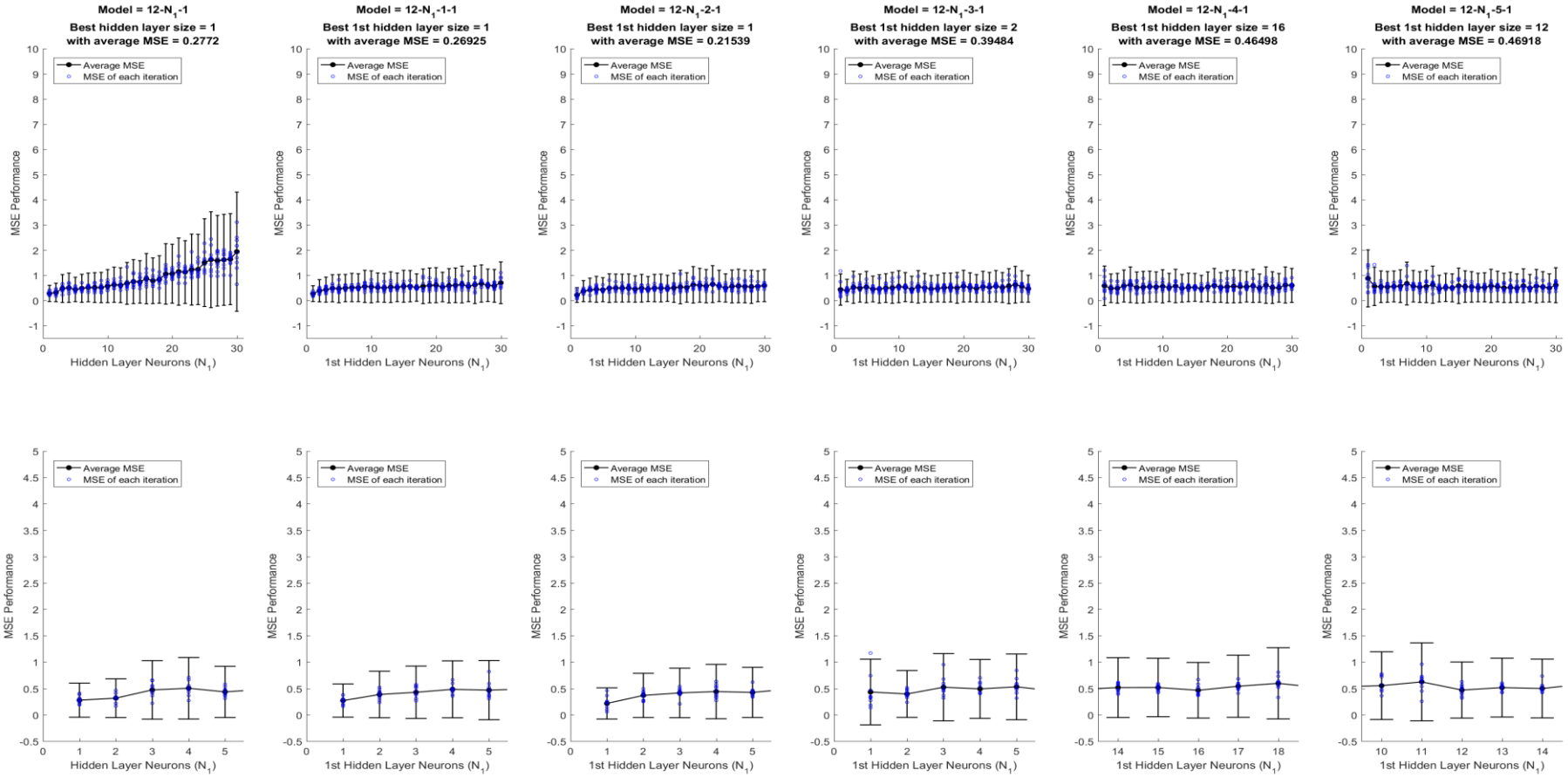

SESSION 8: Average MSE performance across all neural network configurations with top 12 significant input vectors. Error bar indicates 95% CI. Top row of graphs displays all hidden layer neurons, bottom row of graphs zoomed in to the best hidden layer neurons

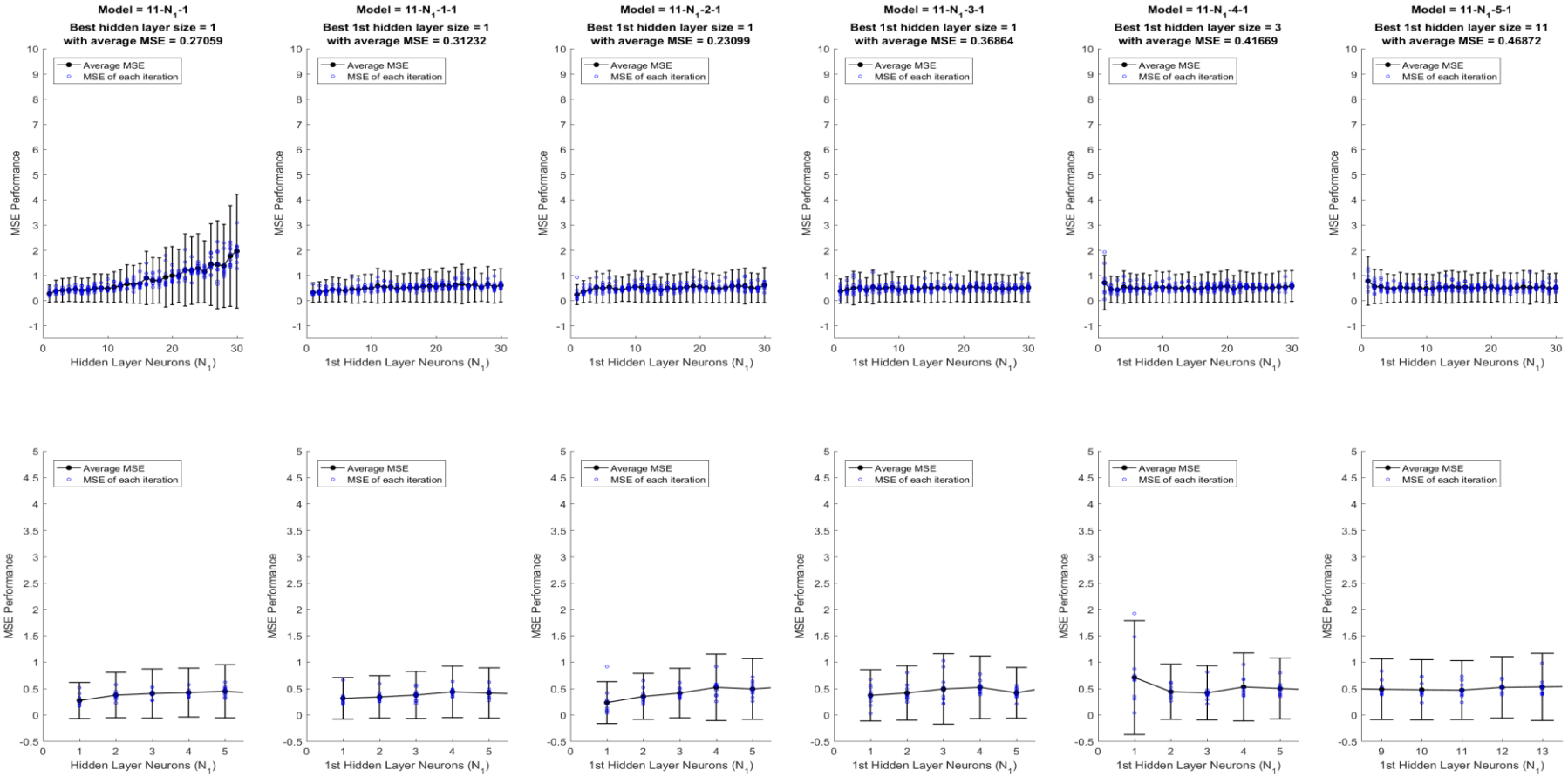

SESSION 9: Average MSE performance across all neural network configurations with top 11 significant input vectors. Error bar indicates 95% CI. Top row of graphs displays all hidden layer neurons, bottom row of graphs zoomed in to the best hidden layer neurons

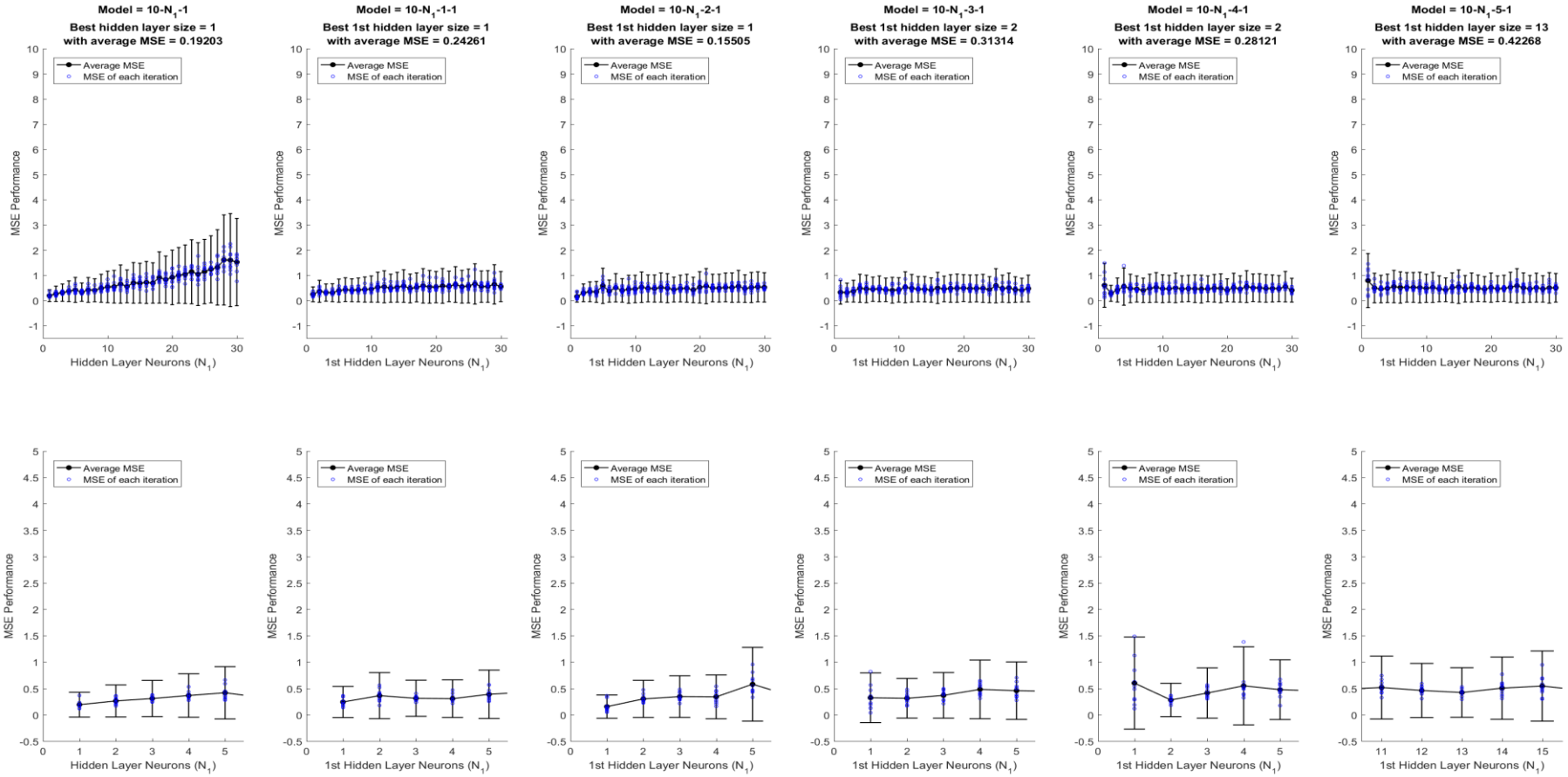

SESSION 10: Average MSE performance across all neural network configurations with top 10 significant input vectors. Error bar indicates 95% CI. Top row of graphs displays all hidden layer neurons, bottom row of graphs zoomed in to the best hidden layer neurons

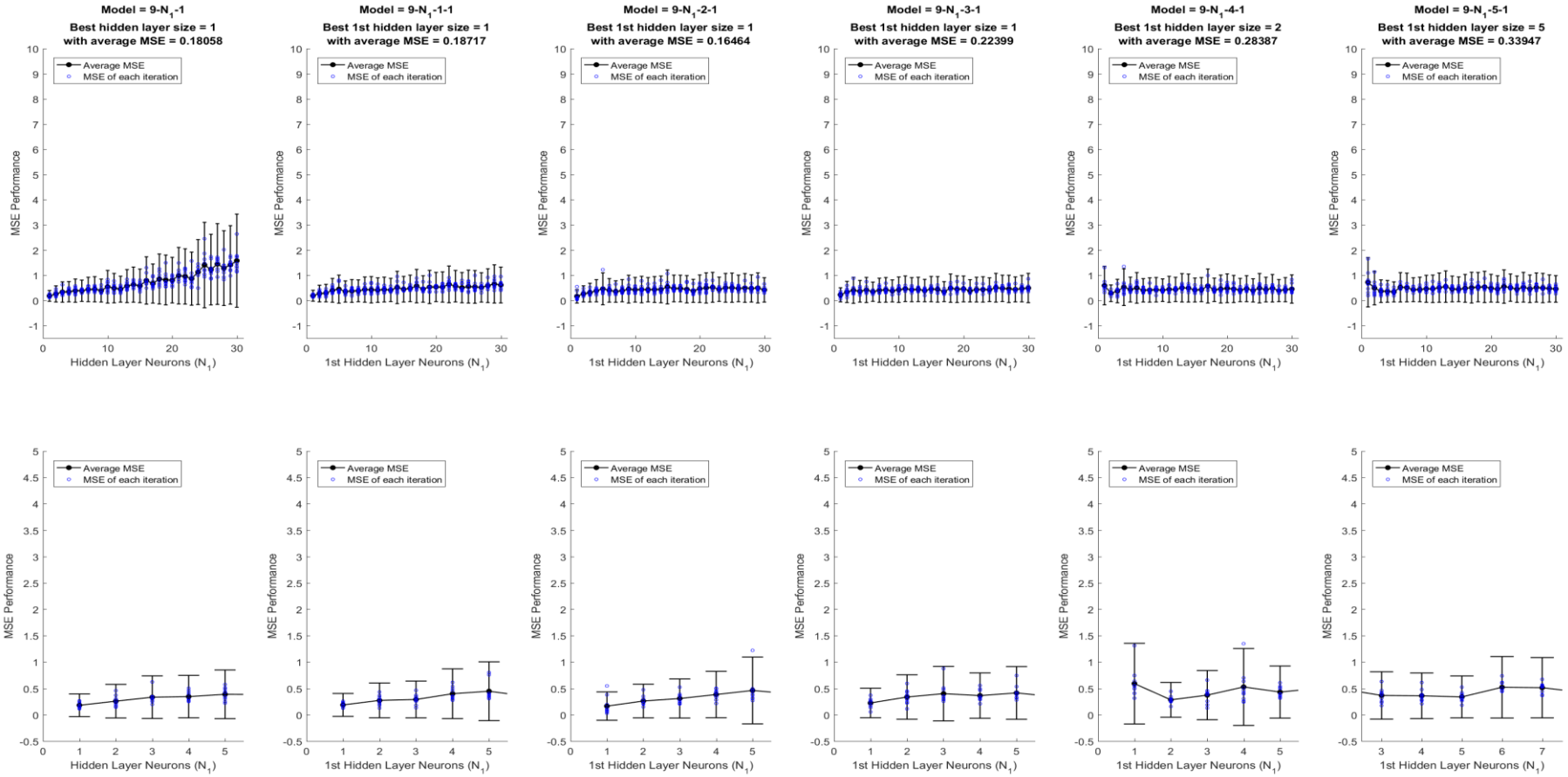

SESSION 11: Average MSE performance across all neural network configurations with top 9 significant input vectors. Error bar indicates 95% CI. Top row of graphs displays all hidden layer neurons, bottom row of graphs zoomed in to the best hidden layer neurons

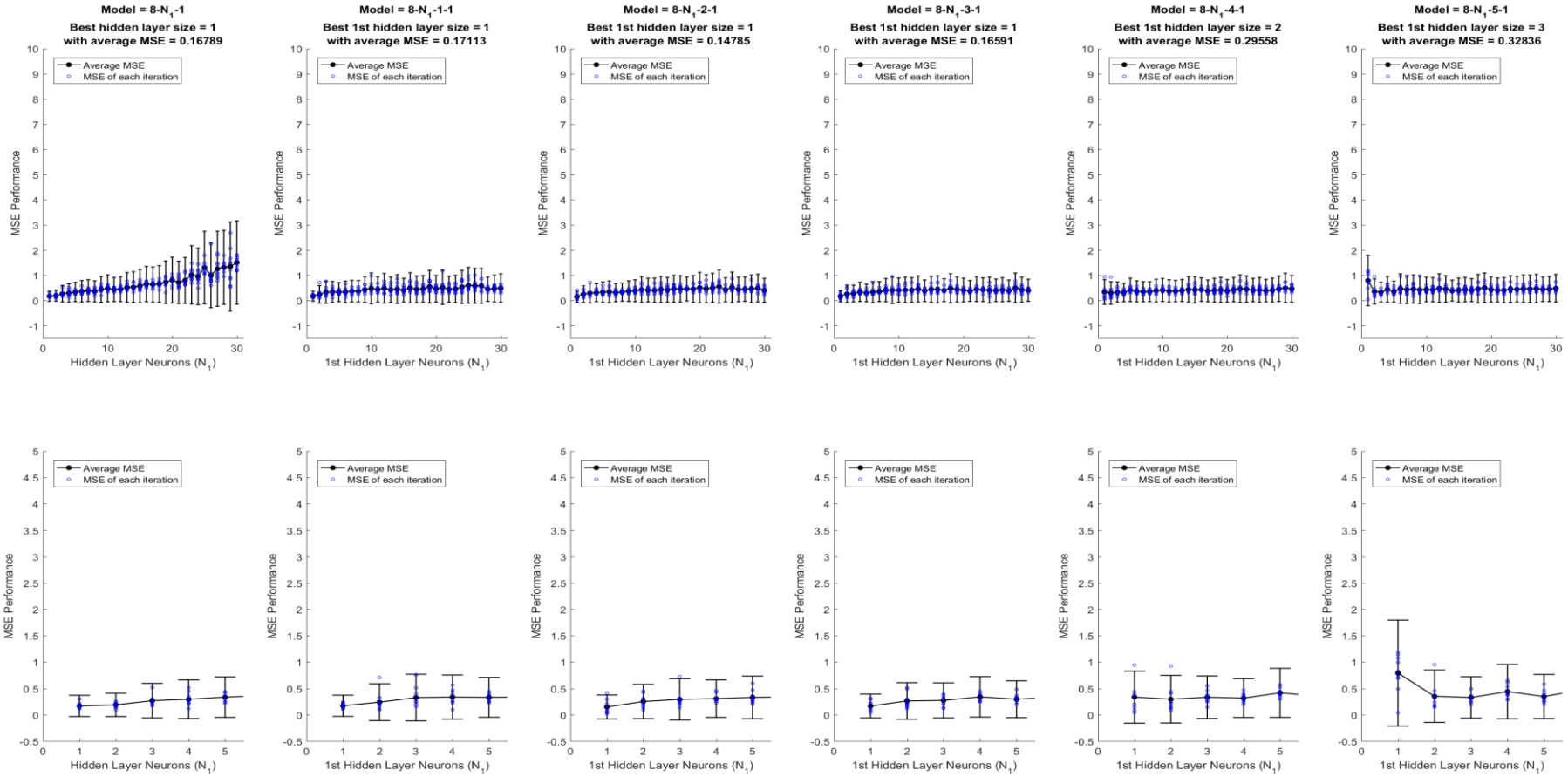

SESSION 12: Average MSE performance across all neural network configurations with top 8 significant input vectors. Error bar indicates 95% CI. Top row of graphs displays all hidden layer neurons, bottom row of graphs zoomed in to the best hidden layer neurons

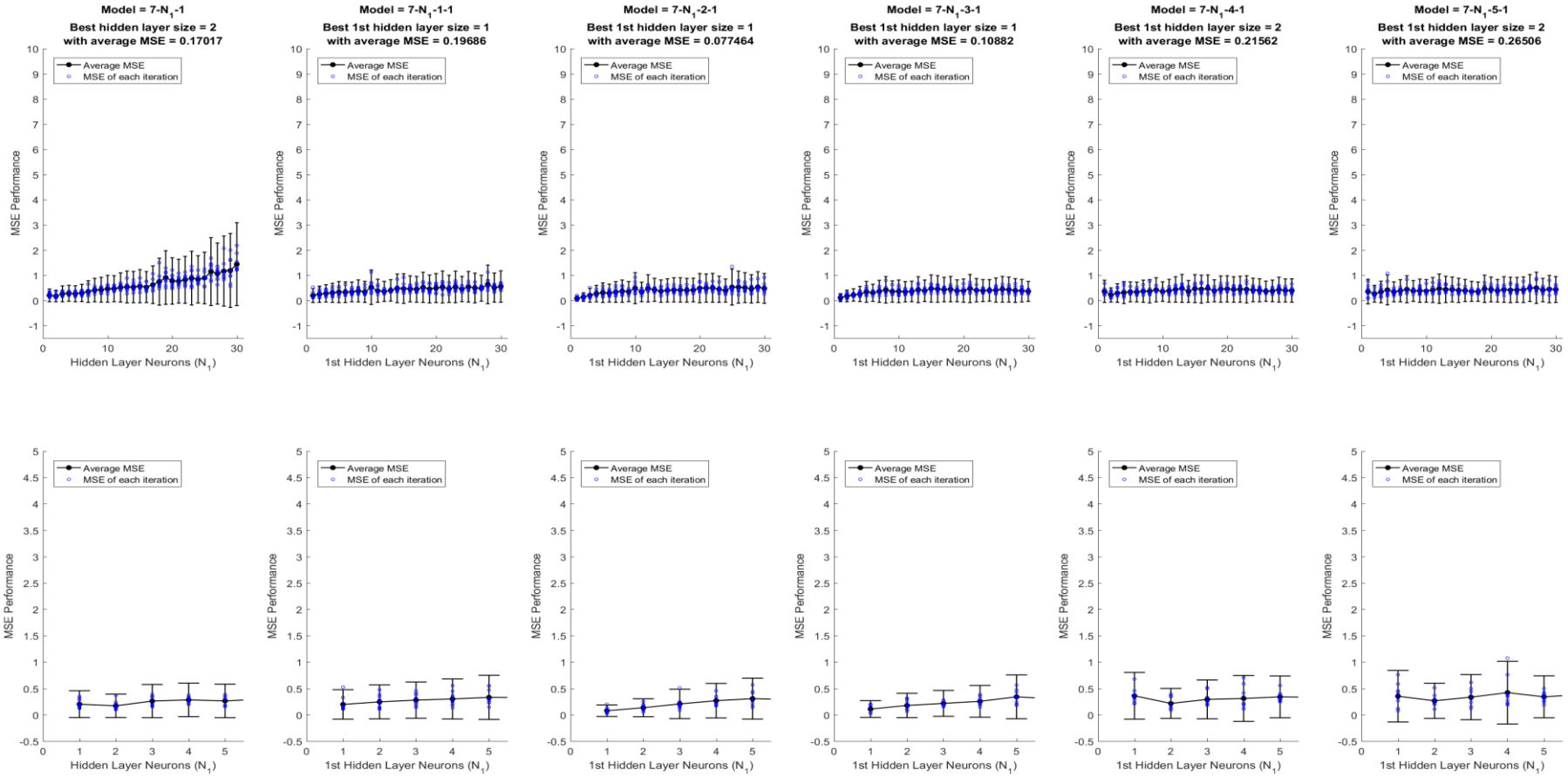

SESSION 13: Average MSE performance across all neural network configurations with top 7 significant input vectors. Error bar indicates 95% CI. Top row of graphs displays all hidden layer neurons, bottom row of graphs zoomed in to the best hidden layer neurons

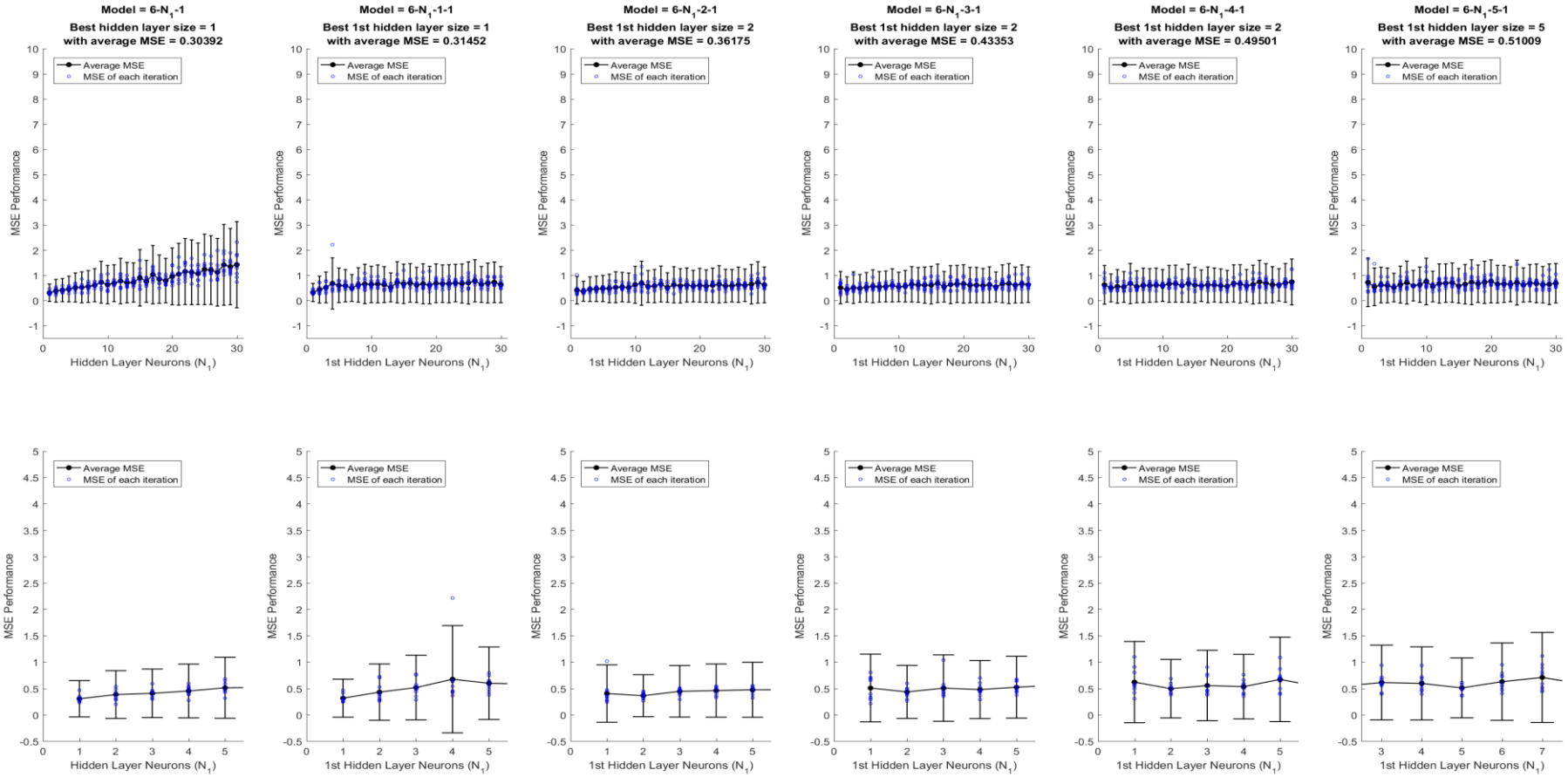

SESSION 14: Average MSE performance across all neural network configurations with top 6 significant input vectors. Error bar indicates 95% CI. Top row of graphs displays all hidden layer neurons, bottom row of graphs zoomed in to the best hidden layer neurons

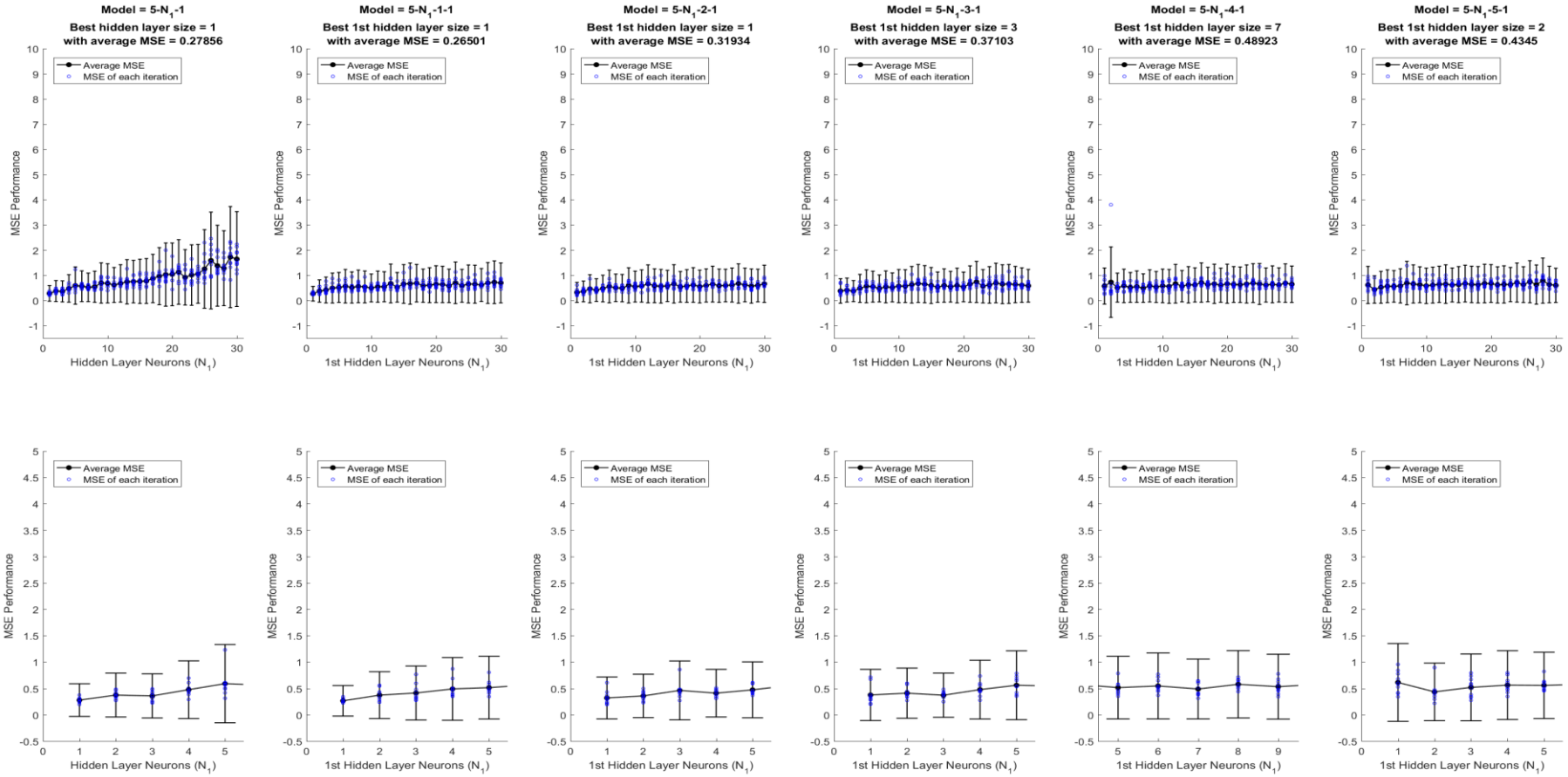

SESSION 15: Average MSE performance across all neural network configurations with top 5 significant input vectors. Error bar indicates 95% CI. Top row of graphs displays all hidden layer neurons, bottom row of graphs zoomed in to the best hidden layer neurons

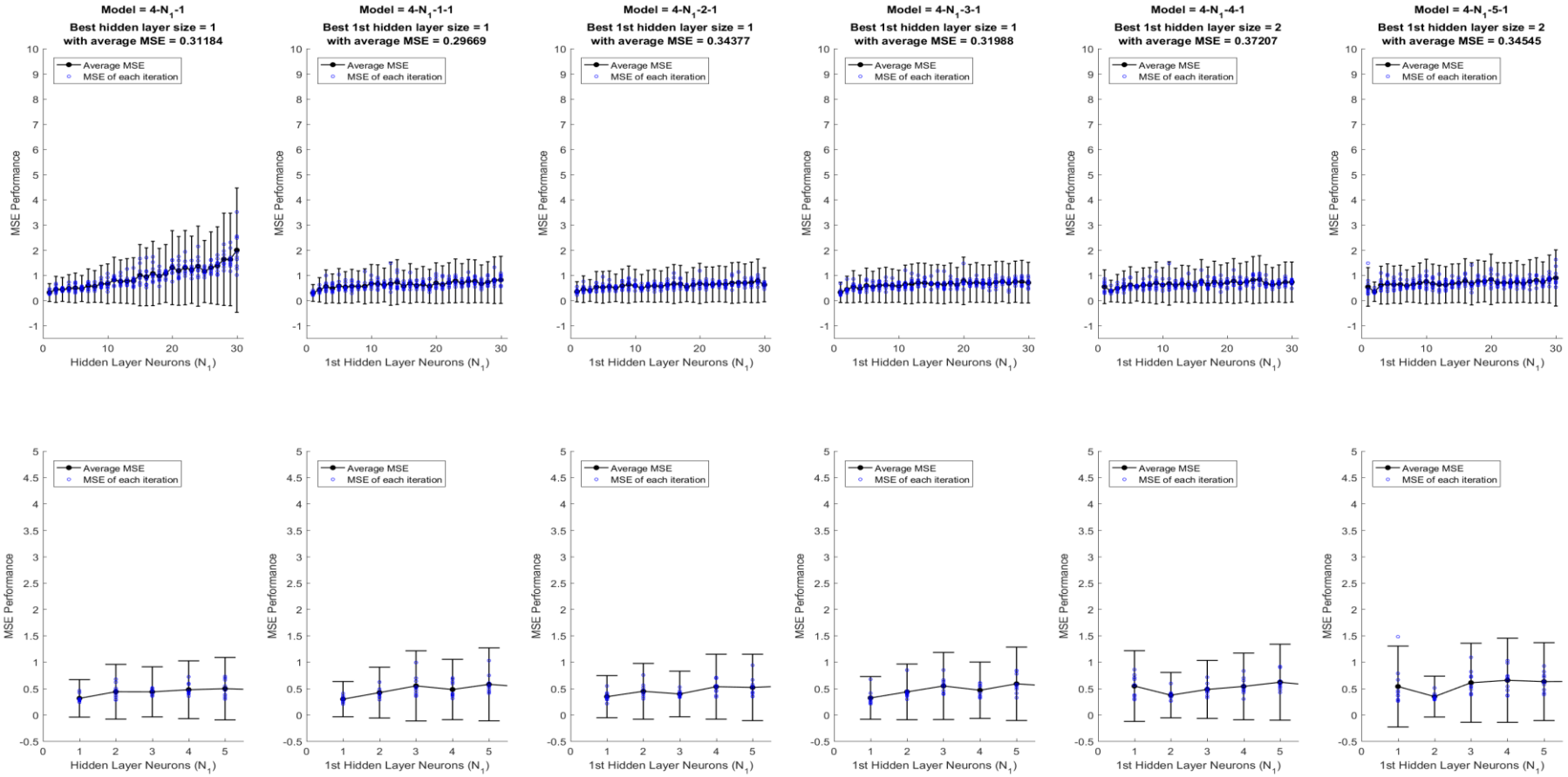

SESSION 16: Average MSE performance across all neural network configurations with top 4 significant input vectors. Error bar indicates 95% CI. Top row of graphs displays all hidden layer neurons, bottom row of graphs zoomed in to the best hidden layer neurons

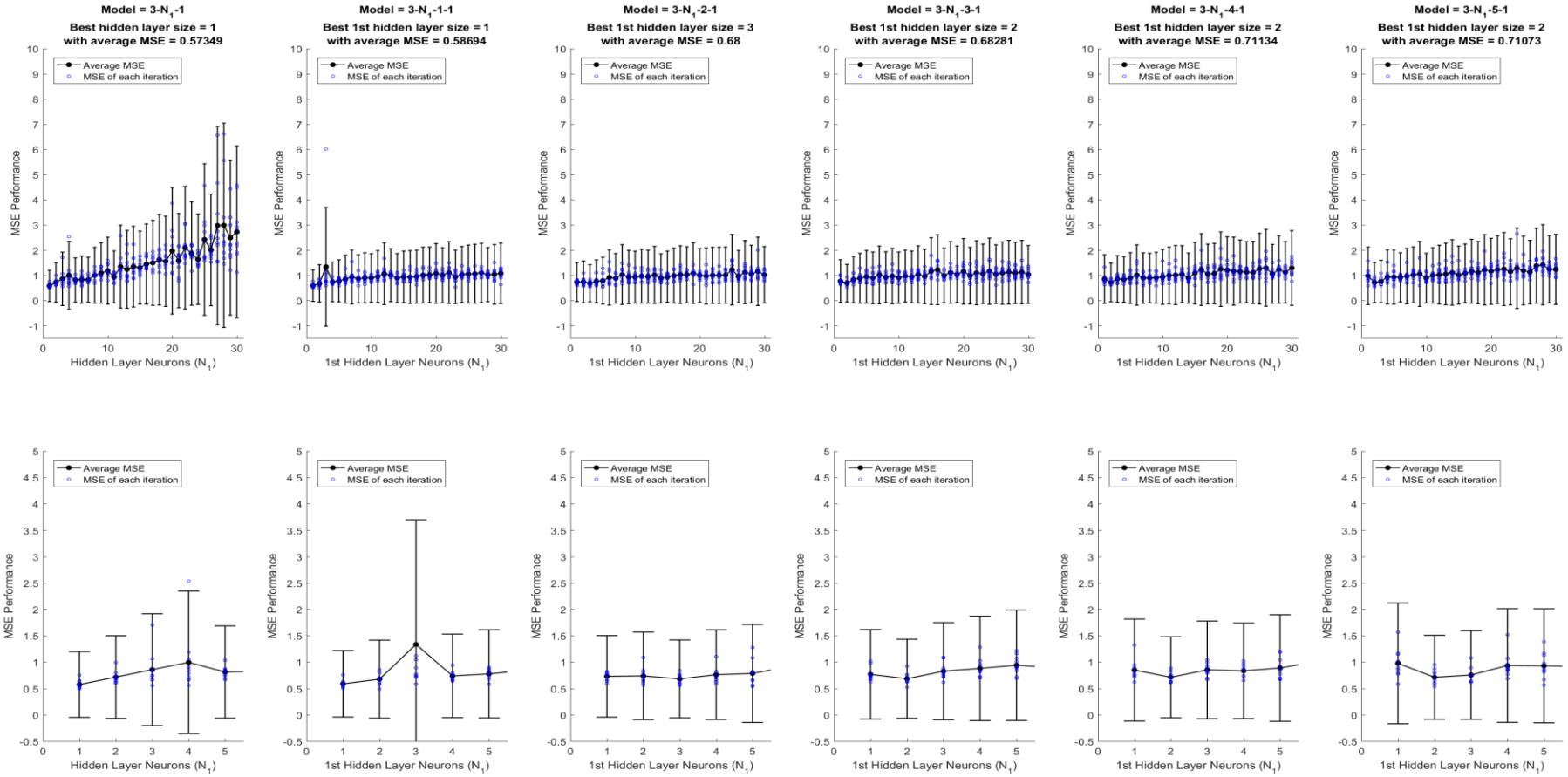

SESSION 17: Average MSE performance across all neural network configurations with top 3 significant input vectors. Error bar indicates 95% CI. Top row of graphs displays all hidden layer neurons, bottom row of graphs zoomed in to the best hidden layer neurons

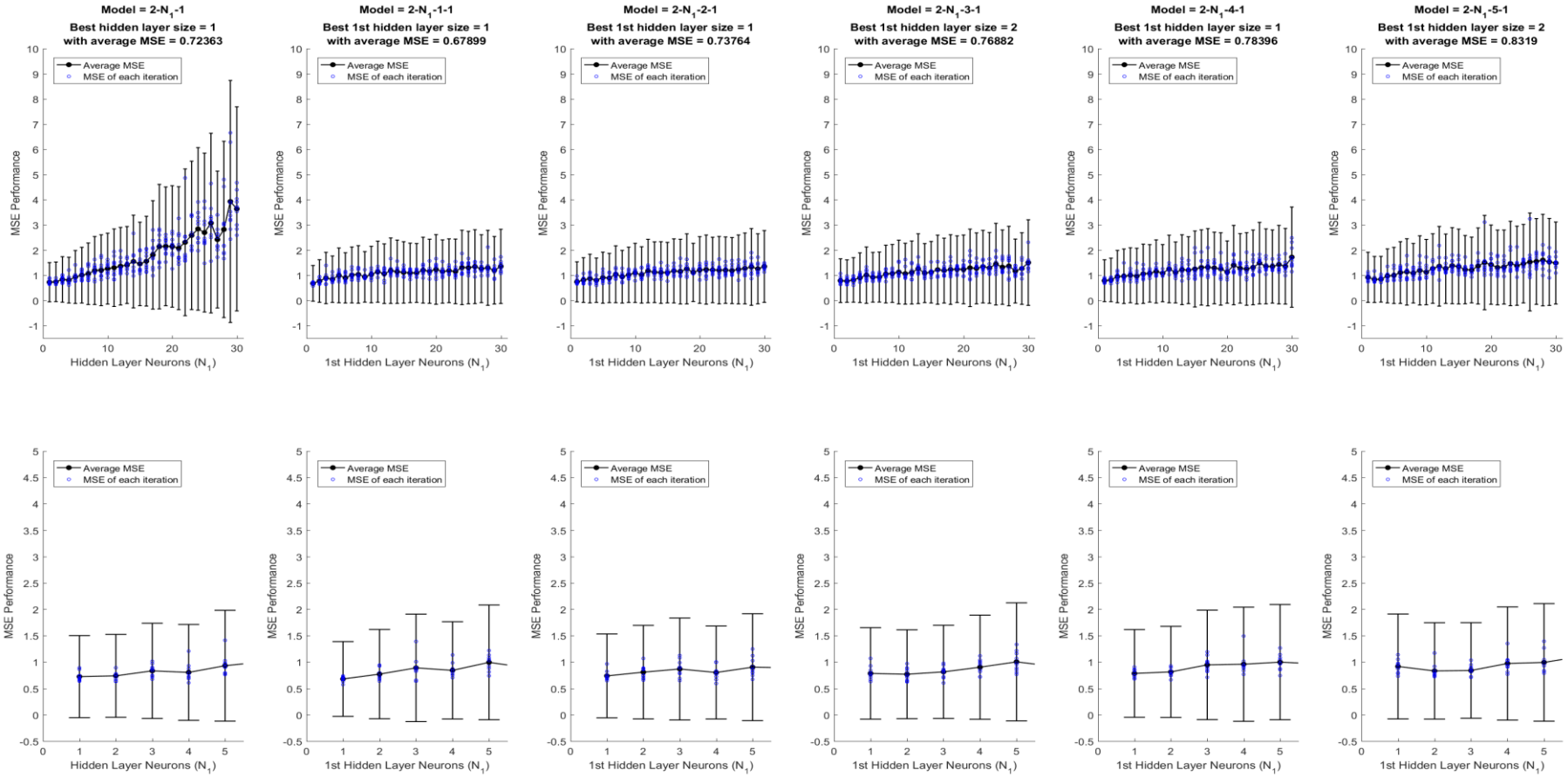

SESSION 18: Average MSE performance across all neural network configurations with top 2 significant input vectors. Error bar indicates 95% CI. Top row of graphs displays all hidden layer neurons, bottom row of graphs zoomed in to the best hidden layer neurons

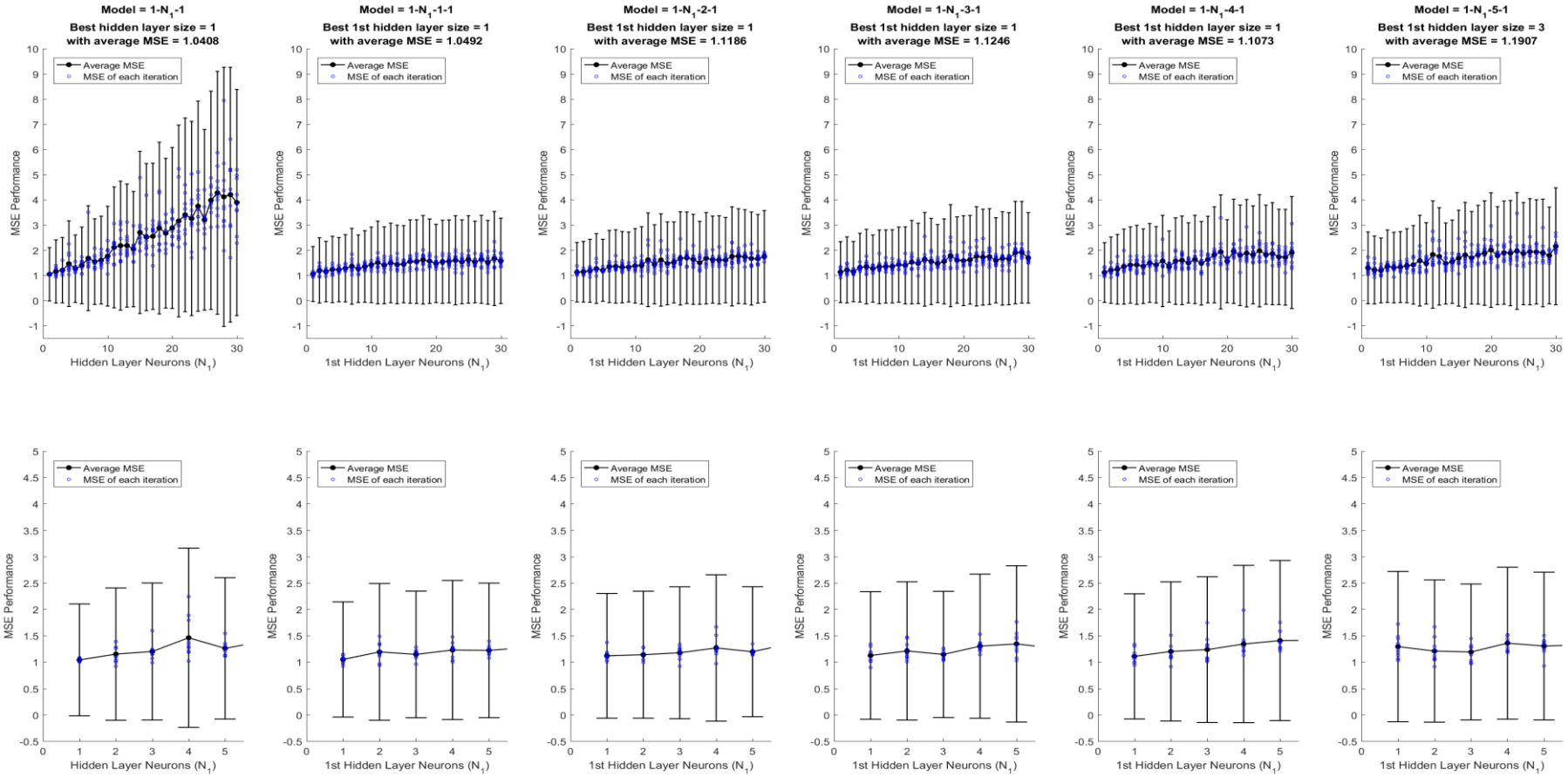

SESSION 19: Average MSE performance across all neural network configurations with top significant input vectors. Error bar indicates 95% CI. Top row of graphs displays all hidden layer neurons, bottom row of graphs zoomed in to the best hidden layer neurons